

3 Higher-level phylogeny of the Ithomiinae (Lepidoptera: Nymphali-
4 dae): classification, patterns of larval hostplant colonization and
5 diversification

6 Keith R. Willmott^{1*} and André V. L. Freitas²

7 ¹McGuire Center for Lepidoptera and Biodiversity, Florida Museum of Natural History, University of Florida, SW 34th Street and Hull Road, PO Box
8 112710, Gainesville, FL 32611-2710, USA, ²Departamento de Zoologia and Museu de História Natural, Instituto de Biologia, Universidade Estadual de
9 Campinas, CP 6109, CEP 13083-970, Campinas, São Paulo, Brazil

10 Accepted 22 February 2006

11

12 **Abstract**

13 We present a higher-level phylogenetic hypothesis for the diverse neotropical butterfly subfamily Ithomiinae, inferred from one of
14 the largest non-molecular Lepidoptera data sets to date, including 106 species (105 ingroup) and 353 characters (306 informative)
15 from adult and immature stage morphology and ecology. Initial analyses resulted in 1716 most parsimonious trees, which were
16 reduced to a single tree after successive approximations character weighting. The inferred phylogeny was broadly consistent with
17 other past and current work. Although some deeper relationships are uncertain, tribal-level clades were generally strongly
18 supported, with two changes required to existing classification. The tribe Melinaeini is polyphyletic and *Athesis* + *Patricia* require a
19 new tribe. *Methona* should be removed from Mechanitini into the restored tribe Methonini. Dircennini was paraphyletic in analyses
20 of all data but monophyletic based on adult morphology alone, and its status remains to be confirmed. *Hypothyris*, *Episcada*,
21 *Godyris*, *Hypoleria* and *Greta* are paraphyletic. A simulation analysis showed that relatively basal branches tended to have higher
22 partitioned Bremer support for immature stage characters. Larval hostplant records were optimized on to a reduced, generic-level
23 phylogeny and indicate that ithomiines moved from Apocynaceae to Solanaceae twice, or that Tithoreini re-colonized Apocynaceae
24 after a basal shift to Solanaceae. Ithomiine clades have specialized on particular plant clades suggesting repeated colonization of
25 novel hostplant niches consistent with adaptive radiation. The shift to *Solanum*, comprising 70% of neotropical Solanaceae, occurs
26 at the base of a clade containing 89% of all ithomiines, and is interpreted as the major event in the evolution of ithomiine larval
27 hostplant relationships.

28 © The Willi Hennig Society 2006.

30 The nymphalid butterfly subfamily Ithomiinae
31 (ithomiines) is one of the best studied groups of
32 Lepidoptera, and has served as a model in research on
33 biogeography, chemical ecology and evolution. The
34 subfamily is exclusively neotropical, containing approxi-
35 mately 370 species (Lamas, 2004; Willmott and Lamas,
36 2005, in prep.) occurring in humid forests from sea level to
37 3000 m, from Mexico to southern Brazil, Paraguay, and
38 across three Caribbean islands.

Adults of all Ithomiinae are unpalatable and warn- 39
ingly colored (Fig. 1), and many are models for palat- 40
able species of other lepidopteran taxa. Observing these 41
butterflies stimulated Bates (1862) to formulate his 42
theory of mimicry, which is now one of the best studied 43
examples of natural selection. Ithomiines are also 44
extensively involved in Müllerian mimicry rings, which 45
they numerically dominate, along with butterflies of the 46
nymphalid subfamily Heliconiinae (Müller, 1879; Bec- 47
caloni, 1997a). Ithomiine unpalatability results from 48
dehydropyrrolizidine alkaloids, which are obtained in 49
the majority of species by adult males feeding on 50
Asteraceae flowers and dried or withered Boraginaceae 51

*Corresponding author: E-mail address: kwillmott@flmnh.ufl.edu

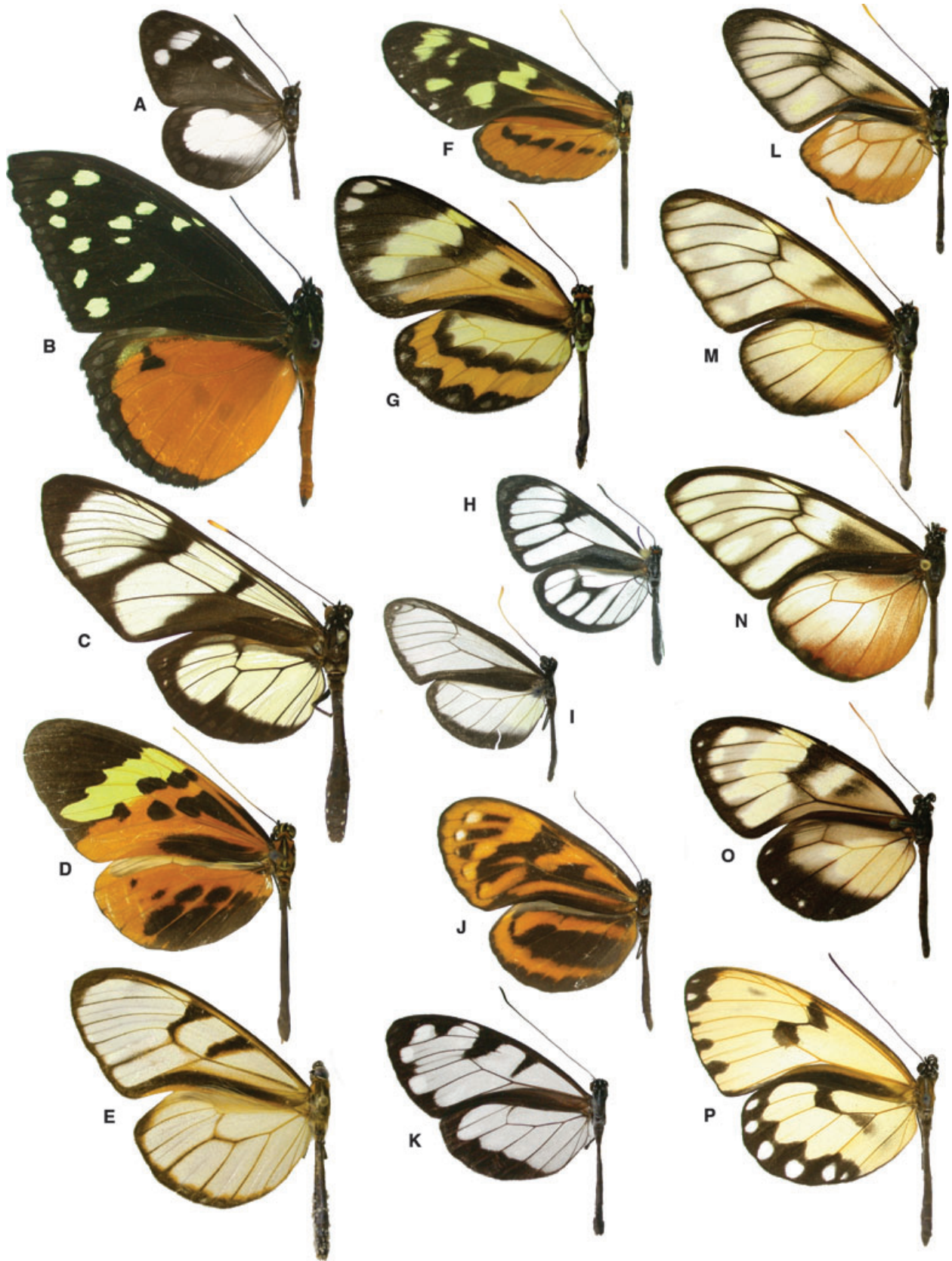


Fig. 1. Adult male representatives of outgroup *Tellervo* and Ithomiinae tribes. (A) *Tellervo zoilus*, Australia; (B) *Tithorea tarricina*, Ecuador; (C) *Methona themisto*, Brazil; (D) *Melinaea menophilus*, Ecuador; (E) *Athesis clearista*, Venezuela; (F) *Mechanitis lysimnia*, Ecuador; (G) *Placidina euryanassa*, Brazil; (H) *Ithomia terra*, Ecuador; (I) *Napeogenes apulia*, Ecuador; (J) *Hyposcada anchiala*, Peru; (K) *Oleria santineza*, Ecuador; (L) *Callithomia lenea*, Ecuador; (M) *Dircenna jemina*, Ecuador; (N) *Pteronymia lonera* Costa Rica; (O) *Godyris zavaleta*, Ecuador; (P) *Veladyris pardalis*, Ecuador.

52 plants (Brown, 1984, 1985; Trigo and Brown, 1990). The
 53 same alkaloids are also the precursors for volatile
 54 pheromones, which males disseminate through hair-like,
 55 alar androconial organs (Edgar et al. 1976; Schulz et al.,
 56 1988, 2004).

57 Many Ithomiinae are abundant, conspicuous and
 58 easily sampled, which has led to a relatively thorough
 59 knowledge of distribution in some groups. Ithomiine
 60 distribution data have therefore been used in identifying
 61 areas of endemism in the neotropical lowlands and
 62 testing the refuge hypothesis (Brown, 1977b, 1982), as
 63 well as examining geographic modes of speciation
 64 2,3 (Whinnett et al., 2005; Jiggins et al. 2005).

65 Perhaps most notably, ithomiines are remarkable in
 66 their larvae feeding almost exclusively on plants of the
 67 family Solanaceae, on which they are one of the
 68 relatively few herbivores (Drummond and Brown,
 69 1987; Brown and Freitas, 1994; Willmott and Mallet,
 70 2004). Although several other insect groups also feed on
 71 Solanaceae, notably Chrysomelidae (Hsiao, 1986), few
 72 are as specialized or abundant in the habitats where
 73 ithomiines occur. This close association between herbi-
 74 vore and host led to the group being used in seminal
 75 studies of insect–plant coevolution (Drummond, 1986;
 76 Brown and Henriques, 1991). These studies found no
 77 evidence for traditional coevolution, or matching clad-
 78 ogenesis of herbivore and host, but nevertheless the
 79 ecology of ithomiine–host interaction is likely to have
 80 been significant in the subfamily’s diversification
 81 (Drummond, 1986; Willmott and Mallet, 2004).

82 Though the Ithomiinae have already proved a model
 83 study group in many fields, a robust phylogenetic
 84 hypothesis, which would permit the use of phylogenetic
 85 comparative methods, is still needed. The Ithomiinae are
 86 defined by a clear morphological synapomorphy, the
 87 presence in males of an elongate patch of erectile, hair-
 88 like androconial scales at the anterior edge of the dorsal
 89 hindwing, apparently first remarked upon by Doubleday
 90 (1847). The subfamily forms a clade with the Tellervinae,
 91 containing the single Australasian genus *Tellervo*,
 92 together with the largely Old World Danainae, of which
 93 the Ithomiinae have been regarded as a tribe (Godman
 94 et al., 1879–80; Haensch, 1909–10; Ackery et al., 1999;
 95 Brower et al., 2006). The close relationship between
 96 these three taxa has been recognized since at least the
 97 time of Doubleday (1847) and confirmed in subsequent
 98 papers (Brower, 2000; Freitas and Brown, 2004), and we
 99 follow Lamas (2004) in according each subfamilial
 100 status.

101 One of the earliest attempts to portray the relation-
 102 ships among Ithomiinae genera was that of Doubleday
 103 (1847), who used characters of the venation and male
 104 foreleg to successfully unite several ithomiine genera and
 105 order them from basal to derived (Fig. 2). His overall
 106 arrangement was refined, but little improved upon, by
 107 subsequent authors (Godman and Salvin, 1879–80;

Haensch, 1909–10), until D’Almeida (1941) and Fox 108
 (1940, 1956) established the currently recognized tribes 109
 and formed the foundation for future work (Fig. 2). 110

Brown and Henriques (1991) provided the first 111
 explicit phylogeny of ithomiine genera, based on ana- 112
 lysis of 90 morphological and ecological characters from 113
 adult and immature stages for representatives of most 114
 genera. This was followed by Brown and Freitas (1994), 115
 in which the immature stage character matrix was 116
 provided in addition to three cladograms based, respect- 117
 ively, on adult, immature and all characters combined 118
 (Fig. 2). These cladograms permitted the first assess- 119
 ment of monophyly of the tribes that had been recog- 120
 nized for the preceding half century. 121

The Tithoreini of Fox (1940, 1956), founded largely 122
 on the possession of a less reduced male foreleg 123
 (apparently a symplesiomorphy), proved to be broadly 124
 paraphyletic, splitting into at least four branches. The 125
 genus *Aeria*, placed in Oleriini by Fox (1956), moved to 126
 a more basal position near *Tithorea*. The highly 127
 autapomorphic genera *Placidina* and *Methona*, placed 128
 in two separate tribes by Fox (1956), moved far from 129
 their putative relatives to form a sister clade to the 130
 Mechanitini. Finally, although the remaining five tribes 131
 formed a monophyletic group, the tribe Dircennini 132
 disintegrated into a broad paraphyletic assemblage 133
 scattered across this clade. In particular, three small, 134
 highly autapomorphic genera, *Callithomia*, *Talaman-* 135
cana (described by Brown and Freitas, 1994; for a single 136
 Costa Rican species) and *Velamysta*, assumed a basal 137
 position for the clade, which contains the majority of 138
 ithomiine species. 139

The cladograms of Brown and Freitas (1994) showed 140
 that a stable tribal classification for the Ithomiinae has 141
 yet to be reached, with four of the generally recognized 142
 eight tribes proving not to be monophyletic. Their study 143
 also demonstrated that immature stages could provide 144
 important information in resolving major, more basal 145
 nodes. For example, larval morphology clearly showed 146
Aeria to be a basal ithomiine, and the larval hostplant 147
 family, Apocynaceae, is otherwise used in the Ithomi- 148
 inae only by the basal genera *Tithorea* and *Elzunia*. 149
 Brown and Freitas (1994) therefore suggested that 150
 future studies concentrate on including more taxa and 151
 trying to obtain life history information for certain key 152
 genera. 153

Our primary goal therefore is to incorporate new data 154
 and taxa from all species clades within the Ithomiinae to 155
 attempt to resolve these currently problematic areas of 156
 ithomiine phylogeny. In particular, we focus on the 157
 monophyly, relationships and classification of the basal 158
 clades (former Tithoreini, Melinaeini and Mechanitini), 159
 the phylogenetic position of certain highly autapomor- 160
 phic and enigmatic genera (including, among others, 161
Methona, *Placidina*, *Callithomia*, *Velamysta* and 162
Talamancana), and the monophyly of the Dircennini. 163

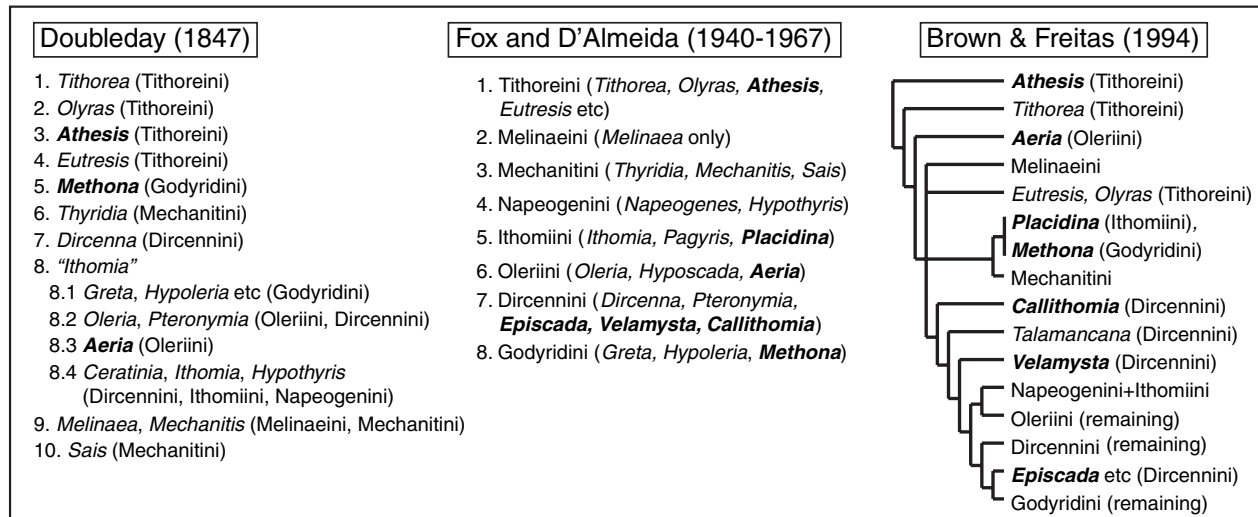


Fig. 2. History of classification and inferred relationships among ithomiine tribes.

164 Because the data set presented here will be combined
 165 with a DNA sequence data set of collaborators (Brower
 166 et al., 2006) for a total evidence analysis in the near
 167 future, we refrain from making taxonomic changes here.

168 Our second goal is to attempt to confirm for the first
 169 time, using cladistic methods, the monophyly of all
 170 recognized genera, or highlight areas in need of future
 171 study. As a basis for discussions of classification in this
 172 paper we use the recent tribal and generic classification
 173 of Lamas (2004), which is based largely on that author's
 174 own morphological knowledge, Brown and Freitas
 175 (1994) and discussions with the authors of this paper.

176 Finally, in the last decade much new hostplant data
 177 have been obtained, so we take this opportunity to
 178 re-examine patterns of host evolution using the phylo-
 179 genetic hypotheses presented here. While the shift to
 180 Solanaceae has been seen as a key event in ithomiine
 181 evolution, the cladograms of Brown and Freitas (1994)
 182 imply that the plant family was either colonized twice, or
 183 that one or more reversals to feeding on Apocynaceae
 184 occurred.

185 Methods

186 Study taxa and outgroup choice

187 In choosing study taxa within the Ithomiinae we
 188 attempted to include representatives from all species
 189 clades, those with immature stage information and
 190 preserved specimens for molecular analysis by collabo-
 191 rators, and type species for genera, where possible.
 192 Species clades are clusters of species with similar or
 193 identical male genitalia and androconia, character sets
 194 that are most reliable in defining monophyletic species
 195 groups (Willmott and Lamas, unpublished data). In

genera lacking clear synapomorphies for species groups
 we selected species to represent most of the morpho-
 logical variation within the genus. We used published
 revisions and our own study to choose representative
 species from 20 genera containing 111 ithomiine species
 (see Table 1). For the remaining 25 genera, containing
 256 species, we examined wing venation, androconia
 and genitalic dissections for males of 229 species to
 define species clades. Omitted species were either clear
 members of monophyletic groups already represented
 by exemplar species (20 spp., based on wing venation
 and androconia), or unavailable for dissection due to
 rarity (seven spp.). Other information (female morphol-
 ogy, wing venation from photographs) suggests that
 these latter species are likely to be closely related to
 examined species and that their omission does not
 compromise this study (see also discussion in Table 1).
 From each species clade one or more representative
 species were selected to maximize available character
 information and to include, usually, the type species. In
Elzunia, *Velamysta* and *Haenschia* the type species was
 not used because it lacked life history and/or molecular
 data and is morphologically very similar to the chosen
 exemplar species. In total we selected 105 ithomiine
 species from all genera for analysis (Appendix 2).

The relationships between the Ithomiinae, Danainae
 and the monotypic Tellervinae remain unclear, so
 initially we included a single species from each of five
 genera representing major lineages of the Danainae
 (*Lycorea*, *Anetia*, *Danaus*, *Euploea* and *Ideopsis*, see
 Ackery and Vane-Wright, 1984) and *Tellervo zoilus*, the
 type species for *Tellervo* (Table 1). Morphologically,
 the Danainae proved to be extremely divergent from the
 Ithomiinae, and many character states could not be
 coded or were autapomorphic. As *Tellervo* is much more
 morphologically similar to Ithomiinae, and a single

Table 1
Summary of species examined and included in phylogenetic analysis

Taxon	Genera	Species	Dissected species (male)	Included species	References
Ithomiinae					
Tithoreini	2	5	4	3	Fox (1956), Brown (1977b)
Aeria	1	3	2	2	Lamas (2004)
Methona	1	7	2	2	Lamas (1973)
Melinaeini	5	18	9	7	Fox (1960), Lamas (1973, 1979), Brown (1977a)
Athesis + Patricia	2	6	4	2	Fox (1956)
Mechanitini	4	16	10	8	Fox (1967), Lamas (1973), Brown (1977a)
Napeogenini	5	56	36	13	Fox and Real (1971), Brown (1980)
Subtotal (revised tribes)	20	111	67	37	
Ithomiini	3	28	19	6	Lamas (1986)
Oleriini	4	63	63	12	
Dircennini ¹	7	92	83	28	Brown and D'Almeida (1970), Brown et al. (1970)
Godyridini ¹	11	73	64	22	Lamas (1980)
Subtotal (non-revised tribes)	25	256	229	68	
Total all tribes	45	367	296	105	
Danainae	11	162	4	–	Ackery and Vane-Wright (1984)
Tellervinae	1	6	1	1	Ackery (1987)

¹The recently described genus *Meizocellis* Brabant, 2004 (type species *Meizocellis infuscans* Brabant, 2004) is regarded as a synonym of *Pteronymia*. The taxon described as the type of *Meizocellis* is regarded as a subspecies of the northern Andean *Pteronymia serrata* Hewitson, which is morphologically almost identical to *Pteronymia alida*, included here in the ingroup. The genus *Oxapampa* Brabant, 2004 (type species *Oxapampa electrea* Brabant, 2004) is somewhat intermediate in male wing venation between *Velamysta* and *Veladyris*, and we suspect that it will prove to form a clade with one or both of these genera. An additional undescribed and apparently closely related species is also known from Peru. Unfortunately, we have been unable to dissect any specimens of *O. electrea* or the undescribed Peruvian species due to their rarity, and no illustrations or discussion of the genitalia of *O. electrea* were given in the original description. Thus, although *Veladyris* and *Velamysta* have a number of unique morphological apomorphies that could readily resolve the relationships of *Oxapampa*, its taxonomic status is still uncertain.

232 character (see Discussion) suggests it is the sister clade,
233 we used *Tellervo* alone as the outgroup for character
234 state polarization.

235 Ithomiinae species names and generic combinations
236 mostly follow Lamas (2004), except as follows (latter
237 name is that used in Lamas, 2004): *Pteronymia carlia* =
238 *Pteronymia sylvo*; *Episcada canaria* = *Episcada doto*
239 *canaria*; *Pteronymia inania* = *Pteronymia dispaena ina-*
240 *nia*; and *Heterosais nephele* = *Heterosais giulia nephele*.
241 The type illustration of *Hymenitis sylvo* Geyer, 1832,
242 appears to show an *Episcada* taxon, probably *Episcada*
243 *carcinia* Schaus, 1902, while additional distribution data
244 and/or morphological differences argue for the remain-
245 ing three changes in name status. No formal name
246 changes are made, however, as these will be discussed in
247 greater detail in forthcoming generic revisions (Lamas
248 and Willmott, in prep.).

249 Character sources

250 This study includes all potential character sources
251 known to us except molecular data (Brower et al., 2006),
252 chromosome number, which varies at the intraspecific
253 level (Brown et al., 2004; Kroutov et al. in prep.), and
254 microscopic characters of the eggs and first instar, which
255 have been studied by Motta (2003). The latter were
256 excluded because of high levels of homoplasy in that
257 data set and our inability to examine many of our
258 exemplar species due to lack of material. Both inform-

259 ative and uninformative characters were included, as the
260 latter may prove to be synapomorphies for genera or
261 species clades represented here by single species.

262 Most Ithomiinae larvae feed on Solanaceae (Drum-
263 mond and Brown, 1987), so immature stages of many
264 species were located by searching Solanaceae plants.
265 Where possible, ovipositing females were also followed,
266 or eggs expressed from gravid females and reared on a
267 range of potential hostplants. The majority of the
268 immature stage information has been obtained by
269 K. Brown (pers. comm.) in many countries, and by
270 K. Brown and AVLF in Brazil, over many years, at both
271 field sites and on cultivated hostplants at the Univer-
272 sidade Estadual de Campinas, Campinas (Freitas, 1993,
273 1996; Brown and Freitas, 1994; Freitas and Brown,
274 2002, 2005; Appendix 2). Additional information for
275 Andean species was collected by KRW during a
276 3-month period in two Ecuadorian cloud-forest localities
277 (Willmott and Mallet, 2004; Appendix 2). Eggs and
278 larvae were usually reared in plastic bags with fresh
279 hostplant leaves provided every 2–3 days. Where poss-
280 ible, eggs and larvae, especially first and last instars,
281 were preserved in locally available industrial alcohol
282 (ethanol). All observations of oviposition behavior,
283 larval behavior, development and appearance were
284 recorded and photographs taken of dorsal and lateral
285 views of larvae, and dorsal, lateral and ventral views of
286 pupae ([http://www.flmnh.ufl.edu/butterflies/neotropica/](http://www.flmnh.ufl.edu/butterflies/neotropica/ith_imm.html)
287 [ith_imm.html](http://www.flmnh.ufl.edu/butterflies/neotropica/ith_imm.html)). At least some immature stage informa-

288 tion was available for all but 20 of the 106 species
289 included in the study (Appendix 3).

290 Adult body morphology was studied using a Wild
291 M4 stereomicroscope with 6–50× magnification and
292 camera lucida. The antennal morphology, color pat-
293 tern and scale morphology of the frons, head, labial
294 palpi, thorax and abdomen were examined for males
295 of all species (no dimorphism was noted). The
296 morphology of the legs, abdomen and genitalia of
297 both sexes were examined by soaking these body parts
298 in 10% KOH for 10 min before dissection and storage
299 in glycerol (Appendix 3). Drawings of the male
300 genitalia in dorsal, lateral, ventral and posterior views,
301 aedeagus in dorsal and lateral view, the terminal 3
302 segments of the female abdomen in dorsal, lateral,
303 ventral and posterior views and the abdomen interior
304 in dorsal view were prepared for all species. Attempts
305 to evert the vesica (internal, tubular membrane) from
306 the aedeagus were successful for all except a few
307 Godyridini in which the aedeagus is extremely narrow.
308 Where possible, a standard 1 mL insulin syringe was
309 inserted into the ductus ejaculatorius and water
310 injected to evert the vesica, but for smaller species
311 the aedeagus was cut in two (after drawing the lateral
312 and dorsal view) just anterior of the zone and then
313 inserted into the syringe needle itself, held in place
314 with forceps. Wing venation was studied in both
315 cleared (with bleach, mounted in Euparal) and
316 uncleared specimens of both sexes. The distribution
317 and morphology of male hindwing androconial scales
318 was studied and drawn for all species by removal of
319 the right forewing to reveal these structures. These
320 scales were examined further with a Hitachi S2500
321 scanning electron microscope at 15 kV, with magnifi-
322 cation 30–5000×, for 86 of the 105 ithomiine species,
323 representing all genera. Included species were all those
324 that showed morphological differences under the
325 stereomicroscope and those whose phylogenetic posi-
326 tion was uncertain. Excluded species are marked with
327 an asterisk in the data matrix (Appendix 2). Sections
328 of wing for SEM study, containing both normal wing
329 scales and androconial scales, were mounted on stubs
330 with PVA glue and coated with a 20 nm layer of
331 gold/palladium (95% gold) using a Cressington Sput-
332 ter Coater. Terminology for genitalic structures fol-
333 lows a combination of Klots (1970), Eliot (1973) and
334 common usage, and is indicated on Fig. 21(D) (male)
335 and Fig. 28(J) (female). The pedunculi of Klots
336 (1970), projections from the anterio-ventral portion
337 of the tegumen, articulate with the vinculum, but as
338 the point of connection is often not discernible we use
339 “vinculum” to include both structures. We use the
340 Comstock and Needham (1918) system for naming
341 wing veins (see Fig. 14A,D,J), referring to cells by the
342 veins bounding them. Terminology for wing scales
343 follows Downey and Allyn (1975).

Character coding

344

All characters were initially equally weighted and
multistate characters unordered. The majority of char-
acters are discrete but in some cases we used continuous
characters, where characters that were discrete in one
part of the tree showed more continuous variation
elsewhere. These characters are conceptually little
different from discrete characters except in being objec-
tively quantifiable. Here, continuous characters repre-
sent either angles or ratios between two variables. The
numerical limits of states were chosen to reflect in
coding the initially observed variation and to minimize
homoplasy, based on cladistic relationships inferred
from other characters. We thus effectively use the same
criterion of parsimony in setting character states (that
number of steps should be minimal), which we use in
searching for optimal tree topologies.

Analyses

361

We used PAUP* 4.0b10 (Swofford, 1998) to analyze
our data, with maximum parsimony as our optimality
criterion. To reduce the problem of tree islands and
maximize the number of most parsimonious topologies
we employed a two-stage search. We first conducted
2000 replicate searches with TBR branch swapping,
obtaining starting trees by stepwise addition using a
random-addition sequence, retaining no more than five
trees per search. Resulting trees were used as starting
trees for a single subsequent heuristic search. Successive
approximations character weighting (SACW) (Farris,
1969) was used to attempt to reduce the number of most
parsimonious trees (MPTs) and improve consensus tree
resolution. Characters were reweighted based on the
maximum value of their consistency index, and subse-
quent two-stage searches were conducted using 1000
replicates retaining no more than two trees per search.

We examined the effect of adult and immature stage
characters on tree topology by conducting separate
analyses of matrices of each data type. All species were
included in analyses of the adult data matrix, but 26
species were excluded from the analysis of the immature
stage matrix due to lack of information (indicated in
Appendix 2). Our goal in these partitioned analyses was
to identify clades supported by both data sets and
therefore likely to prove robust and to evaluate whether
the time required to obtain immature stage data is
justified in such studies. The incongruence length
difference (ILD) test (Farris et al., 1995) is widely used
to examine for supposed inconsistencies in phylogenetic
signal between data partitions (e.g., Freitas and Brown,
2004). However, as we believe that the best phylogenetic
hypothesis results from a combined analysis of all data
(e.g., Nixon and Carpenter, 1996; Baker and DeSalle,
1997; Wahlberg et al., 2005), and given possible

397 inconsistencies in the ILD test as a measure of incon-
398 gruence (Dolphin et al., 2000; Barker and Lutzoni,
399 2002; Darlu and Lecointre, 2002), we do not use it here.

400 Strict consensus trees are used to summarize shortest
401 tree topologies. We estimated the strength of support for
402 branches based on our data by bootstrapping, as well as
403 by partitioned Bremer support values (Bremer, 1988,
404 1994), to evaluate the relative contribution of two major
405 data partitions (adult versus immature stage characters)
406 to the tree topology in the total evidence analysis. Two
407 hundred bootstrap replicates were run for each analysis.
408 Searches for each bootstrap replicate used starting trees
409 obtained by stepwise addition with 20 random-addition
410 sequences, retaining no more than two trees from each
411 search. Bremer support was calculated using constraint
412 searches generated by TreeRot v.2 (Sorenson, 1999) and
413 run in PAUP. Each constrained search included 100
414 replicate TBR searches with no more than five trees
415 retained per search. Decay indices for trees obtained
416 after SACW were derived using the same character
417 weights used in the final round of searches.

418 Brown and Freitas (1994) suggested that immature
419 stage characters might provide particularly important
420 support to more basal nodes, a common viewpoint in
421 Lepidoptera phylogenetic studies that we wished to
422 test (e.g., Kitching, 1984, 1985; Harvey, 1991; Tyler
423 et al., 1994; Parsons, 1996). Our null expectation is
424 that for a given node the ratios of PBS values between
425 data partitions will be the same as the ratio of
426 characters between data partitions. We therefore
427 identify those nodes that have an immature stage
428 PBS value exceeding this expected value as “strongly
429 supported” by immature stage characters. We assigned
430 each node a score based on the nodal distance to the
431 base of the tree, with the basal node scored 0, and
432 calculated the average base-node distance of nodes
433 strongly supported by immature stage characters (for
434 $n = N_{\text{imm}}$ nodes). To determine whether this average
435 distance was lower than expected by chance (i.e.,
436 nodes tend to be more basal) we obtained a null
437 distribution of averages by generating 500 random
438 samples of N_{imm} nodes from the empirical base-node
439 distance values. The proportion of null averages that
440 are lower than the observed average provides an
441 estimate of the probability that nodes supported by
442 immature stage characters are nearer the base of the
443 tree than expected by chance alone. Random samples
444 of base-node distances were generated in Microsoft
445 Excel 2003 by pairing the column of empirical base-
446 node values with a column of random numbers (“=
447 RAND()”), then reordering both columns by the
448 random number column. The first N_{imm} base-node
449 distances were then used to calculate a null average
450 base-node distance for N_{imm} nodes. This process was
451 repeated 500 times by recording the initial series of
452 actions (reordering the empirical values and calcula-

ting the average of the first N_{imm} base-node distances) 453
in a macro and replicating the macro text 500 times. 454

Character changes were examined using ACCTRAN 455
optimization and are given for major clades in Table 2. 456

Evolution of hostplant choice 457

We examined the evolution of hostplant choice in the 458
Ithomiinae by optimization of hostplant character states 459
on to a generic-level cladogram (reduced from our 460
preferred species-level cladogram). Within genera there 461
is little evidence, to date, of major differences in 462
hostplant clades between species groups, so examining 463
broad patterns at the generic level is sensible. Hostplant 464
was coded as a single multistate character with states 465
representing major plant clades based on phylogenies 466
presented by Olmstead et al. (1999). Plant clades were 467
arbitrarily defined to represent the smallest clades 468
utilized by any single ithomiine genus, and are members 469
of distinct tribes (or higher taxa) in all cases except 470
Lycianthes and *Capsicum*. Although *Lycianthes* and 471
Capsicum form a clade, because *Napeogenes* feed only 472
on *Lycianthes* the two genera were kept distinct. 473
Hostplant records for Ithomiinae were compiled from 474
Drummond and Brown (1987), Brown and Freitas 475
(1994), Beccaloni (1997b), Haber (2001), Willmott and 476
Mallet (2004), Janzen and Hallwachs (2005) and AVLF 477
(unpublished data), and are summarized in Table 3. 478

Ithomiines were coded for hostplant usage in two 479
ways, first with each genus (or species, if genus 480
polyphyletic) being coded as polymorphic including all 481
known records of plant clades (Char H1, end of 482
Appendix 1), and secondly as monomorphic for only 483
the dominant plant clade (Char H2, end of Appendix 1). 484
Velamysta has only two host records, one on *Lycianthes* 485
and one on *Cuatresia* (*Withania* + *Physalis* + *Iocho-* 486
ma clade), and so was coded polymorphic in both cases. 487
Character coding for each genus/terminal taxon is given 488
in Table 3. Character states were optimized with maxi- 489
mum parsimony using ACCTRAN in MacClade 3.05 490
(Maddison and Maddison, 1995) on to a generic-level 491
cladogram reduced from the consensus tree resulting 492
from successive approximations weighting of the entire 493
matrix. 494

Results 495

Characters 496

A total of 353 characters (306 informative, 45 497
uninformative, two constant) were coded (Appendix 498
1), including 75 from the immature stages (ecology: 499
eight; egg: five; first instar: four; last instar: 36; pupa: 22) 500
and 278 from adult stages (ecology and chemistry: six; 501
body: 27; venation: 37; wing scales and androconia: 56; 502

Table 2
Clades, synapomorphies and autapomorphies. Note: Synapomorphies are given for genera with more than one species analyzed. Current generic synonyms and revised tribes in parentheses

Clade no.	Clade name	Unambiguous synapomorphies ¹	Ambiguous synapomorphies ²
1	Ithomiinae	23:0, 67:0, 70:1, 84:0, 86:0, 90:0, 93:0, 94:0, 95:0, 96:0, 97:0, 107:1, 114:1, 135:0, 143:0, 146:0, 148:0, 156:1 , 205:0, 266:0, 270:0, 282:0, 292:0, 298:0, 319:0, 323:0, 329:1, 338:0 49:1, 261:1, 9:1, 22:1, 54:0, 55:1 , 56:0, 59:1, 90:1, 91:1, 93:3, 95:6 , 96:5, 97:7 , 99:1, 105:1 , 114:2, 121:1, 140:1, 147:1, 154:1, 169:1, 227:1, 230:1 , 240:2, 242:1 , 246:1 , 278:5, 295:5, 297:1 , 298:1, 299:1 , 326:1, 341:3 65:4, 68:2, 73:1, 161:1, 167:1(m) , 170:1, 180:0, 307:2 34:2 , 50:1, 75:0, 76:1, 90:3, 144:1, 184:2 , 193:1 , 249:1, 278:3 , 285:1, 308:1, 311:2, 331:1 103:0, 107:0, 109:1, 264:1, 276:1 4:1, 61:1, 76:1, 78:1, 331:1	11:1, 34:0, 60:0, 88:0, 115:0, 250:0, 284:0 39:1, 58:1, 100:2, 179:2, 286:1, 88:1, 101:0, 115:2, 164:0, 284:2, 304:1, 317:1, 319:1
2	<i>Methona</i> , Methonini	95:6, 96:5, 97:7 , 99:1, 105:1 , 114:2, 121:1, 140:1, 147:1, 154:1, 169:1, 227:1, 230:1 , 240:2, 242:1 , 246:1 , 278:5, 295:5, 297:1 , 298:1, 299:1 , 326:1, 341:3 65:4, 68:2, 73:1, 161:1, 167:1(m) , 170:1, 180:0, 307:2 34:2 , 50:1, 75:0, 76:1, 90:3, 144:1, 184:2 , 193:1 , 249:1, 278:3 , 285:1, 308:1, 311:2, 331:1 103:0, 107:0, 109:1, 264:1, 276:1 4:1, 61:1, 76:1, 78:1, 331:1	11:0, 62:1, 79:1, 153:2 , 159:2, 254:1 58:0, 115:3, 179:1
3	Tithoreini <i>Aeria</i>	17:1, 124:1, 153:3(s) , 154:1, 167:3 97:2, 159:2, 284:1, 350:1 , 352:1 4:0, 96:6 , 121:1, 135:1, 143:1, 171:1 , 227:1, 241:2, 251:3 , 253:1, 312:1, 315:2, 319:2 , 351:1, 353:1 87:1 , 91:2, 120:0, 208:1	17:1, 81:1 , 86:1, 95:1, 100:0, 153:4 , 172:2, 183:2 34:3, 40:1, 62:1, 63:3, 79:1, 119:1, 122:1, 177:1, 183:3, 250:1, 254:1, 284:5, 317:1 25:2, 39:1, 58:1, 118:1, 146:1 , 158:1, 172:2, 191:1, 194:1, 326:1 6:1, 51:1, 88:1, 172:3, 250:2 158:0, 191:0, 194:0, 254:0
4	<i>Tithorea</i> + <i>Elzunia</i>	17:1, 124:1, 153:3(s) , 154:1, 167:3 97:2, 159:2, 284:1, 350:1 , 352:1 4:0, 96:6 , 121:1, 135:1, 143:1, 171:1 , 227:1, 241:2, 251:3 , 253:1, 312:1, 315:2, 319:2 , 351:1, 353:1 87:1 , 91:2, 120:0, 208:1	11:0, 62:1, 79:1, 153:2 , 159:2, 254:1 58:0, 115:3, 179:1
5	<i>Melinaeini</i>	17:1, 124:1, 153:3(s) , 154:1, 167:3 97:2, 159:2, 284:1, 350:1 , 352:1 4:0, 96:6 , 121:1, 135:1, 143:1, 171:1 , 227:1, 241:2, 251:3 , 253:1, 312:1, 315:2, 319:2 , 351:1, 353:1 87:1 , 91:2, 120:0, 208:1	17:1, 81:1 , 86:1, 95:1, 100:0, 153:4 , 172:2, 183:2 34:3, 40:1, 62:1, 63:3, 79:1, 119:1, 122:1, 177:1, 183:3, 250:1, 254:1, 284:5, 317:1 25:2, 39:1, 58:1, 118:1, 146:1 , 158:1, 172:2, 191:1, 194:1, 326:1 6:1, 51:1, 88:1, 172:3, 250:2 158:0, 191:0, 194:0, 254:0
6	<i>Paititia</i> + <i>Olyras</i>	17:1, 124:1, 153:3(s) , 154:1, 167:3 97:2, 159:2, 284:1, 350:1 , 352:1 4:0, 96:6 , 121:1, 135:1, 143:1, 171:1 , 227:1, 241:2, 251:3 , 253:1, 312:1, 315:2, 319:2 , 351:1, 353:1 87:1 , 91:2, 120:0, 208:1	17:1, 81:1 , 86:1, 95:1, 100:0, 153:4 , 172:2, 183:2 34:3, 40:1, 62:1, 63:3, 79:1, 119:1, 122:1, 177:1, 183:3, 250:1, 254:1, 284:5, 317:1 25:2, 39:1, 58:1, 118:1, 146:1 , 158:1, 172:2, 191:1, 194:1, 326:1 6:1, 51:1, 88:1, 172:3, 250:2 158:0, 191:0, 194:0, 254:0
7	<i>Athyrtis</i> + <i>Melinaea</i>	17:1, 124:1, 153:3(s) , 154:1, 167:3 97:2, 159:2, 284:1, 350:1 , 352:1 4:0, 96:6 , 121:1, 135:1, 143:1, 171:1 , 227:1, 241:2, 251:3 , 253:1, 312:1, 315:2, 319:2 , 351:1, 353:1 87:1 , 91:2, 120:0, 208:1	11:0, 62:1, 79:1, 153:2 , 159:2, 254:1 58:0, 115:3, 179:1
8	<i>Melinaea</i>	17:1, 124:1, 153:3(s) , 154:1, 167:3 97:2, 159:2, 284:1, 350:1 , 352:1 4:0, 96:6 , 121:1, 135:1, 143:1, 171:1 , 227:1, 241:2, 251:3 , 253:1, 312:1, 315:2, 319:2 , 351:1, 353:1 87:1 , 91:2, 120:0, 208:1	11:0, 62:1, 79:1, 153:2 , 159:2, 254:1 58:0, 115:3, 179:1
9	<i>Melinaea</i>	17:1, 124:1, 153:3(s) , 154:1, 167:3 97:2, 159:2, 284:1, 350:1 , 352:1 4:0, 96:6 , 121:1, 135:1, 143:1, 171:1 , 227:1, 241:2, 251:3 , 253:1, 312:1, 315:2, 319:2 , 351:1, 353:1 87:1 , 91:2, 120:0, 208:1	11:0, 62:1, 79:1, 153:2 , 159:2, 254:1 58:0, 115:3, 179:1
10	<i>Melinaea</i>	17:1, 124:1, 153:3(s) , 154:1, 167:3 97:2, 159:2, 284:1, 350:1 , 352:1 4:0, 96:6 , 121:1, 135:1, 143:1, 171:1 , 227:1, 241:2, 251:3 , 253:1, 312:1, 315:2, 319:2 , 351:1, 353:1 87:1 , 91:2, 120:0, 208:1	11:0, 62:1, 79:1, 153:2 , 159:2, 254:1 58:0, 115:3, 179:1
11	<i>Athesis</i> + <i>Patricia</i>	17:1, 124:1, 153:3(s) , 154:1, 167:3 97:2, 159:2, 284:1, 350:1 , 352:1 4:0, 96:6 , 121:1, 135:1, 143:1, 171:1 , 227:1, 241:2, 251:3 , 253:1, 312:1, 315:2, 319:2 , 351:1, 353:1 87:1 , 91:2, 120:0, 208:1	11:0, 62:1, 79:1, 153:2 , 159:2, 254:1 58:0, 115:3, 179:1
12	<i>Mechanitiini</i>	17:1, 124:1, 153:3(s) , 154:1, 167:3 97:2, 159:2, 284:1, 350:1 , 352:1 4:0, 96:6 , 121:1, 135:1, 143:1, 171:1 , 227:1, 241:2, 251:3 , 253:1, 312:1, 315:2, 319:2 , 351:1, 353:1 87:1 , 91:2, 120:0, 208:1	11:0, 62:1, 79:1, 153:2 , 159:2, 254:1 58:0, 115:3, 179:1
13	<i>Sais</i> + <i>Scada</i>	17:1, 124:1, 153:3(s) , 154:1, 167:3 97:2, 159:2, 284:1, 350:1 , 352:1 4:0, 96:6 , 121:1, 135:1, 143:1, 171:1 , 227:1, 241:2, 251:3 , 253:1, 312:1, 315:2, 319:2 , 351:1, 353:1 87:1 , 91:2, 120:0, 208:1	11:0, 62:1, 79:1, 153:2 , 159:2, 254:1 58:0, 115:3, 179:1
14	<i>Scada</i>	17:1, 124:1, 153:3(s) , 154:1, 167:3 97:2, 159:2, 284:1, 350:1 , 352:1 4:0, 96:6 , 121:1, 135:1, 143:1, 171:1 , 227:1, 241:2, 251:3 , 253:1, 312:1, 315:2, 319:2 , 351:1, 353:1 87:1 , 91:2, 120:0, 208:1	11:0, 62:1, 79:1, 153:2 , 159:2, 254:1 58:0, 115:3, 179:1
15	<i>Forbestra</i> + <i>Mechanitis</i> <i>Forbestra</i> <i>Mechanitis</i>	17:1, 124:1, 153:3(s) , 154:1, 167:3 97:2, 159:2, 284:1, 350:1 , 352:1 4:0, 96:6 , 121:1, 135:1, 143:1, 171:1 , 227:1, 241:2, 251:3 , 253:1, 312:1, 315:2, 319:2 , 351:1, 353:1 87:1 , 91:2, 120:0, 208:1	11:0, 62:1, 79:1, 153:2 , 159:2, 254:1 58:0, 115:3, 179:1
16	<i>Forbestra</i> + <i>Mechanitis</i> <i>Forbestra</i> <i>Mechanitis</i>	17:1, 124:1, 153:3(s) , 154:1, 167:3 97:2, 159:2, 284:1, 350:1 , 352:1 4:0, 96:6 , 121:1, 135:1, 143:1, 171:1 , 227:1, 241:2, 251:3 , 253:1, 312:1, 315:2, 319:2 , 351:1, 353:1 87:1 , 91:2, 120:0, 208:1	11:0, 62:1, 79:1, 153:2 , 159:2, 254:1 58:0, 115:3, 179:1
17	<i>Mechanitiini</i>	17:1, 124:1, 153:3(s) , 154:1, 167:3 97:2, 159:2, 284:1, 350:1 , 352:1 4:0, 96:6 , 121:1, 135:1, 143:1, 171:1 , 227:1, 241:2, 251:3 , 253:1, 312:1, 315:2, 319:2 , 351:1, 353:1 87:1 , 91:2, 120:0, 208:1	11:0, 62:1, 79:1, 153:2 , 159:2, 254:1 58:0, 115:3, 179:1
18	<i>Sais</i> + <i>Scada</i> <i>Scada</i>	17:1, 124:1, 153:3(s) , 154:1, 167:3 97:2, 159:2, 284:1, 350:1 , 352:1 4:0, 96:6 , 121:1, 135:1, 143:1, 171:1 , 227:1, 241:2, 251:3 , 253:1, 312:1, 315:2, 319:2 , 351:1, 353:1 87:1 , 91:2, 120:0, 208:1	11:0, 62:1, 79:1, 153:2 , 159:2, 254:1 58:0, 115:3, 179:1
19	<i>Forbestra</i> + <i>Mechanitis</i> <i>Forbestra</i> <i>Mechanitis</i>	17:1, 124:1, 153:3(s) , 154:1, 167:3 97:2, 159:2, 284:1, 350:1 , 352:1 4:0, 96:6 , 121:1, 135:1, 143:1, 171:1 , 227:1, 241:2, 251:3 , 253:1, 312:1, 315:2, 319:2 , 351:1, 353:1 87:1 , 91:2, 120:0, 208:1	11:0, 62:1, 79:1, 153:2 , 159:2, 254:1 58:0, 115:3, 179:1
20	<i>Placidina</i> + <i>Pagyris</i> <i>Pagyris</i> <i>Ithonia</i>	17:1, 124:1, 153:3(s) , 154:1, 167:3 97:2, 159:2, 284:1, 350:1 , 352:1 4:0, 96:6 , 121:1, 135:1, 143:1, 171:1 , 227:1, 241:2, 251:3 , 253:1, 312:1, 315:2, 319:2 , 351:1, 353:1 87:1 , 91:2, 120:0, 208:1	11:0, 62:1, 79:1, 153:2 , 159:2, 254:1 58:0, 115:3, 179:1
21	<i>Napeogenini</i>	17:1, 124:1, 153:3(s) , 154:1, 167:3 97:2, 159:2, 284:1, 350:1 , 352:1 4:0, 96:6 , 121:1, 135:1, 143:1, 171:1 , 227:1, 241:2, 251:3 , 253:1, 312:1, 315:2, 319:2 , 351:1, 353:1 87:1 , 91:2, 120:0, 208:1	11:0, 62:1, 79:1, 153:2 , 159:2, 254:1 58:0, 115:3, 179:1
22	<i>Aremfoxia</i> + <i>Epityches</i>	17:1, 124:1, 153:3(s) , 154:1, 167:3 97:2, 159:2, 284:1, 350:1 , 352:1 4:0, 96:6 , 121:1, 135:1, 143:1, 171:1 , 227:1, 241:2, 251:3 , 253:1, 312:1, 315:2, 319:2 , 351:1, 353:1 87:1 , 91:2, 120:0, 208:1	11:0, 62:1, 79:1, 153:2 , 159:2, 254:1 58:0, 115:3, 179:1
23	<i>Napeogenes</i>	17:1, 124:1, 153:3(s) , 154:1, 167:3 97:2, 159:2, 284:1, 350:1 , 352:1 4:0, 96:6 , 121:1, 135:1, 143:1, 171:1 , 227:1, 241:2, 251:3 , 253:1, 312:1, 315:2, 319:2 , 351:1, 353:1 87:1 , 91:2, 120:0, 208:1	11:0, 62:1, 79:1, 153:2 , 159:2, 254:1 58:0, 115:3, 179:1
24	<i>Napeogenes</i>	17:1, 124:1, 153:3(s) , 154:1, 167:3 97:2, 159:2, 284:1, 350:1 , 352:1 4:0, 96:6 , 121:1, 135:1, 143:1, 171:1 , 227:1, 241:2, 251:3 , 253:1, 312:1, 315:2, 319:2 , 351:1, 353:1 87:1 , 91:2, 120:0, 208:1	11:0, 62:1, 79:1, 153:2 , 159:2, 254:1 58:0, 115:3, 179:1

Table 2
Continued

Clade no.	Clade name	Unambiguous synapomorphies ¹	Ambiguous synapomorphies ¹
25	<i>Hyaliris</i>	90:2, 124:1, 239:1, 246:2, 323:1 86:1, 88:2, 240:2	66:2, 143:0 65:2, 66:2, 70:0, 74:1, 109:1, 164:2, 184:1, 222:0, 254:0, 284:1
26	Olerini	75:0, 88:1, 183:1, 227:1, 253:1, 283:1	67:1, 79:0, 80:0, 121:1, 169:0, 294:1
27	<i>Megoleria</i> + <i>Hyposcada</i>	3:1, 63:1(ms) , 83:1, 92:1, 247:1, 282:1	64:1, 73:2, 114:1, 118:0, 119:0, 243:2, 279:1, 320:2
28	<i>Hyposcada</i>	11:2(m) , 250:0 251:2, 278:5	18:1, 226:1, 294:0, 308:0
29	<i>Oleria</i>	40:0, 61:0, 91:2, 244:1, 262:1, 281:1 , 293:1, 329:0, 338:0	54:1, 65:0, 66:1, 68:0, 90:0
30	(<i>Ollantaya</i>)	300:1	19:0, 20:0, 79:1, 120:0, 173:2, 334:1
31		18:1, 287:1	59:1, 67:0, 177:0, 241:2
32		17:5, 41:1, 46:0, 117:0, 125:1, 153:5 , 154:2 , 248:2, 251:2, 278:5, 288:7, 300:2, 326:1, 327:1	32:0, 35:0, 60:0, 177:0, 180:0, 268:1, 284:3, 308:0
	<i>Callithomia</i>	88:3, 93:5, 118:2, 119:2, 140:2, 216:2 , 223:5 , 231:1 , 240:0, 241:3, 257:4 , 270:1, 305:2 , 341:1, 344:1	20:0, 30:1, 35:1, 42:1, 43:1, 58:1, 64:1, 65:4, 66:0, 70:1, 74:0, 78:0, 90:2, 109:0, 143:1, 164:1, 187:1
33	Dircennini (excl. <i>Callithomia</i>)	12:1, 16:1, 18:1, 33:0, 51:2, 63:2, 338:8	3:3, 59:1, 68:0, 122:0, 243:2, 345:1
34	<i>Hyalenna</i> +	115:1, 183:0	92:1, 204:1, 225:4, 266:1, 267:1
35	<i>Dircenna</i>	5:1, 8:1, 21:1, 45:1(m) , 53:1(m) , 57:1, 58:1,	90:0, 110:1, 172:2, 227:0, 345:0
	<i>Dircenna</i> ss	93:1, 102:1, 141:1, 164:0, 185:1	90:1, 92:0, 110:0, 122:1, 266:0, 267:0, 268:0
36		125:0, 169:0, 236:1 , 244:1, 270:1, 307:2, 338:4 , 352:1	38:2, 64:1, 122:1, 125:0, 126:1, 169:0, 184:3, 187:1, 307:2, 338:3
37	<i>Episcada</i> , in part	36:0, 37:0, 61:0, 66:1, 176:1, 219:2, 223:2, 244:1, 333:1	92:0, 115:3, 122:2, 266:0, 267:0, 268:0, 339:1
38	<i>Episcada</i> , in part + <i>Ceratinia</i>	226:1, 270:2, 340:1	180:1, 224:2
39	(<i>Ceratiscada</i>)	112:1, 163:1 , 183:1	56:0, 84:1, 109:0, 184:0
	<i>Ceratinia</i>	88:3, 121:1	
	<i>Huenschia</i> + <i>Pteronymia</i>	91:2	
40		16:0, 35:1, 114:1, 140:2, 141:1	5:1, 39:1, 41:0, 56:1, 122:1
	<i>Pteronymia</i>	269:2(s)	16:0, 35:1, 42:1, 48:1(m) , 68:2, 204:0
41	Godyridini	128:1, 179:0, 212:1, 288:1	
		119:0, 144:1, 161:1, 167:2(m) , 179:0, 288:9	17:4, 65:1, 73:5, 79:0, 118:0, 140:3, 170:1, 180:1, 240:2, 241:2, 268:0, 304:1, 352:2
42		217:2 , 223:2, 225:5, 323:2	307:2
43		37:0, 186:1, 187:2, 284:4, 289:1, 291:1, 305:1	42:1, 57:1, 131:1, 140:1, 345:0, 352:0
		94:1, 115:3, 128:1, 134:1 , 144:2, 164:1, 165:1 ,	304:2
	<i>Heterosais</i>	180:0, 195:1, 206:1 , 219:2, 226:1, 227:3, 294:1, 334:2	
		41:0, 66:0, 133:1 , 179:1	
44	<i>Godyris</i> (excl. <i>G. mantura</i>)	1:1(m) , 79:1, 119:1, 130:1, 161:0, 237:1 , 244:1	38:1, 57:2, 140:2, 170:0, 307:0, 338:0
45		216:1 , 220:1 , 225:0, 227:2, 247:1, 284:3, 343:1 , 344:1	67:1, 70:1, 93:1, 102:1, 114:1, 141:1, 210:1, 224:3, 345:1
46		122:1, 172:3 , 174:1, 187:0, 210:1	38:5, 57:1, 304:2
47	<i>Meclungia</i> + <i>Brevioleria</i>	177:1, 243:1, 248:0	66:1, 131:0, 161:0 170:1
	<i>Brevioleria</i>	164:0, 168:2, 173:2, 294:2, 334:1	3:0, 12:0, 16:0, 37:1
48	<i>Greta diaphanus</i> + <i>morgane</i>	12:0, 16:0, 37:1, 41:1, 66:2, 94:4, 115:3, 144:0, 244:1, 272:1	57:0, 90:0, 131:0, 145:1, 177:2, 183:4, 226:1, 252:2, 275:1, 277:1
49		161:0, 169:1, 187:0, 225:0, 284:5, 294:1, 327:0	126:1, 170:0, 304:0, 326:0, 341:2
50		92:1, 132:1, 137:1, 140:1, 180:0, 223:2, 227:2, 258:1 , 338:8	59:0, 298:1, 307:0
	<i>Pseudoscada</i>	67:1, 71:1, 126:1, 162:1, 173:0, 187:0, 227:3, 334:0, 336:1 , 338:9 94:0	60:1, 298:0 17:4, 38:1, 42:2, 59:1, 66:0, 85:1, 145:0

¹Bold type indicates a unique synapomorphy for members of a clade, where for some species within clade: (m) = missing character information; (n) = nonapplicable character; (s) = some species with different derived character state.

Table 3
Continued

		Plant clade and character state										Charac- ter			
Subfamily	Tribe	Genus	Apocynaceae (state 0)	Gesneriaceae (state 1)	<i>Brumfalsia</i> (state 2)	<i>Cestrum</i> clade (state 3)	<i>Nicantra</i> clade (state 4)	<i>Datura</i> clade (state 5)	<i>Solanum</i> clade (state 6)	<i>Solandra</i> clade (state 7)	<i>Capsicum</i> <i>Capsicum</i> (state 8)	<i>Lycianthes</i> <i>Lycianthes</i> (state 9)	<i>Withania</i> + <i>Iochroma</i> + <i>Physalis</i> clades (state A)	H1	H2
Godryidini		<i>Brevioleria</i>	2						1					3	3
Godryidini		<i>Hypoleria</i>	5						1					36	3
Godryidini		<i>Greta</i>	6						1					369	3
Godryidini		<i>Pseudoscada</i>	41						6					36	3

male abdomen and genitalia: 105; female abdomen and genitalia: 45; wing pattern: 2). Fourteen characters were continuous. 503
504
505

Total evidence analysis with equal weighting 506

In the equally weighted search including all characters and taxa, the initial search found 707 trees of length 1828 steps, while the subsequent search increased the number of MPTs to 1716, also of 1828 steps (CI = 0.32, RI = 0.73) The strict consensus of these trees is shown in Fig. 3. The majority of nodes had bootstrap support > 50%, with Bremer support as high as 13 (*Callithomia*), 18 (*Scada*) and 22 (*Methona*). Partitioned Bremer support indicated substantial conflict between the two data partitions (immature and adult stage), with only 16 of the 69 resolved nodes (23%) having positive support for both partitions. 507
508
509
510
511
512
513
514
515
516
517
518

Five of the eight currently recognized tribes (Lamas, 2004) were recovered as monophyletic, with the status of Mechanitini and Melinaeini unresolved and Dircennini paraphyletic, at least. The basal node is a polytomy of eight clades, resulting from five distinct topologies summarized with a representative genus from each clade in Fig. 4(A). In all trees a single clade is sister to remaining clades, either *Tithorea* (*Tithorea* + *Elzunia* + *Aeria*) one tree or *Methona* (four trees). Trees 3–5 are identical except in the placement of *Athesis* (*Athesis* + *Patricia*). In all cases neither Mechanitini or Melinaeini was monophyletic, and in four of the five trees their representative clades are far removed from one another. 519
520
521
522
523
524
525
526
527
528
529
530
531
532

The tribe Dircennini was paraphyletic, with *Callithomia* sister to a clade containing Godryidini and remaining Dircennini. The basal node of the latter clade was a polytomy of nine branches, resulting from 11 distinct topologies. In five of these topologies, members of the Dircennini form a clade sister to Godryidini. The remaining six consist of three basic topologies, summarized in Fig. 4(B), with the three unfigured topologies being similar to 1 with alternative topologies in the *Dircenna* + *Hyalenna* + *Haenschia* clade. 533
534
535
536
537
538
539
540
541
542

Total evidence analysis with successive approximations character weighting 543
544

A single round of SACW reduced the number of MPTs to a single tree, and tree length stabilized at 600 steps after a further round of weighting (CI = 0.51, RI = 0.81) (Fig. 5). Branches were relatively well supported, with 81 branches having a bootstrap value > 50% (average 81%), and Bremer support as high as 12.6 (*Methona*). Conflict between the immature stage and adult stage data sets was reduced substantially by SACW, with 61 of the 103 nodes (69%) having no conflict in partitioned Bremer support values (both 545
546
547
548
549
550
551
552
553
554

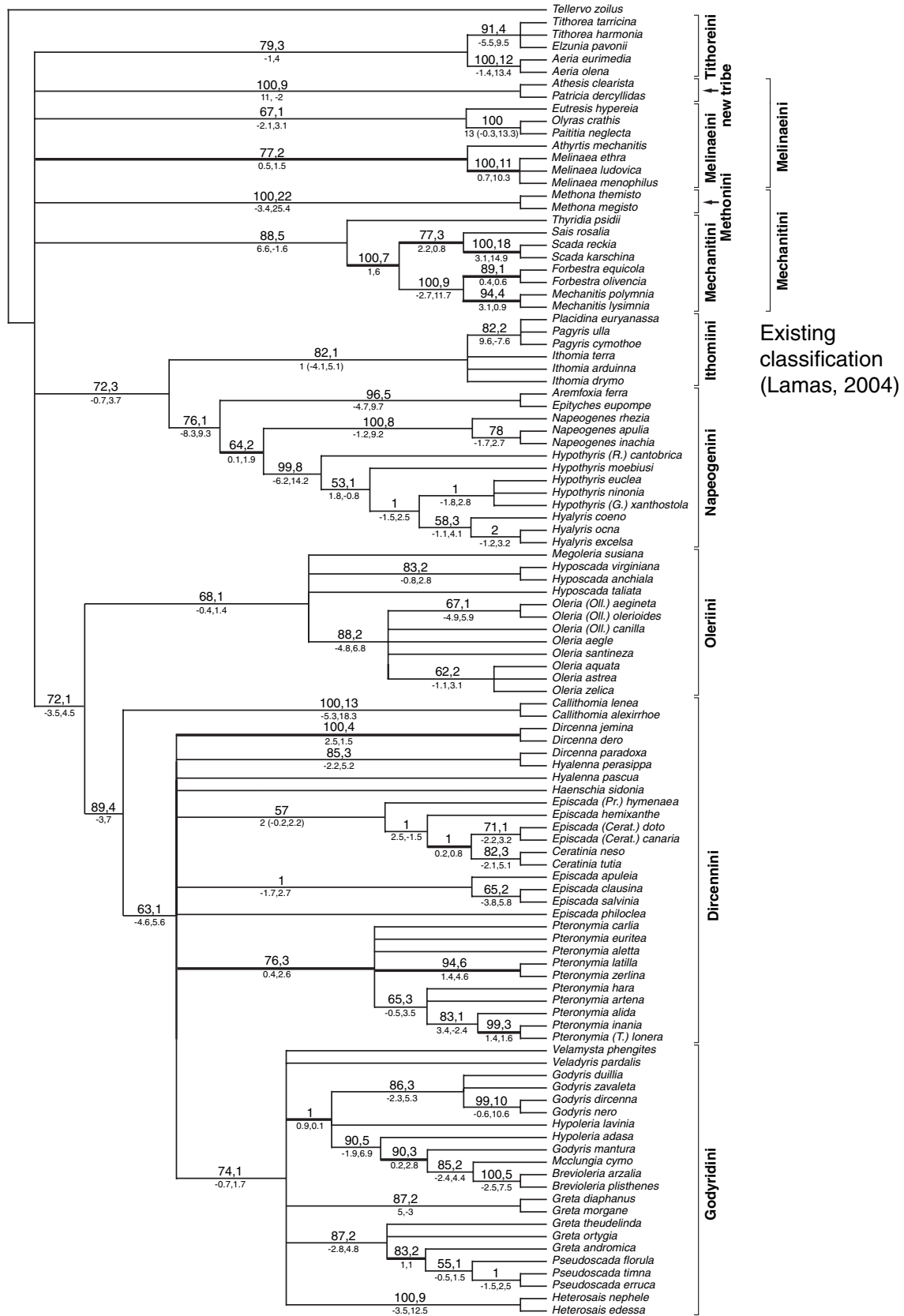


Fig. 3. Strict consensus of 1716 most parsimonious trees (length 1828, CI 0.32) for complete data matrix with 353 equally weighted characters. Bootstrap and Bremer support values above branches, partitioned Bremer support below (immature stages, chars 1–75, ecology and adult, chars 76–353). Branches in bold have positive Bremer support for both data partitions.

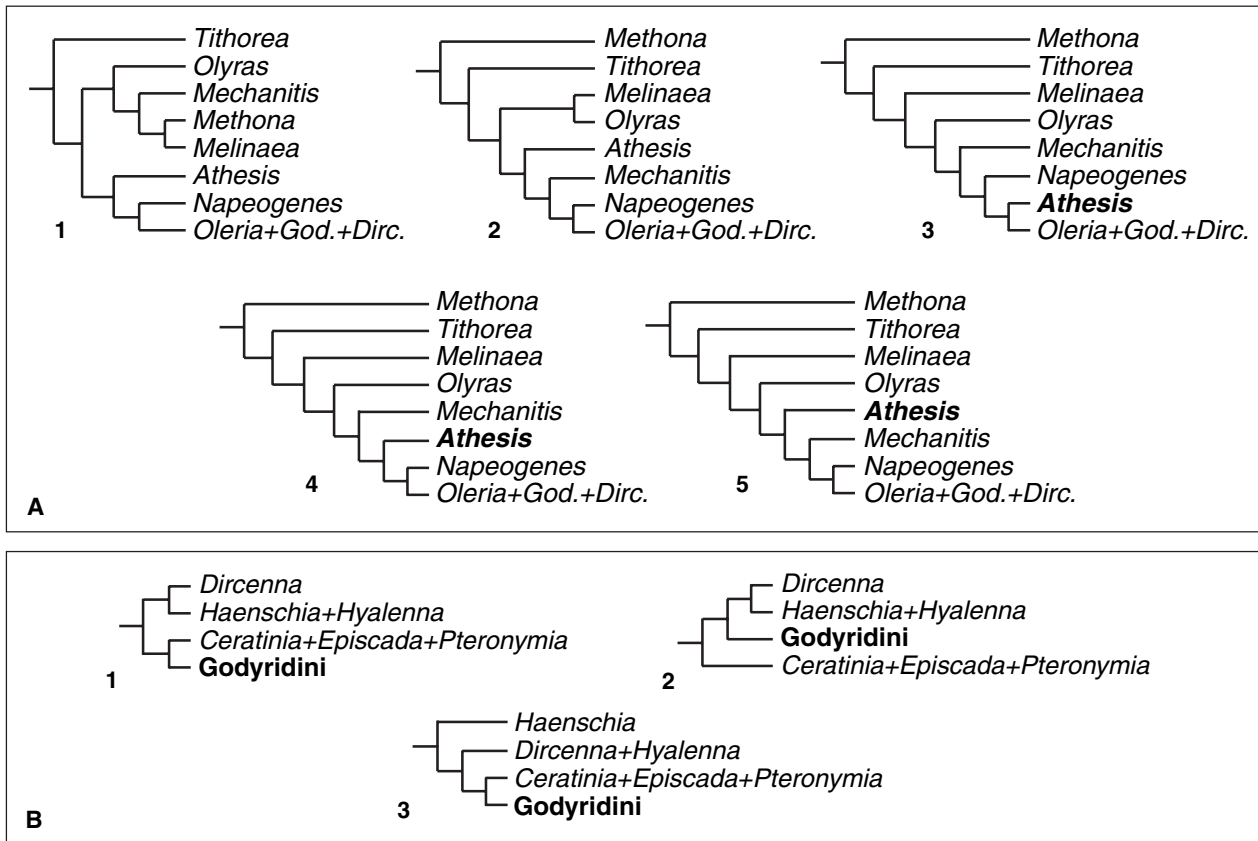


Fig. 4. Alternative tree topologies collapsed in consensus trees. (A) Alternative reduced MPTs from equally weighted analysis of all characters (Fig. 3), tribal level. (B) Alternative reduced MPTs from equally weighted analysis of all characters (Fig. 3), within Dircennini + Godyridini only, excluding *Callithomia*.

partitions were positive, or one of the partitions was zero). Notably, poorly supported parts of the tree include the relationships between clade 17 and remaining tribal-level clades, between species in *Episcada* and *Ceratinia*, and between most of the Godyridini genera.

Much of the topology is similar to that of the equally weighted analysis, with the same five tribes monophyletic and Mechanitini, Melinaeini and Dircennini not monophyletic. However, *Methona* was placed as sister to *Aeria* + *Tithorea*, a topology not found in the equally weighted analysis, and this combined clade (clade 2) was sister to all other ithomiines (clade 5). Within clade 5, *Melinaea*, *Athyrtis*, *Paititia*, *Eutresis* and *Olyras* formed a clade sister to the remaining ithomiines (clade 10), as in some equally weighted trees. Within clade 10, *Athesis* + *Patricia* formed a clade sister to the remaining species (clade 12). Clade 12 consisted of Mechanitini (excluding *Methona*) sister to remaining tribes (clade 17). Clade 17 was similar topologically to the unweighted analysis, but Dircennini excluding

Callithomia formed a clade sister to Godyridini, as in some equally weighted trees.

Partitioned analyses

The analysis of adult characters only (236 informative) found 2610 MPTs of length 1409 (CI = 0.33, RI = 0.74). One round of SACW reduced the number of MPTs to 3, which stabilized at length 483 after an additional round of weighting (CI = 0.52, RI = 0.81). The strict consensus of these three MPTs (Fig. 6A) differs from that from the equally weighted analysis (not shown) mainly in resolving the basal node, which was a polytomy of six clades including *Aeria*, *Tithorea* + *Elzunia*, *Methona*, *Athesis* + *Patricia*, Oleriini + Dircennini + Godyridini and Melinaeini + Mechanitini + Napeogenini.

With only immature stage characters included (70 informative), multiple MPTs of 349 steps (CI = 0.33, RI = 0.78) were found, with the search stopped at 10 000 trees. After SACW the number of MPTs remained above 10 000 (length 118.1 steps, CI = 0.52,

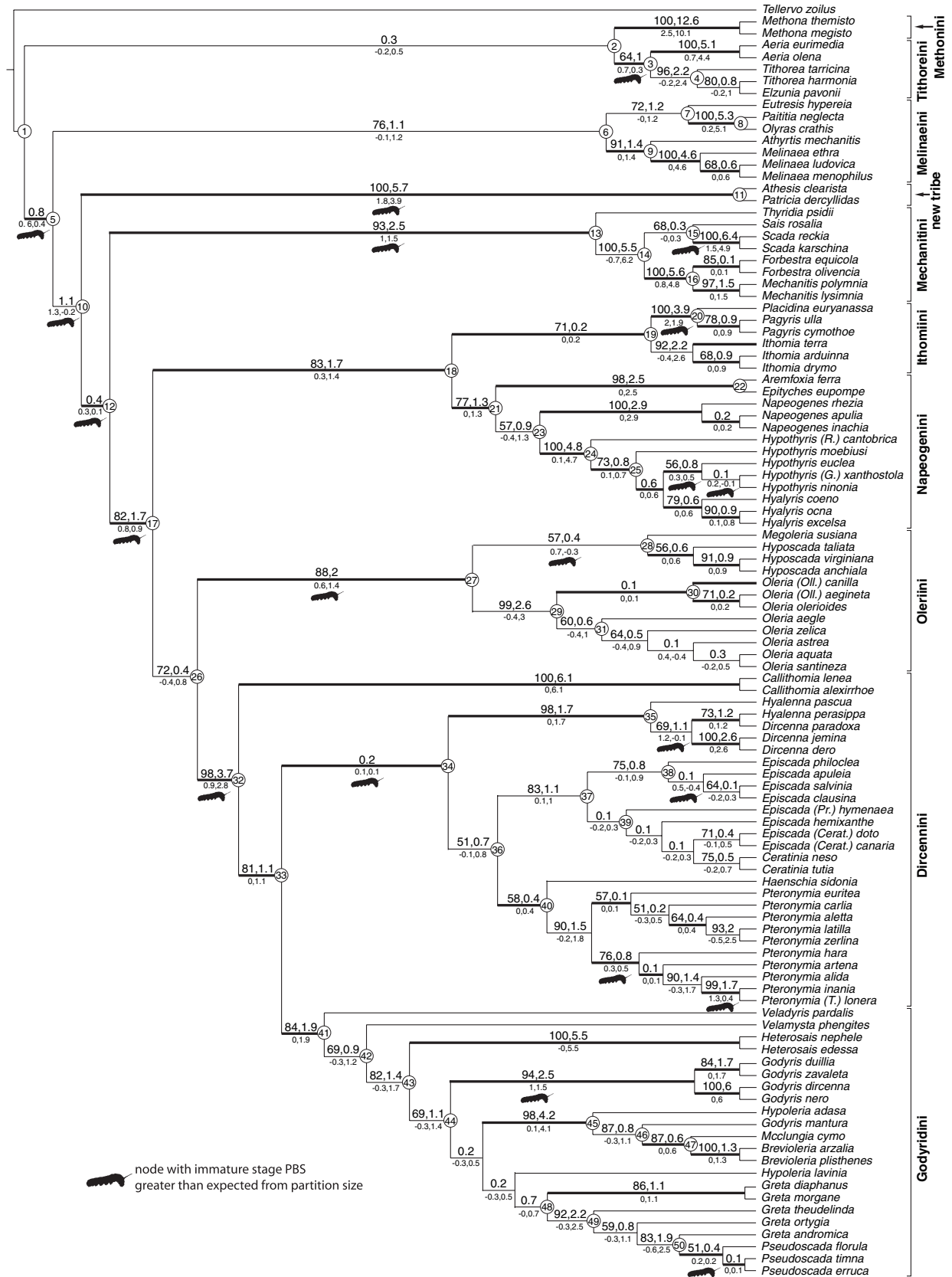


Fig. 5. Single most parsimonious tree (length 600, CI 0.51) for complete data matrix with 353 characters, after successive approximations weighting. Bootstrap and Bremer support values above branches, partitioned Bremer support below (immature stages, chars 1–75, adult, chars 76–353). Branches in bold have non-conflicting partitioned Bremer support values. Nodes discussed in text and Table 2 are numbered.

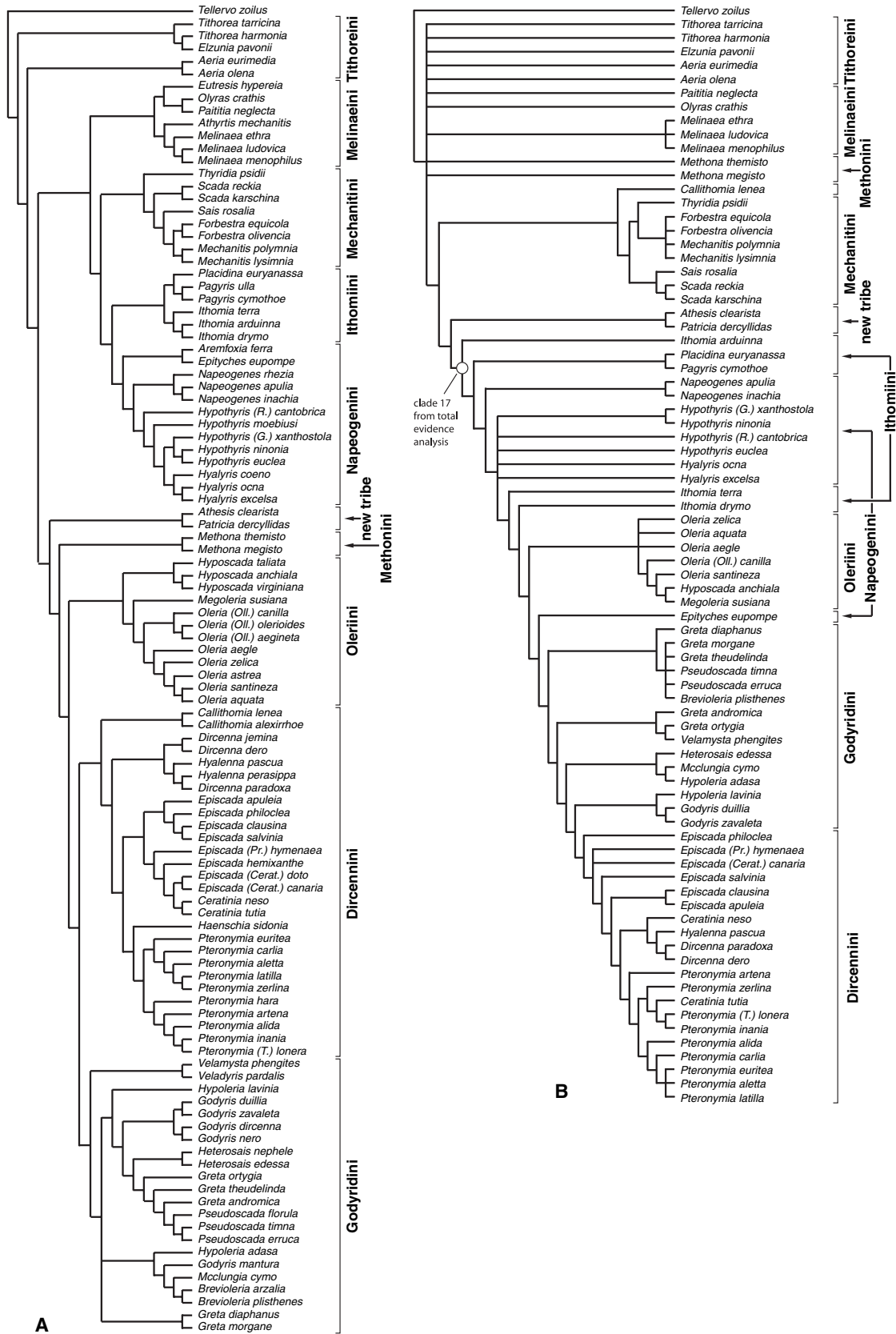


Fig. 6. Strict consensus trees for partitioned character analyses. (A) Strict consensus of three MPTs (length 1857, CI = 0.31) from analysis of 236 informative adult and ecological characters after successive approximations character weighting. (B) Strict consensus of 10 000 MPTs (length 349, CI = 0.33) from analysis of 70 informative characters from immature stages. Taxa without immature stage data excluded.

597 RI = 0.83) with a slight increase in resolution of the
598 strict consensus tree (Fig. 6B), although the basal node
599 remained a polytomy of 11 clades.

600 The adult SACW consensus tree recovered the same
601 tribal level clades as the total evidence SACW
602 consensus tree, with the exception of *Aeria* + *Tithorea*
603 and in placing *Callithomia* with remaining Dircennini,
604 implying Dircennini as currently conceived (Lamas,
605 2004) is monophyletic. In contrast, the immature stage
606 SACW consensus tree recovered only four of the 10
607 tribal level clades found in the total evidence SACW
608 consensus tree. However, the deeper topology of the
609 adult SACW tree differs significantly from the total
610 evidence SACW tree in placing Melinaeini, Mechaniti-
611 ni, Ithomiini and Napeogenini as a single clade.
612 Although relationships between members of these
613 clades are poorly resolved in the immature stage
614 SACW tree, this tree nevertheless has the major clade
615 17 as in the total evidence SACW analysis. Adding
616 immature stage data to adult data therefore had the
617 most significant effect on topology among the more
618 basal nodes.

619 *Homoplasy and distribution of support from partitioned* 620 *data sets*

621 Immature stage characters were more homoplasious
622 than adult stage characters. The average consistency
623 index for informative immature stage characters (1–75)
624 in the total evidence SACW analysis was 0.42, while
625 that for adult characters (76–353) was 0.52. In
626 partitioned analyses, consistency and retention index
627 values for MPTs were similar in the immature and
628 adult data sets, even though the larger adult data
629 matrix would be expected to have lower indices
630 (Sanderson and Donoghue, 1989). In addition, 7%
631 of immature stage character states could not be coded
632 because of missing data; had these characters been
633 known they would almost certainly have introduced
634 additional homoplasy.

635 In the total evidence SACW analysis, 21 nodes had
636 immature stage PBS values higher than expected from
637 the ratio of immature to adult characters in the data
638 matrix, and simple inspection of Fig. 5 suggests that
639 these nodes tend to be more basal. The average
640 number of nodes between the base of the tree and a
641 given node was 9.17 ($n = 103$), the average for nodes
642 supported by higher immature stage PBS values than
643 expected was 7.76 ($n = 21$), and the average for nodes
644 supported by higher adult stage PBS values than
645 expected was 9.52 ($n = 82$). In the simulation analysis,
646 of the 500 random samples of 21 nodes, 13 had
647 average nodal distances of less than 7.76, indicating
648 that immature stage characters tend to support bran-
649 ches nearer the base of the tree than expected by
650 chance alone ($P = 0.026$). However, the distribution

of support across the tree from adult characters did
not differ from null expectations ($P = 0.302$).

Generic monophyly

The majority of currently recognized genera (Lamas,
2004) were found to be monophyletic in the total
evidence SACW analysis. *Tithorea* was paraphyletic
with respect to *Elzunia*, although there was only low,
conflicting Bremer support for this hypothesis.
Hypothyris contained *Hyaliris*, although, again, there
was weak bootstrap and Bremer support for nodes
within the inclusive clade (clade 24). Neither *Hyalenna*
nor *Dircenna* proved to be monophyletic, though both
form a strongly supported clade, with *Hyalenna pascu*
sister to all other *Hyalenna* and *Dircenna* and *Hyalenna*
perasippa sister to *Dircenna paradoxa*. *Episcada* was
paraphyletic with respect to *Ceratinia*, which clustered
E. canaria, *E. doto* and *E. hemixanthe*. Within the
Godyridini, *Godyris* proved to be polyphyletic, with *G.*
mantura forming a very strongly supported clade with
Brevioleria, *Mcclungia* and *Hypoleria adasa*. *Greta* was
paraphyletic with the inclusion of the monophyletic
Pseudoscada, with strong bootstrap and Bremer support
values.

Evolution of hostplant choice

Hostplant records were obtained for 164 ithomiine
species and *c.* 270 plant species, representing
butterfly–plant species interactions (Table 3). Genera
with no confirmed records include *Paititia* (one sp.),
Athyrtis (one sp.), *Sais* (one sp.), *Aremfoxia* (one sp.),
Haenschia (four spp.) and *Veladyris* (one sp.). Although
most ithomiine tribes and genera are polyphagous to
some extent, almost all show a distinct preference for a
particular plant clade (Table 3). Generic polyphagy
typically reflects specific polyphagy (e.g., *Pteronymia*
artena has been recorded on both *Solanum* and *Lycian-*
thes) rather than any finer scale specialization among
species groups. The evolution of hostplant choice is
shown in Fig. 7, representing monomorphic coding of
dominant hostplant clades only (Char H2, Table 3).
Polymorphic coding of all recorded plant clades (Char
H1, Table 3) produced similar results (not shown),
except that the inferred ancestral character state for
Napeogenini + Ithomiini was *Solanum*.

Discussion

Characters

A large amount of new character information was
uncovered during this study. The immature stage data
set of Brown and Freitas (1994) was significantly

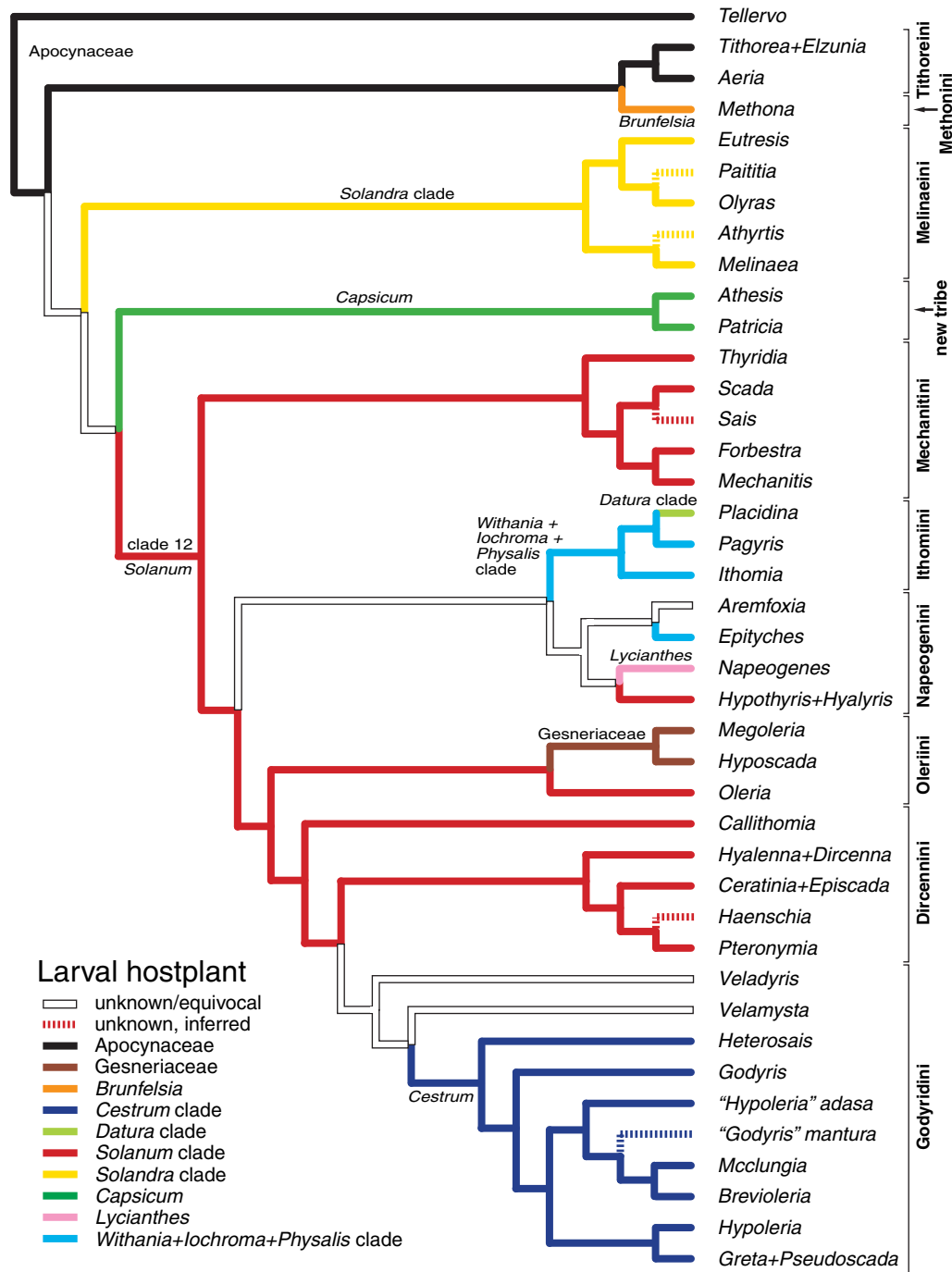


Fig. 7. Optimization of preferred larval hostplant clades on to Ithomiinae generic level tree reduced from the SACW tree.

699 expanded and reevaluated with addition of new life
 700 history information, both for species that had been
 701 partially studied and for those that we formerly had no
 702 knowledge. As in the sister subfamily Danainae (Ackery
 703 and Vane-Wright, 1984), adult morphology also provided
 704 a wealth of characters. Both subfamilies have a rich
 705 diversity of androconial structures (e.g., Danainae,
 706 Boppré and Vane-Wright, 1989), and while these struc-

707 tures are much less elaborate in the Ithomiinae, they still
 708 provided 78 characters, almost all of which have not
 709 been coded previously, with 21 coded through scanning
 710 electron microscopy. Other novel character sources
 711 included body color and scale pattern (11 characters),
 712 the vesica and cornuti (13 characters), and in particular
 713 the female abdomen and genitalia (45 characters), about
 714 which Fox (1956, p. 17) once remarked: ‘There is very

715 little variation in the chitinous female genitalia, and I
716 have made no attempt to analyze them systematically.’
717 It is clear, then, that morphology can continue to
718 provide important new character information even in
719 groups that have been relatively well studied.

720 Despite the comparatively few characters coded from
721 immature stages, there are two lines of evidence that
722 suggest that these characters are especially important for
723 resolving more basal nodes. First, while analyses of
724 adult data alone or combined adult and immature stage
725 data showed little difference in the more terminal clades,
726 there were marked differences among more basal nodes
727 (Figs 5 and 6). Considering the higher homoplasy of
728 immature stage characters this result must be due to
729 relatively strong support for more basal nodes in the
730 immature stage data compared with the adult data,
731 demonstrating that the data sets are complementary.
732 Secondly, partitioned Bremer support suggested that
733 basal nodes tended to be more strongly supported by
734 immature stage data than expected, and the simulation
735 analysis confirms this hypothesis. In the context of a
736 combined evidence analysis therefore immature stages
737 provide particularly strong support for more basal
738 nodes. The time and expense in obtaining life history
739 information is therefore likely to be repaid in phylo-
740 genetic studies alone, as concluded in previous papers
741 using this source of information (Kitching, 1984, 1985;
742 Brown and Freitas, 1994; Freitas and Brown, 2004).

743 *Deep tree topology*

744 The inferred phylogeny from the total evidence
745 analysis after SACW represents our preferred hypo-
746 thesis for ithomiine relationships and forms the basis
747 for the following discussion. The SACW tree was
748 broadly similar to other phylogenetic studies (Brown
749 and Freitas, 1994; Brower et al., 2006), and would
750 have been recognizable even to Doubleday as he
751 prepared his classification of the subfamily over
752 150 years ago (Doubleday, 1847). The subfamily is
753 divisible into two sections: genera placed by Fox in
754 the Tithoreini, Melinaeini and Mechanitini, and the
755 remaining genera, in the Napeogenini, Ithomiini,
756 Oleriini, Dircennini and Godyridini, which form a
757 clade (clade 17). The latter five tribes were also found
758 to form a clade by Brown and Freitas (1994; with the
759 exception of *Placidina*) and by Brower et al. (2006),
760 and are convincingly united by the pale first instar
761 thoracic legs (Char 13:1) and pitchfork-shaped ground
762 scales in transparent wing areas (Char 146:3), among
763 other synapomorphies. Within clade 17 Dircennini and
764 Godyridini form a strongly supported clade, although
765 their sister group is uncertain, with the Oleriini
766 identified in our analysis but Napeogenini by Brower
767 et al. (2006). Brown and Freitas (1994) found a third
768 topology, with Oleriini + Napeogenini + Ithomiini

forming a clade. No unique synapomorphies support
769 Oleriini as sister to Dircennini + Godyridini (clade
770 26), and only a single character is relatively convin-
771 cing, the fusion of the expanded base of the uncus
772 with the appendices angulares (Char 283:1). 773

774 Within the first section the relationships between
775 major clades remains uncertain. Clade 5 is not upheld by
776 any very convincing characters (except possibly a larval
777 shift to Solanaceae—see below) and has weak support,
778 although clade 10 is supported by the loss of body rings
779 in the first instar larva (Char 15:1) and absence of a
780 dorsal black stripe on the 8–9th abdominal segment
781 suture in the last instar larva (Char 72:1). Clade 12
782 excludes *Methona* and all ithomiines placed by Fox in
783 Tithoreini (Fox, 1956), and is also found in analyses of
784 molecular data (Brower et al., 2006). Despite low
785 bootstrap and Bremer support it has several significant
786 apomorphies, including: loss of larval subdorsal fila-
787 ments (Char 22:1, also inferred to be independently lost
788 in *Methona*), gain of a lateral larval stripe (Char 46:1,
789 later lost in clade 32, Dircennini + Godyridini), white
790 to yellow ventral larval color (Char 51:1, changing to
791 51:2 in clade 33) and fused male foreleg tibia and tarsus
792 (Char 100:2, independently fused in *Aeria* and some
793 *Melinaea* and *Methona*).

Tribal classification

795 *Aeria*, *Tithorea* and *Elzunia*, the only ithomiine genera
796 known to feed on Apocynaceae, form a clade (Fig. 5,
797 clade 3), with moderate support from both immature
798 and adult stages, and were treated as the Tithoreini by
799 Lamas (2004). As Apocynaceae are also the larval
800 hostplants of the outgroup *Tellervo*, this association is
801 either a symplesiomorphy or synapomorphy, depending
802 on optimization. Only one character (Char 167:1), the
803 extent of male dorsal hindwing androconial scales, is a
804 unique autapomorphy for Tithoreini, and cannot be
805 assessed in the genus *Elzunia* due to partial loss of these
806 scales. Nevertheless, the monophyly of Tithoreini seems
807 likely and has been corroborated in other studies
808 (Motta, 2003; Brower et al., 2006).

809 The affinities of the small genus *Methona* remain
810 almost as unclear as they have ever been. This genus
811 appears in different positions in most analyses, and the
812 final hypothesis of a sister relationship with Tithoreini is
813 novel but was also suggested by Brower et al. (2006).
814 However, bootstrap, Bremer and character support for
815 this relationship are weak, with only two unambiguous
816 synapomorphies, both also occurring in other relatively
817 close genera. Whatever the relationships of the genus, it
818 is so highly autapomorphic we believe it should be
819 treated in its own tribe, for which the name Methonini
820 (Mielke and Brown, 1979), is already available.

821 The tribe Melinaeini as currently conceived (Lamas,
822 2004) is paraphyletic, with *Athesis* + *Patricia* forming a

823 separate, strongly supported clade in all analyses (Har-
824 vey, 1991; Brown and Freitas, 1994; Brower et al., 2006)
825 that is diagnosed by numerous synapomorphies. With
826 the removal of the latter two genera, which require a
827 new tribe, Melinaeini (clade 6) is monophyletic and
828 relatively strongly supported.

829 Mechanitini are monophyletic and strongly supported,
830 with the inclusion of *Thyridia*, which was, however,
831 suggested by Brower et al. (2006) to be sister to
832 *Methona*. Particularly convincing synapomorphies for
833 the genera in Mechanitini include lateral tubercles just
834 above the prolegs (Char 27:1), the four-segmented
835 female foretarsus (Char 102:1), anteriorly projecting
836 gnathos (Char 285:1), and attenuated corpus bursae
837 (Char 349:1).

838 Oleriini, Ithomiini and Napeogenini are each mono-
839 phyletic and well supported, with *Placidina* strongly
840 supported as a member of Ithomiini, sister to *Pagyris*, in
841 both partitioned analyses and the total evidence analy-
842 sis. The monotypic south-east Brazilian *Epityches*,
843 suggested by Brown and Freitas (1994) to possibly
844 merit its own tribe, was well supported as sister to the
845 monotypic Andean *Aremfoxia*, with both forming a
846 clade sister to remaining Napeogenini. The sister rela-
847 tionship between Ithomiini and Napeogenini was also
848 robust, and the topology of the clade containing these
849 two tribes (clade 18) is the same as that found by Brower
850 et al. (2006).

851 The analyses of Brown and Freitas (1994) found
852 *Callithomia*, *Velamysta* and *Pteronymia lonera* (as *Tal-*
853 *amancana lonera*) to be sister to remaining Dircennini
854 + Godyridini. The total evidence SACW tree also
855 placed *Callithomia* in a similar position, but *Velamysta*
856 is within the well supported Godyridini and *P. lonera* is
857 sister to *P. inania* within *Pteronymia*. Adult characters
858 alone recovered a monophyletic Dircennini, as did
859 Brower et al. (2006), so a combined morphological
860 and molecular analysis should establish the true sys-
861 tematic position of *Callithomia*.

862 Generic classification

863 This study represents the first attempt to test the
864 monophyly of ithomiine genera using cladistic methods,
865 and a number of problems were uncovered in the four
866 most diverse tribes. In Napeogenini, the only one of
867 these tribes that has been subjected to recent systematic
868 revision, *Hypothyris* proved paraphyletic with respect to
869 *Hyaliris*. In their revision of both of these genera, Fox
870 and Real (1971, p. 100) stated: “[*Hyaliris*] is distin-
871 guished from *Hypothyris* not so much by any single, well
872 emphasized, consistent structural difference, as by the
873 fact that in nearly every morphologic detail, there is
874 some variation, often slight ... sufficient to justify
875 generic separation.” Fox and Real (1971) also placed
876 *Hypothyris cantobrica* and *H. xanthostola* in the

monotypic *Rhodussa* and *Garsauritis*, respectively. 877
While *H. cantobrica* is basal to remaining species, 878
H. xanthostola appeared here as sister to *H. ninonia*, 879
the type of the *Hypothyris*, justifying the recent synon- 880
ymy of *Garsauritis* (Lamas, 2004). Even though *Hyaliris* 881
was monophyletic, there are no clear synapomorphies, 882
especially when other members of the genus are consid- 883
ered, and a species-level study is necessary to resolve the 884
classification of this assemblage. 885

886 Ten years ago Brown and Freitas (1994) described the 886
genus *Ollantaya* to include *Ithomia canilla* Hewitson, 887
Ithomia aegineta Hewitson and *Leucothyris baizana* 888
Haensch. However, *Ollantaya* was recently synonymized 889
with *Oleria* by Lamas (2004). The first two of these 890
species form a clade sister to remaining *Oleria*, with the 891
inclusion of *Hyposcada olerioides* D’Almeida, a result 892
confirmed by molecular data (A. Whinnett, pers. 893
comm.). An undescribed species from the Peruvian 894
Andes is also an apparent member of this clade (Lamas 895
and Willmott, in prep.), but morphological and molecu- 896
lar data place *Leucothyris baizana* near to *Oleria* 897
santineza (Willmott, unpub. data, A. Whinnett, unpub. 898
data.). *Ollantaya* might therefore be resurrected for 899
canilla, *aegineta*, *olerioides* and the new species, but the 900
systematic position of *Oleria aegle* is uncertain, as it 901
lacks the synapomorphies of either *Ollantaya* or remain- 902
ing *Oleria*. Hopefully, molecular data (Whinnett and 903
Leadbeater, in prep.) will provide a solution. 904

905 The systematics of *Hyalenna* and *Dircenna* have been 905
addressed by Willmott and Lamas (2005), who conclu- 906
ded that *Ithomia paradoxa* should be transferred to 907
Hyalenna. Elsewhere in the Dircennini, there are clear 908
problems with the classification of *Episcada*, *Ceratinia* 909
and relatives. *Ceratinia* forms a clade with several 910
species often placed in different genera, including 911
Episcada canaria, *E. doto* (formerly both placed in 912
Ceraticscada), *E. hemixanthe* (formerly placed in *Pteron-*
913 *ymia*) and *E. hymenaea* (formerly placed in *Prittwitzia*). 914
Despite weak branch support for relationships in this 915
clade, there is no evidence that *Episcada* as currently 916
conceived is monophyletic, and a species-level analysis 917
including molecular data is necessary. 918

919 In the Godyridini, there is strong evidence showing 919
Godyris mantura to be distantly related to other *Godyris*. 920
This species shares a number of synapomorphies with 921
Ithomia cleomella Hewitson and two undescribed 922
Andean species and should be placed in a new genus 923
(Willmott and Lamas, in prep.). *Hypoleria adasa* clus- 924
tered with *G. mantura*, *Mcchungia* and *Brevioleria*, with 925
strong branch support, so *Hypoleria* will need to be 926
subdivided. Finally, the small genus *Pseudoscada* 927
appeared within *Greta*, one of the largest ithomiine 928
genera, a position with strong branch and character 929
support. The type species of *Greta*, *G. diaphanus*, formed 930
a relatively isolated clade with *G. morgane*, so *Greta* 931
should probably be restricted to include only these two 932

933 species. While it seems likely that certain other *Greta*
 934 species form a monophyletic group, especially the high
 935 Andean *G. theudelinda*, *G. ortygia* and most remaining
 936 species, there are no synapomorphies yet known that
 937 support this hypothesis and a species-level analysis is
 938 called for.

939 *Larval hostplant choice and ithomiine diversification*

940 The tight association between the diverse, exclusively
 941 neotropical Ithomiinae and their speciose, largely
 942 neotropical larval hostplant family Solanaceae has been
 943 studied in admirable depth and detail by Keith Brown
 944 and co-workers since the early 1980s (e.g., Brown,
 945 1984, 1985, 1987; Drummond, 1986; Brown et al., 1991;
 946 Trigo et al., 1996). Early studies of the Ithomiinae–
 947 Solanaceae interface tested Ehrlich and Raven, 1965)
 948 the hypothesis of plant–herbivore coevolution, but
 949 found little positive evidence for simultaneous diversi-
 950 fication (Brown, 1985). Our results support earlier
 951 conclusions that there is no evidence for phylogenetic
 952 tracking between Solanaceae hosts and ithomiine her-
 953 bivores (Drummond, 1986; Brown, 1987). For example,
 954 the relatively basal Melinaeini use the relatively derived
 955 *Solandra* clade, while Godryidini specialize on the
 956 relatively primitive *Cestrum* (Olmstead et al., 1999)
 957 (Table 3; Fig. 7).

958 The origin of Ithomiinae larval feeding on Solanaceae
 959 has been seen as a key event in the diversification of the
 960 butterfly group (Brown, 1987; Brown and Henriques,
 961 1991). *Tellervo*, the likely sister to the Ithomiinae, feeds
 962 on Apocynaceae (Ackery, 1987), as do many Danainae
 963 (Ackery and Vane-Wright, 1984), and this seems a
 964 plausible ancestral hostplant for the subfamily. Never-
 965 theless, our phylogenetic hypothesis (and that of Brower
 966 et al., 2006) suggests either that two independent shifts
 967 occurred on to Solanaceae (*Methona* and clade 5), or
 968 that the shift on to Solanaceae by the ancestor of the
 969 subfamily was followed by reversal to Apocynaceae by
 970 Tithoreini (clade 3). Exclusion of larval hostplant as a
 971 character in the matrix does not affect this scenario.
 972 Discrimination between these two hypotheses may not
 973 be possible using phylogenetic methods, but resolution
 974 of the position of *Methona*, which feeds exclusively on
 975 the Solanaceae genus *Brunfelsia*, might settle the ques-
 976 tion. Brown (1987, p. 380) reported that *Aeria* larvae did
 977 not accept any Solanaceae in captivity and Freitas
 978 (1999) found that *Methona* can accept *Prestonia* (Apo-
 979 cynaceae) in experiments of host shift, so two origins of
 980 Solanaceae feeding is perhaps the more plausible hypo-
 981 thesis given our phylogeny. Regardless of how Solana-
 982 ceae was colonized, however, we suggest that it was not
 983 a shift to Solanaceae *per se* that facilitated Ithomiinae
 984 diversification, but further specialization on distinct
 985 Solanaceae clades, which are usually exclusive to a single
 986 ithomiine clade (Fig. 7).

In addition to *Methona*, the two basal tribes Meli- 987
 naeini and new tribe (*Athesis* + *Patricia*) are also 988
 specialists on different plant clades, also used very 989
 infrequently by other ithomiine tribes. All Melinaeini 990
 are entirely restricted to the *Solandra* clade, on which 991
 only two other ithomiines have been recorded feeding 992
 (*Pteronymia carlia*, Dircenninio unidentified species, 993
 probably *Hypothyris*). Oleriini and Mechanitini can also 994
 readily accept *Juanulloa* (*Solandra* clade) as an alternat- 995
 1000-ive hostplant in captivity (Freitas and Brown, 1994; 996
 Freitas, 1999). Many members of the *Solandra* clade are 997
 hemi-epiphytes, and female Melinaeini are usually 998
 scarce in the forest understorey, presumably because 999
 they spend much time searching for hostplants in the 1000
 canopy (Beccaloni, 1997b). *Athesis* and *Patricia* have 1001
 almost identical immature stages, both feeding on 1002
Capsicum, which is used occasionally in nature by 1003
Epityches and *Ithomia* in the sister tribes Napeogenini 1004
 and Ithomiini. 1005

The vast genus *Solanum* is used by members of six 1006
 tribes, the Mechanitini, Ithomiini, Napeogenini, Oleri- 1007
 ini, Dircennini and Godryidini (Table 3). Brown (1987) 1008
 proposed that existing adaptations among Ithomiinae to 1009
 classes of secondary chemicals in ancestral hostplants 1010
 permitted colonization of new, chemically similar and 1011
 already diversified hosts. He suggested that at least four 1012
 radiations of Ithomiinae showed similar patterns of host 1013
 colonization, with shifts on to *Capsicum* and the 1014
Solandra clade leading to feeding on *Solanum*, and a 1015
 cladogram indicating hypothesized patterns was present- 1016
 ed by Brown and Henriques (1991, fig. 4.6). Our 1017
 phylogeny and optimization of hostplant states suggests, 1018
 however, that only a single shift on to *Solanum* 1019
 occurred, at the base of clade 12 (Fig. 7). Although we 1020
 found no evidence for the ancestral hostplant before this 1021
 shift, both the *Solandra* clade and *Capsicum* are occa- 1022
 sionally used by members of clade 12 and thus possible 1023
 candidates. 1024

Clade 12 includes all species with non-“danaoid” 1025
 larvae, which lack complete body color rings and flexible 1026
 thoracic tubercles. Among the basal tribes of Ithomiinae 1027
 outside clade 12, data suggesting chemical protection of 1028
 the immature stages are known only for the tribe 1029
 Tithoreini, whose larvae have been shown to sequester 1030
 pyrrolizidine alkaloids from their apocynaceous host- 1031
 plants (Trigo and Brown, 1990). There are no data of 1032
 this kind available for *Methona*, Melinaeini or *Athe- 1033
 1034
 1035
 1036
 1037
 1038
 1039
 1040
 1041
 1042*sis + *Patricia*, but the aposematic larval color pattern
 and behavior in these clades are similar to those of
 Tithoreini (Fig. 9H,R) and of most danaines (Freitas
 and Brown, 1994). Larvae within these tribes may also
 therefore have some chemical protection and larvae of
Methona are reportedly rejected by young birds (Mas-
 suda and Trigo, pers. comm.). In contrast, the largely
 cryptic larvae of species in clade 12 appear to be
 palatable to predators (with two possible exceptions,

1043 Freitas et al., 1996; Massuda and Trigo, pers. comm.),
 1044 although a novel defense mechanism has recently been
 1045 discovered involving chemical camouflage from predat-
 1046 ory ants through similarity of larval and plant cuticular
 1047 lipids (Portugal and Trigo, 2005). Additional informa-
 1048 tion on behavior and chemical protection within Ithomi-
 1049 iinae will therefore surely lead to a better understanding
 1050 of the ecological shifts associated with the origin of
 1051 clade 12.

1052 Although all tribes in clade 12 feed on *Solanum*, there
 1053 are at least four main shifts in preferred hostplant. The
 1054 Ithomiini are concentrated on a clade of small, chem-
 1055 ically similar genera (Brown, 1987) and *Napeogenes* feed
 1056 almost exclusively on *Lycianthes*, with both sharing
 1057 these resources with a few other ithomiines. The shift by
 1058 *Megoleria* and *Hyposcada* on to Gesneriaceae, which is
 1059 used only by these two sister genera, remains to be
 1060 investigated. Finally, another important host shift
 1061 occurs near the base of the Godryridini, the second
 1062 largest ithomiine tribe, on to *Cestrum*, the second largest
 1063 Solanaceae genus. Brown (1987) suggested that this shift
 1064 might have been facilitated by the presence of a similar,
 1065 pungent oil in *Cestrum* and *Solanum* section *Geminata*
 1066 (the predominant group used by the Dircennini), and
 1067 our phylogeny is consistent with this hypothesis, with
 1068 *Cestrum*-feeders evolving from a *Solanum*-feeding ances-
 1069 tor.

1070 The overall picture then, of specialization by ithomi-
 1071 iine tribes and generic clades on particular plant clades,
 1072 with relatively little overlap, suggests the possibility of
 1073 multiple instances of adaptive radiation driven by new
 1074 ecological opportunities (Simpson, 1953). Schluter
 1075 (2000) outlined four criteria for diagnosing adaptive
 1076 radiation, including common ancestry, a correspon-
 1077 dence between divergent traits and different niches,
 1078 evidence that particular traits enhance fitness within
 1079 particular niches, and correlation between key adapta-
 1080 tions and increased speciation rate. The first and last of
 1081 these criteria can be considered in the light of our
 1082 results, while the second and third are now briefly
 1083 reviewed.

1084 Within clades of sympatric ithomiines, larvae fre-
 1085 quently specialize on different, but often related, host-
 1086 plant species (Willmott and Mallet, 2004). Whether such
 1087 specialization might represent resource partitioning to
 1088 reduce competition from other herbivores (as proposed
 1089 for *Heliconius* butterflies; Benson, 1978), limit attacks by
 1090 parasitoids and predators, or is a by-product of other
 1091 niche shifts, such as a change in adult microhabitat,
 1092 remains largely unexplored. Two other divergent traits
 1093 likely correlated with larval hostplant are adult wing
 1094 pattern and microhabitat preference. Adults of all
 1095 Ithomiinae have warningly colored wing patterns that
 1096 advertise their unpalatability, and are mimetic, facilita-
 1097 ting learning in predators (Bates, 1862; Müller, 1879).
 1098 Ithomiine communities may contain up to eight or more

distinct types of warning color pattern, or mimicry rings 1099
 (Beccaloni, 1997a), with evidence for comimetic species 1100
 flying within the same area of forest (DeVries et al., 1101
 1999) and at the same height above ground (Beccaloni, 1102
 1997b). Species that share larval hostplant are often 1103
 mimetic (Willmott and Mallet, 2004), suggesting that 1104
 plant microhabitat and adult flight microhabitat are 1105
 linked (Beccaloni, 1997b). However, despite the accu- 1106
 mulating evidence for correlations between traits and 1107
 hostplants, little research to date has tested whether 1108
 such traits directly enhance fitness. 1109

1110 Considering the remaining two criteria for adaptive 1110
 radiation, our results indicate that most ithomiines 1111
 which specialize on the same hostplant clade do form 1112
 monophyletic groups (Fig. 7), with the occasional 1113
 exclusion of one to a few other clades. Exploitation of 1114
 a new clade of plants can be seen as a key innovation 1115
 providing access to a formerly underutilized or vacant 1116
 resource, and may be accompanied by a suite of 1117
 adaptations. Thus colonization of the largely hemi- 1118
 epiphytic *Solandra* clade might require ovipositing 1119
 Melinaeini females to identify new hostplants, novel 1120
 mimicry patterns in adults to provide protection from 1121
 predators in the subcanopy, and larval ability to 1122
 overcome plant physical and chemical defenses and 1123
 avoid predation and parasitism. The two largest tribes, 1124
 Dircennini and Godryridini, which dominate understory 1125
 ithomiine communities and feed on the diverse *Solanum* 1126
 and *Cestrum* growing there, have the most highly 1127
 transparent wing patterns, a trait hypothesized to 1128
 enhance protection from predators in low light condi- 1129
 tions (Brown, 1988). 1130

1131 Access to new hostplants is likely to provide oppor- 1131
 tunities for adaptive speciation, so we might expect 1132
 plant diversity to be correlated with herbivore diversity 1133
 and important host shifts to be associated with an 1134
 increase in speciation rate. Using the phylogeny and 1135
 optimized hostplant character states we inferred the 1136
 number of ithomiine species that feed on each plant 1137
 clade, and there is indeed a strong positive correlation 1138
 between plant and associated herbivore clade diversity, 1139
 at least within the Solanaceae (Table 4; Fig. 32; 1140
 $P < 0.01$). This is not simply an artifact of more diverse 1141
 ithomiine clades having a broader host range, as there is 1142
 no correlation between plant generic diversity and 1143
 ithomiine diversity (Table 4). Larger ithomiine clades 1144
 might also have broader geographic ranges and access to 1145
 more plant species, but there is no strong correlation 1146
 between clade and range size, with many small ithomiine 1147
 genera (e.g., *Mechanitis*, *Tithorea*, *Dircenna*, *Ceratinia*) 1148
 being very widespread (Willmott, unpublished data). 1149

1150 *Solanum* comprises about 70% of neotropical Solan- 1150
 aceae (Hunziker, 1979), and clade 12 (*Solanum* feeders) 1151
 comprises 89% of the Ithomiinae, so the shift on to 1152
Solanum is perhaps the most significant event in 1153
 ithomiine hostplant evolution. Although host shifts 1154

away from *Solanum* occur in several clades within clade 12, we suggest such shifts are likely to have been facilitated by the evolution of morphological, biochemical and/or behavioral traits, which accompanied the original shift to *Solanum*. Using the test of clade imbalance proposed by Slowinski and Guyer (1989), clade 12 (328 spp.) is significantly more diverse than its sister clade 11 (*Athesis* + *Patricia*, six spp.; $P = 0.04$), but given uncertainties regarding topology in this part of the tree, the test provides no strong support for increased speciation. Nevertheless, the correlation between other host shifts and higher taxonomic categories is notable. Although the rank and inclusiveness of higher taxa are arbitrary, the features that led initially to their recognition, namely relatively greater character distance between them in comparison with character distances between their members, are consistent with an increase in speciation rate.

To conclude, ecological study to date suggests that shifts in hostplant species are likely to be associated with a number of trait shifts in ithomiines, of which microhabitat and wing pattern (Jiggins et al., 2001) in particular are likely to lead to reproductive isolation. Hostplant interactions are thus likely to have played a key role in Ithomiinae speciation. Phylogenetic patterns are consistent with this hypothesis, and it seems likely that the diversity of new niches presented by *Solanum* and other plant clades was important in increasing ithomiine diversification through ecological speciation.

1184 Conclusions and future work

The phylogeny presented here is the most detailed hypothesis to date of ithomiine relationships, and in combination with molecular data (Brower et al., 2006) will provide a solid foundation for tribal classification. While some tribal relationships are firmly supported (Napeogenini + Ithomiini, Dircennini + Godyradini, and monophyly of these four tribes plus Oleriini), others (especially between Tithoreini, *Methona*, Melinaeini and *Athesis* + *Patricia*) are weakly resolved and tend to differ depending on what characters are included, in both morphological and molecular data sets. It therefore seems unlikely that combination of existing data sets alone will convincingly resolve these relationships, and we suggest that additional character sources such as those from the egg and first instar larva (e.g., Motta, 2003) and additional gene regions (e.g., *tektin*, Whinnett et al., 2005) should be examined.

There exist clear problems with generic classification in each of the four most diverse tribes (Napeogenini, Oleriini, Dircennini and Godyradini), with at least five genera paraphyletic or polyphyletic. Morphological characters identified here will permit a revision of several of these genera (e.g., *Godyris mantura* and

relatives), but more intensive morphological and molecular sampling will be required in other cases (e.g., *Episcada*, *Ceratinia* and relatives). The position of the recently described genus *Haenschia* remains poorly resolved and any information on the immature stages could prove significant in establishing its true position.

Knowledge of ithomiine hostplants may be the most detailed available for any diverse (> 200 spp.) neotropical butterfly group and there are clear macroevolutionary patterns emerging. Nevertheless, there remains much work to be done in the field of ithomiine hostplant ecology. We have little knowledge of whether hostplant differences are maintained by adult microhabitat specialization or female recognition of specific chemical cues (Brown, 1987), and which of these adaptations occurs first. Furthermore, much detailed ecological study is required to determine whether host shifts are driven by improved larval growth rates, reduced predation and parasitism, adult microhabitat shifts, or other factors. Finally, more detailed molecular phylogenies will permit identification of periods of increased speciation rate (Nee et al., 1996) and therefore provide a better understanding of the role of adaptive radiation in the evolution of the Ithomiinae.

Acknowledgments

We thank the museum curators who permitted us to examine and borrow specimens for morphological study, including Phil Ackery (Natural History Museum, London), Lee and Jackie Miller (Allyn Museum, Sarasota, now at Florida Museum of Natural History, Gainesville), Wolfram Mey (Museum für Naturkunde, Berlin), Matthias Nuã (Staatliches Museum für Tierkunde, Dresden), Heinz Schröder (Senckenberg Museum, Frankfurt am Main), Axel Hausmann (Zoologische Sammlung des Bayerischen Staates, Munich), Miguel Monné (Museu Nacional do Rio de Janeiro, Rio de Janeiro), Olaf Mielke (Universidade Federal do Paraná, Curitiba), Marcelo Duarte (Museu de Zoologia da Universidade de São Paulo, São Paulo), Bob Robbins (National Museum of Natural History, Washington, DC) and Eric Quinter (American Museum of Natural History, New York). We are very grateful to Gerardo Lamas for his assistance with numerous taxonomic matters and insightful discussions into Ithomiinae systematics and morphology, and Keith Brown for his exceptional work on ithomiines, enthusiasm and encouragement which have proved so inspirational in our own research. We thank Dick Vane-Wright and two anonymous reviewers for thoughtful comments on the manuscript and Andrei Sourakov for providing immature stage specimens of *Greta diaphanus*. KRW thanks Julia Robinson-Dean, Ismael and Raul Aldas

1261 for field assistance, Sandy Knapp for identifying
 1262 Solanaceae hostplants, and S. Knapp and Michael
 1263 Nee for comments on Solanaceae diversity. Permits
 1264 for fieldwork in Ecuador were provided by the
 1265 Ministerio del Ambiente and Museo Ecuatoriano de
 1266 Ciencias Naturales, Quito. Museum and field work of
 1267 KRW was funded by Leverhulme Trust Standard
 1268 Research Project grant F/00696/C, and field work by
 1269 the National Geographic Society (Research and
 1270 Exploration grant no. 5751-96) and National Science
 1271 Foundation (Biodiversity Surveys & Inventories grant
 1272 no. 0103746). AVLF was funded by Fapesp, Faepex
 1273 and the National Science Foundation (Fapesp grants
 1274 00/01484-1 and 04/05269-9 to AVLF; BIOTA-FAP-
 1275 ESP program—98/05101-8; NSF DEB-0316505).
 1276 AVLF thanks Ronaldo Bastos Francini (Unisantos,
 1277 Santos), Paulo Cesar Motta (UnB, Brasília), Keith
 1278 S. Brown Jr., José Roberto Trigo, João Vasconcellos-
 1279 Neto (Unicamp, Campinas), Marco Aurélio Pizo
 1280 (Unisinos, São Leopoldo) and Sandra Inês Uribe
 1281 (Unalmed, Medellín) for assistance in fieldwork and
 1282 for providing material for many species of Ithomiinae.

1283 References

- 1284 Ackery, P.R., 1987. The danaid genus *Tellervo* (Lepidoptera, Nym-
 1285 phalidae)—a cladistic approach. *Zool. J. Linn. Soc.* 89, 203–274.
- 1286 Ackery, P.R., Vane-Wright, R.I., 1984. Milkweed Butterflies. Their
 1287 Cladistics and Biology. British Museum (Natural History), Lon-
 1288 don.
- 1289 Ackery, P.R., De Jong, R., Vane-Wright, R.I., 1999. The butterflies:
 1290 Hedyloidea, Hesperioidea and Papilionoidea. In: Kristensen,
 1291 N.P. (Ed.) *Lepidoptera: Moths and Butterflies. 1. Evolution,*
 1292 *Systematics and Biogeography. Handbook of Zoology, 4(35),*
 1293 *Lepidoptera.* De Gruyter, Berlin, pp. 263–300.
- 1294 Arms, K., Feeny, P., Lederhouse, R.C., 1974. Sodium: stimulus for
 1295 puddling behavior by tiger swallowtail butterflies, *Papilio glaucus*.
 1296 *Science* 185, 372–374.
- 1297 Baker, R.H., DeSalle, R., 1997. Multiple sources of character
 1298 information and the phylogeny of Hawaiian drosophilids. *Syst.*
 1299 *Biol.* 46, 654–673.
- 1300 Barker, F.K., Lutzoni, F.M., 2002. The utility of the Incongruence
 1301 Length Difference Test. *Syst. Biol.* 51, 625–637.
- 1302 Bates, H.W., 1862. Contributions to an insect fauna of the Amazon
 1303 Valley. *Lepidoptera: Heliconidae.* *Trans. Linn. Soc. Lond.* 23, 495–
 1304 566.
- 1305 Beccaloni, G.W., 1997a. Ecology, natural history and behaviour of
 1306 ithomiine butterflies and their mimics in Ecuador (Lepidoptera:
 1307 Nymphalidae: Ithomiinae). *Trop. Lepid.* 8, 103–124.
- 1308 Beccaloni, G.W., 1997b. Vertical stratification of ithomiine butterfly
 1309 (Nymphalidae: Ithomiinae) mimicry complexes: the relationship
 1310 between adult flight height and larval host-plant height. *Biol.*
 1311 *J. Linn. Soc.* 62, 313–341.
- 1312 Benson, W.W., 1978. Resource partitioning in passion vine butterflies.
 1313 *Evolution.* 32, 493–518.
- 1314 Boppre, M., Vane-Wright, R.I., 1989. Androconial systems in Dana-
 1315 ina (Lepidoptera): functional morphology of *Amauris*, *Danaus*,
 1316 *Tirumala* and *Euploea*. *Zool. J. Linn. Soc.* 97, 101–133.
- 1317 Brabant, R., 2004. Un nouvel Ithomiide, originaire du centre du
 1318 12 Perou. *Lambillionea*, 104, 423–428.
- Bremer, K., 1988. The limits of amino acid sequence data in
 angiosperm phylogenetic reconstruction. *Evolution*, 42, 795–803. 1319 1320
- Bremer, K., 1994. Branch support and tree stability. *Cladistics*, 1, 295–
 304. 1321 1322
- Brévignon, C., 2003. Inventaire des Ithomiinae de Guyane Française
 (Lepidoptera, Nymphalidae). *Lambillionea*, 103, 41–58. 1323 1324
- Brower, A.V.Z., 2000. Phylogenetic relationships among the Nym-
 phalidae (Lepidoptera) inferred from partial sequences of the
 wingless gene. *Proc. R. Soc. Lond. B*, 267, 1201–1211. 1325 1326 1327
- Brower, A.V.Z., Freitas, A.V.L., Lee, M.-M., Silva Brandão, K.L.,
 Whinnett, A., Willmott, K.R., 2006. Phylogenetic relationships
 among the Ithomiini (Lepidoptera: Nymphalidae) inferred from
 one mitochondrial and two nuclear gene regions. *Syst. Entomol.*, in
 press. 1328 1329 1330 1331 1332
- 1333 Brown, K.S., 1967. Chemotaxonomy and chemomimicry: the case of
 3-hydroxy-kynurenine. *Syst. Zool.* 16, 213–216. 1334
- Brown, K.S., 1977a. Geographical patterns of evolution in neo-
 tropical Lepidoptera: differentiation of the species of *Melinaea*
 and *Mechanitis* (Nymphalidae: Ithomiinae). *Syst. Entomol.* 2,
 161–197. 1335 1336 1337 1338
- Brown, K.S., 1977b. Centros de evolução, refúgios quaternários
 e conservação de patrimônios genéticos na região neotropical:
 padrões de diferenciação em Ithomiinae (Lepidoptera: Nymphali-
 dae). *Acta Amaz.* 7, 75–137. 1339 1340 1341 1342
- Brown, K.S., 1980. A review of the genus *Hypothyris* Hübner
 (Nymphalidae), with descriptions of three new subspecies and the
 early stages of *H. daphnis*. *J. Lep. Soc.* 34, 152–172. 1343 1344 1345
- Brown, K.S., 1982. Historical and ecological factors in the biogeog-
 raphy of aposematic neotropical butterflies. *Am. Zool.* 22, 453–
 471. 1346 1347 1348
- Brown, K.S., 1984. Adult-obtained pyrrolizidine alkaloids defend
 ithomiine butterflies against a spider predator. *Nature* 309, 707–
 709. 1349 1350 1351
- Brown, K.S., 1985. Chemical ecology of dehydropyrrolizidine alka-
 loids in adult Ithomiinae (Lepidoptera: Nymphalidae). *Rev. Bras.*
Biol. 44, 453–460. 1352 1353 1354
- Brown, K.S., 1987. Chemistry at the Solanaceae/Ithomiinae interface.
Ann. Missouri Bot. Gdn. 74, 359–397. 1355 1356
- Brown, K.S., 1988. Mimicry, aposematism and crypsis in neotropical
 Lepidoptera: the importance of dual signals. *Bull. Soc. Zool.*
Fr. 113, 83–119. 1357 1358 1359
- Brown, K.S., D’Almeida, R.F., 1970. The Ithomiinae of Brazil
 (Lepidoptera: Nymphalidae). II. A new genus and species of
 Ithomiinae with comments on the tribe Dircennini d’Almeida.
Trans. Am. Entomol. Soc. 96, 1–18. 1360 1361 1362 1363
- Brown, K.S., Freitas, A.V.L., 1994. Juvenile stages of Ithomiinae :
 overview and systematics (Lepidoptera: Nymphalidae). *Trop.*
Lepid. 5, 9–20. 1364 1365 1366
- Brown, K.S., Henriques, S.A., 1991. Chemistry, co-evolution, and col-
 onisation of Solanaceae leaves by ithomiine butterflies. In: Hawkes,
 J.G., Lester, R.N., Nee, M., Estrada, N. (Eds.), *Solanaceae III:*
Taxonomy, Chemistry, Evolution. Linnean Society of London,
 London, pp. 51–68. 1367 1368 1369 1370 1371
- Brown, K.S., Mielke, O.H.H., Ebert, H., 1970. Os Ithomiinae do
 Brasil. I. *Prittwitzia* g. n. para *Ithomyia hymenaea* Prittwitz. e suas
 subespécies (Lepidoptera, Nymphalidae). *Rev. Bras. Biol.* 30, 269–
 273. 1372 1373 1374 1375
- Brown, K.S., Trigo, J.R., Francini, R.B., Morais, A.B.B., Motta, P.C.,
 1991. Aposematic insects on toxic host plants: coevolution,
 colonization and chemical emancipation. In: Price, P.W., Lewin-
 sohn, T.M., Fernandes, G.W., Benson, W.W. (Eds.), *Plant–Animal*
Interactions: Evolutionary Ecology in Tropical and Temperate
Regions. J. Wiley, New York, pp. 357–402. 1376 1377 1378 1379 1380 1381
- Brown, K.S., Schoultz, B.V., Suomalainen, E., 2004. Chromosome
 evolution in Neotropical Danainae and Ithomiinae (Lepidoptera).
Hereditas 141, 216–236. 1382 1383 1384

- 1385 Comstock, J.H., Needham, J.G., 1918. The wings of insects. *Am. Nat.* 32, 231–257.
- 1387 D'Almeida, R.F., 1941. Contribuição ao estudo dos Mechanitidae (Lep. Rhopalocera) (4a. nota). *Pap. Avuls. Dept. Zool. Sec. Agric.* 1, 79–85.
- 1390 Darlu, P., Leconitre, G., 2002. When does the incongruence length difference test fail? *Mol. Biol. Evol.* 19, 432–437.
- 1392 DeVries, P.J., Lande, R., Murray, D., 1999. Associations of co-mimetic ithomiine butterflies on small spatial and temporal scales in a neotropical rainforest. *Biol. J. Linn. Soc.* 67, 73–85.
- 1395 Dolphin, K., Belshaw, R., Orme, C.D.L., Quicke, D.L.J., 2000. Noise and incongruence: interpreting results of the incongruence length difference test. *Mol. Phylogenet. Evol.* 17, 401–406.
- 1398 Doubleday, E., 1847. The Genera of Diurnal Lepidoptera: Comprising their Generic Characters, a Notice of their Habits and Transformations, and a Catalogue of the Species of Each Genus 1, 87–106, pl. Longman, Brown, Green & Longmans, London, pp. 16–19.
- 1403 Downey, J.C., Allyn, A.C., 1975. Wing-scale morphology and nomenclature. *Bull. Allyn Mus.* 31, 1–32.
- 1405 Drummond, B.A., 1986. Coevolution of ithomiine butterflies and solanaceous plants. In: D'Arcy, W.G. (Ed.), *Solanaceae: Biology and Systematics*. Columbia University Press, New York, pp. 307–327.
- 1409 Drummond, B.A., Brown, K.S., 1987. Ithomiinae (Lepidoptera: Nymphalidae): summary of known larval food plants. *Ann. Missouri Bot. Gdn.* 74, 341–358.
- 1412 Edgar, J.A., Culvenor, C.C.J., Pliske, T.E., 1976. Isolation of lactone, structurally related to the esterifying acids of pyrrolizidine alkaloids, from the costal fringes of male Ithomiinae. *J. Chem. Ecol.* 2, 263–270.
- 1416 Ehrlich, P.R., Raven, P.H., 1965. Butterflies and plants: a study in coevolution. *Evolution*, 18, 586–608.
- 1418 Eliot, J.N., 1973. The higher classification of the Lycaenidae (Lepidoptera): a tentative arrangement. *Bull. Br. Mus. Nat. Hist. (Entomol.)*, 28, 373–506.
- 1421 Farris, J.S., 1969. A successive approximations approach to character weighting. *Syst. Zool.* 18, 374–385.
- 1423 Farris, J.S., Källersjö, M., Kluge, A.G., Bult, C., 1995. Constructing a significance test for incongruence. *Syst. Biol.* 44, 570–572.
- 1425 Fox, R.M., 1940. A generic review of the Ithomiinae (Lepidoptera, Nymphalidae). *Trans. Am. Entomol. Soc.* 66, 161–207.
- 1427 Fox, R.M., 1956. A monograph of the Ithomiidae (Lepidoptera). Part I. *Bull. Am. Mus. Nat. Hist.* 111, 1–76.
- 1429 Fox, R.M., 1960. A monograph of the Ithomiidae (Lepidoptera). Part II. The tribe Melinaeini Clark. *Trans. Am. Entomol. Soc.* 86, 109–171.
- 1432 Fox, R.M., 1967. A monograph of the Ithomiidae (Lepidoptera). Part III. The tribe Mechanitini Fox. *Mem. Am. Entomol. Soc.* 22, 1–190.
- 1435 Fox, R.M., Real, H.G., 1971. A monograph of the Ithomiidae (Lepidoptera). Part IV. The tribe Napeogenini Fox. *Mem. Am. Entomol. Inst.* 15, 1–368.
- 1438 Freitas, A.V.L., 1993. Biology and population dynamics of *Placidula euryanassa*, a relict ithomiine butterfly (Nymphalidae: Ithomiinae). *J. Lepid. Soc.* 47, 87–105.
- 1441 Freitas, A.V.L., 1996. Population biology of *Heterosais edessa* (Nymphalidae) and its associated Atlantic Forest Ithomiinae community. *J. Lepid. Soc.* 50, 273–289.
- 1444 Freitas, A.V.L., 1999. Nymphalidae (Lepidoptera), filogenia com base em caracteres de imaturos, com experimentos de troca de plantas hospedeiras. PhD Thesis. Universidade Estadual de Campinas, Campinas.
- 1448 Freitas, A.V.L., Brown, K.S., 2002. Immature stages of *Sais rosalia* (Nymphalidae, Ithomiinae). *J. Lepid. Soc.* 56, 104–106.
- 1450 Freitas, A.V.L., Brown, K.S., 2004. Phylogeny of the Nymphalidae (Lepidoptera). *Syst. Biol.* 53, 363–383.
- Freitas, A.V.L., Brown, K.S., 2005. Immature stages of *Napeogenes sulphurina* Bates, 1862 (Lepidoptera, Nymphalidae, Ithomiinae) from Northeastern Brazil. *J. Lepid. Soc.* 59, 35–37.
- Freitas, A.V.L., Trigo, J.R., Brown, K.S., Witte, L., Hartmann, T., Barata, L.E.S., 1996. Tropane and pyrrolizidine alkaloids in the ithomiines *Placidula euryanassa* and *Miraleria cymothoe* (Lepidoptera: Nymphalidae). *Chemoecology*, 7, 61–67.
- Galluser, S., Guadagnuolo, R., Rahier, R., 2004. Genetic (RAPD) diversity between *Oleria onega agarista* and *Oleria onega* ssp. (Ithomiinae, Nymphalidae, Lepidoptera) in north-eastern Peru. *Genetica* 121, 65–74.
- Godman, F.D., Salvin, O., 1879–1880. *Biologia Centrali-Americana. Insecta. Lepidoptera-Rhopalocera*. Dulau & Co., Bernard Quaritch, London, 1, 6–56, pls. 1–4 (1879), 57–62, pl. 5 (1880).
- Haber, W.A., 1978. Evolutionary Ecology of Tropical Mimetic Butterflies (Lepidoptera: Ithomiinae). PhD Thesis. University of Minnesota, Minnesota.
- Haber, W.A., 2001. Guide to Costa Rican Ithomiinae. <http://www.cs.umb.edu/~whaber/Monte/Ithomid/Intro.html>.
- Haensch, R., 1909–10. 3. Familie: Danaidae. In: Seitz, A. (Ed.), *Die Gross-Schmetterlinge der Erde*, 5. Alfred Kernen, Stuttgart, pp. 113–171. pls. 31–41.
- Hall, J.P.W., Willmott, K.R., 2000. Patterns of feeding behaviour in adult male iroinid butterflies and their relationship to morphology and ecology. *Biol. J. Linn. Soc.* 69, 1–23.
- Hall, S.K., 1996. Behaviour and natural history of *Greta oto* in captivity (Lepidoptera: Nymphalidae: Ithomiinae). *Trop. Lepid.* 7, 161–165.
- Harvey, D.J., 1991. Higher classification of the Nymphalidae. In: Nijhout, H.F. (Eds.), *The Development and Evolution of Butterfly Wing Patterns*. Smithsonian Institution, Washington, pp. 255–273.
- Hsiao, T.H., 1986. Specificity of certain chrysolimid beetles for Solanaceae. In: D'Arcy, W.G. (Ed.), *Solanaceae: Biology and Systematics*. Columbia University Press, New York, pp. 345–363.
- Hunziker, A.T., 1979. South American Solanaceae: a synoptic survey. In: Hawkes, J.G., Lester, R.N., Skelding, A.D. (Eds.), *The Biology and Taxonomy of the Solanaceae*. Academic Press, London, pp. 49–85.
- Janzen, D.H., Hallwachs, W., 2005. Philosophy, navigation and use of a dynamic database (ACG Caterpillars SRNP) for an inventory of the macrocaterpillar fauna, and its food plants and parasitoids, of the Area de Conservacion Guanacaste (ACG), northwestern Costa Rica. <http://janzen.sas.upenn.edu>.
- Jiggins, C.D., Naisbit, R.E., Coe, R.L., Mallet, J., 2001. Reproductive isolation caused by colour pattern mimicry. *Nature*, 411, 302–305.
- Jiggins, C.D., Mallarino, R., Willmott, K.R., Bermingham, E., 2005. What can phylogenies tell us about speciation? The case of *Ithomia* (Lepidoptera: Nymphalidae). *Evolution*, submitted.
- Kitching, I.J., 1984. The use of larval chaetotaxy in butterfly systematics, with special reference to the Danaini (Lepidoptera: Nymphalidae). *Syst. Entomol.* 9, 49–61.
- Kitching, I.J., 1985. Early stages and classification of the milkweed butterflies (Lepidoptera: Danaeinae). *Zool. J. Linn. Soc.* 85, 1–97.
- Klots, A.B., 1970. 20. Lepidoptera. In: Tuxen, S.L. (Ed.), *Taxonomist's Glossary of Genitalia in Insects*, 2nd edn. Munksgaard, Copenhagen, pp. 115–130.
- Lamas, G., 1973. Taxonomia e evolução dos gêneros *Ituna* Doubleday (Danaeinae) e *Paititia* gen. n., *Thyridia* Hübn. e *Methona* Doubleday (Ithomiinae) (Lepidoptera, Nymphalidae). PhD Thesis. Universidade de São Paulo, São Paulo.
- Lamas, G., 1979. *Paititia neglecta*, gen. n., sp. n. from Peru (Nymphalidae: Ithomiinae). *J. Lepid. Soc.* 33, 1–5.
- Lamas, G., 1980. A revision of the genera *Hypomenitis* Fox and *Veladyris* Fox (Lepidoptera: Nymphalidae, Ithomiinae). *Rev. Ciencias*, 72, 36–46.

- 1519 Lamas, G., 1986. Revisión del género *Pagyris* Boisduval (Lepidoptera,
1520 Nymphalidae: Ithomiinae). *An. Inst. Biol. U. Nac. Aut. Mex.*
1521 (Zool.) 56, 259–276.
- 1522 Lamas, G., 2004. Ithomiinae. In: Heppner, J.B. (Ed.), Checklist: Part
1523 4A. Hesperioidea—Papilionoidea. Atlas of Neotropical Lepidop-
1524 tera, Vol. 5A. Association for Tropical Lepidoptera/Scientific
1525 Publishers, Gainesville, pp. 172–191.
- 1526 Maddison, W.P., Maddison, D.R., 1995. Macclade: Analysis of
1527 Phylogeny and Character Evolution, Version 3.05. Sinauer Asso-
1528 ciated, Sunderland, MA.
- 1529 Motta, P.C., 2003. Phylogenetic relationships of Ithomiinae based on
1530 first-instar larvae. In: Boggs, C., Ehrlich, P., Watt, W.B. (Eds.),
1531 Butterflies as Model Systems. Chicago University Press, Chicago,
1532 pp. 409–429.
- 1533 Müller, F., 1879. *Ituna and Thyridia*: a remarkable case of mimicry in
1534 butterflies. *Proc. Entomol. Soc. Lond.* 2, Xx–Xxix.
- 1535 Nee, M., 2001a. Solanaceae systematics for the 21st century. In: Van
1536 Den Berg, R.G., Barendse, G.W.M., Van der Weerden, G.M.,
1537 Mariani, C. (Eds.), Solanaceae V: Advances in Taxonomy and
1538 Utilization. Nijmegen University Press, Nijmegen, pp. 3–22.
- 1539 Nee, M., 2001b. An overview of *Cestrum*. In: Van Den Berg, R.G.,
1540 Barendse, G.W.M., Van der Weerden, G.M., Mariani, C. (Eds.),
1541 Solanaceae V: Advances in Taxonomy and Utilization. Nijmegen
1542 University Press, Nijmegen, pp. 109–136.
- 1543 Nee, S., Barraclough, T.G., Harvey, P., 1996. Temporal changes in
1544 biodiversity: detecting patterns and identifying causes. In: Gaston,
1545 K.J. (Ed.), Biodiversity: a Biology of Numbers and Difference.
1546 Blackwell Scientific, Oxford, pp. 230–252.
- 1547 Nixon, K.C., Carpenter, J.M., 1996. On simultaneous analysis.
1548 *Cladistics* 12, 221–241.
- 1549 Olmstead, R.G., Sweere, J.A., Spangler, R.E., Bohs, L., Palmer, J.D.,
1550 1999. Phylogeny and provisional classification of the Solanaceae
1551 based on chloroplast DNA. In: Nee, M., Symon, D.E., Lester,
1552 R.N., Jessop, J.P. (Eds.), Solanaceae IV. Royal Botanic Gardens,
1553 Kew, Richmond, pp. 111–137.
- 1554 Parsons, M.J., 1996. Gondwanan evolution of the troidine swallowtails
1555 (Lepidoptera: Papilionidae): cladistic reappraisals using mainly
1556 immature stage characters, with focus on the Birdwings *Ornithop-*
1557 *tera* Boisduval. *Bull. Kitakyushu Mus. Nat. Hist.* 15, 43–118.
- 1558 Portugal, A.H.A., Trigo, J., 2005. Similarity of cuticular lipids between
1559 caterpillar and its host plants: a way to make prey undetectable for
1560 predatory ants? *J. Chem. Ecol.* 31, 2551–2561.
- 1561 Sanderson, M.J., Donoghue, M.J., 1989. Patterns of variation in levels
1562 of homoplasy. *Evolution* 43, 1781–1795.
- 1563 Schluter, D., 2000. The Ecology of Adaptive Radiation. Oxford
1564 University Press, Oxford.
- 1565 Schulz, S., Francke, W., Edgar, J., Schneider, D., 1988. Volatile
1566 compounds from androconial organs of danaine and ithomiine
1567 butterflies. *Zeit. Naturforsch.* 43c, 99–104.
- 1568 Schulz, S., Beccaloni, G., Brown, K.S., Boppré, M., Freitas, A.V.L.,
1569 Ockenfels, P., Trigo, J.R., 2004. Semiochemicals derived from
1570 pyrrolizidine alkaloids in male ithomiine butterflies (Lepidoptera,
1571 Nymphalidae: Ithomiinae). *Biochem. Syst. Ecol.* 32, 699–713.
- 1572 Simpson, G.G., 1953. The Major Features of Evolution. Columbia
1573 University Press, New York.
- 1574 Slowinski, J.B., Guyer, C., 1989. Testing the stochasticity of patterns
1575 of organismal diversity: an improved null model. *Am. Nat.* 134,
1576 907–921.
- 1577 Sorenson, M.D., 1999. Treerot, Version 2. Boston University, Boston.
- 1578 Sourakov, A., Emmel, T.C., 1995. Life history of *Greta diaphana* from
1579 the Dominican Republic. *Trop. Lepid.* 6, 155–157.
- 1580 Swofford, D.L., 1998. PAUP*. Phylogenetic Analysis Using Parsi-
1581 mony (*and Other Methods), Version 4. Sinauer Associates,
1582 Sunderland, MA.
- 1583 Trigo, J.R., Brown, K.S., 1990. Variation of pyrrolizidine alkaloids in
1584 Ithomiinae: a comparative study between species feeding on
1585 Apocynaceae and Solanaceae. *Chemoecology* 1, 22–29.
- Trigo, J.R., Brown, K.S., Witte, L., Hartmann, T., Ernst, L., Euclides, 1586
L., Barata, S., 1996. Pyrrolizidine alkaloids: different acquisition 1587
and use patterns in Apocynaceae and Solanaceae feeding ithomiine 1588
butterflies (Lepidoptera: Nymphalidae). *Biol. J. Linn. Soc.* 58, 1589
99–123.
- Tyler, H.A., Brown, K.S., Wilson, K.H., 1994. Swallowtail butterflies 1591
of the Americas. A Study in Biological Dynamics, Ecological 1592
Diversity, Biosystematics and Conservation. Scientific Publishers, 1593
Gainesville, FL. 1594
- Wahlberg, N., Braby, M.J., Brower, A.V.Z., de Jong, R., Lee, 1595
M.-M., Nylin, S., Pierce, N.E., Sperling, F.A.H., Vila, R., 1596
Warren, A.D., Zakharov, E., 2005. Synergistic effects of com- 1597
bining morphological and molecular data in resolving the 1598
phylogeny of butterflies and skippers. *Proc. R. Soc. Lond. B,* 1599
272, 1577–1586. 1600
- Whinnett, A., Brower, A.V.Z., Lee, M.-M., Willmott, K.R., Mallet, J., 1601
2005. The phylogenetic utility of tektin, a novel region for inferring 1602
systematic relationships amongst Lepidoptera. *Ann. Entomol. Soc.* 1603
Am. in press. 1604
- Willmott, K.R., Lamas, G., 2005. A phylogenetic reassessment of 1605
Hyalenna Forbes and *Dircenna* Doubleday, with a revision of 1606
Hyalenna (Lepidoptera: Nymphalidae: Ithomiinae). *Syst. Entomol., in press.* 1607
1608
- Willmott, K.R., Mallet, J., 2004. Correlations between adult mimicry 1609
and larval hostplants in ithomiine butterflies. *Proc. R. Soc. Lond. B* 1610
(*Biol. Lett.*) Suppl. 271, S266–S269. 1611
- Young, A.M., 1974. A natural historical account of *Oleria zelica* 1612
pagasa (Lepidoptera: Nymphalidae: Ithomiinae) in a Costa Rican 1613
mountain rainforest. *Studies Neotr. Fauna*, 9, 123–139. 1614
- Young, A.M., 1978. Notes on the biology of the butterfly *Hypoleria* 1615
cassotis (Bates) (Nymphalidae: Ithomiinae) in Northeastern Costa 1616
Rica. *Brenesia* 14/15, 97–108. 1617
- Appendix 1. Character list** 1618
- Immature stages* 1619
- Egg and hostplant** 1620
1. *Egg with lateral aspect*: (0) ellipsoidal (Fig. 8B); (1) 1621
truncate (Fig. 8A). There is much variation in the 1622
overall shape of the egg, coded in Char. 3, but the egg 1623
of known *Godyris* is unique in resembling a truncated 1624
cone, distinct from other rounded or ellipsoidal eggs. 1625
2. *Egg with apex*: (0) rounded (Fig. 8B); (1) pointed 1626
(Fig. 8D). Because Char. 1 also concerns shape of the 1627
apex, this character was coded as equivocal for species 1628
with state 1:1. 1629
3. *Egg with ratio between vertical and horizontal axes*, 1630
 r : (0) $1.2 < r < 1.5$ (Fig. 8A); (1) $1.5 < r < 1.7$ 1631
(Fig. 8B); (2) $r > 1.7$ (Fig. 8C); (3) $r < 1.2$ (Fig. 8D). 1632
4. *Egg relative size*: (0) > 2.4 (e.g., Fig. 8D); (1) < 2.4 1633
(e.g., Fig. 8B). Relative size is the cube root of egg 1634
volume (mm^3) (estimated by width \times height \times breadth) 1635
divided by forewing length (cm). 1636
5. *Egg with longitudinal ridges with elevated carinae* 1637
near micropyle: (0) absent (Fig. 8B); (1) present 1638
(Fig. 8G). 1639
6. *Eggs placed*: (0) in isolation (Fig. 8A–C); (1) in 1640
clusters (Fig. 8D,E). Most Ithomiinae lay isolated eggs, 1641
moving between each oviposition. Placing eggs in 1642

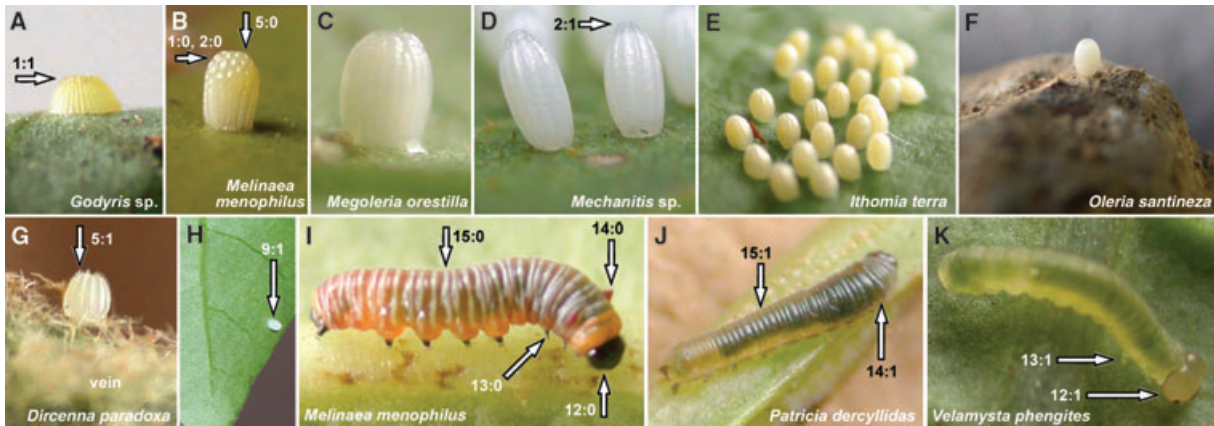


Fig. 8. Ovum, lateral view: (A) *Godyris* sp. (probably *G. panthyle panthyle*) (KRW-210), Ecuador; (B) *Melinaea menophilus zaneka* (KRW-187), Ecuador; (C) *Megoleria o. orestilla* (KRW-285), Ecuador; (D) *Mechanitis* sp., Costa Rica; (E) *Ithomia t. terra* (KRW-267), Ecuador; (F) *Oleria santineza* ssp. n. (KRW-161), egg deposited on stone, Ecuador; (G) *Dircenna paradoxa praestigiosa* (KRW-263), Ecuador; (H) *Methona themisto*, Brazil. First instar larva, dorsolateral view: (I) *Melinaea menophilus zaneka* (KRW-187), Ecuador; (J) *Patricia deryllidas hazelea* (KRW-273), Ecuador; (K) *Velamysta p. phengites* (KRW-184), Ecuador.

1643 clusters from a single position has arisen rarely but
1644 occurs throughout the subfamily.

1645 7. *Oviposition*: (0) on the larval hostplant (Fig. 8A–E);
1646 (1) on other substrates adjacent to the larval hostplant
1647 (Fig. 8F). While most Ithomiinae place eggs on the
1648 larval hostplant, several (but not all) *Oleria* have been
1649 observed to lay eggs on other substrates. One female of
1650 *Oleria santineza* was observed inspecting a fallen leaf of
1651 the larval hostplant *Solanum abitaguense* before laying
1652 five eggs on dead and dried leaves (of other plant
1653 species) and stones (Fig. 8F) around the leaf. One
1654 female of *Oleria fasciata* inspected several *Solanum*
1655 *anceps*, the larval hostplant, before eventually laying a
1656 single egg on a seedling of an unrelated plant species *c.*
1657 0.2 m from the nearest *S. anceps*. *Oleria onega* has also
1658 been recorded to lay eggs off the hostplant (Galluser
1659 et al., 2004), and the trait may also occur in other
1660 highland *Oleria* (H. Greeney, pers. comm.).

1661 8. *If oviposition occurs on the larval hostplant* (Char.
1662 7:0), then preferential placement of the egg near a leaf
1663 vein or a hole is: (0) not marked (Fig. 8H); (1) marked
1664 (Fig. 8G). In species coded state 1, eggs are laid next
1665 to a leaf vein or area of feeding damage about half
1666 the time.

1667 9. *If oviposition occurs on the larval hostplant* (Char.
1668 7:0), then eggs are placed: (0) at random with respect to
1669 leaf border (Fig. 8D); (1) near the leaf border (Fig. 8H).

1670 10. *If oviposition occurs on the larval hostplant* (Char.
1671 7:0), then chosen leaf surface is: (0) underside (Fig. 8H);
1672 (1) upperside (Fig. 8D,E). Most species place eggs
1673 exclusively on the leaf underside, but in *Mechanitis*
1674 and *Ithomia terra*, all of which also lay eggs in clusters,
1675 eggs are always placed on the upperside.

1676 11. *Larval hostplant family*: (0) Apocynaceae
1677 (Fig. 9T); (1) Solanaceae (e.g., Fig. 8A,B); (2) Gesner-

1678 iaceae (Fig. 8C). Apocynaceae is the hostplant family of
1679 *Tellervo*, the most likely sister taxon to the Ithomiinae,
1680 and is common throughout the closely related Danainae
1681 (Ackery and Vane-Wright, 1984; Ackery, 1987). Among
1682 the Ithomiinae it occurs in only three primitive genera
1683 (Drummond and Brown, 1987). Remaining ithomiines
1684 all feed on Solanaceae with the exception of the two
1685 sister genera, *Megoleria* and *Hyposcada*, which feed on
1686 Gesneriaceae (Drummond and Brown, 1987; Willmott,
1687 pers. obs.; G. Beccaloni, pers. comm.; H. Greeney, pers.
1688 comm.).

1689 *Larva: first instar. 12. First instar with color of*
1690 *cephalic capsule*: (0) dark (Fig. 8I); (1) pale to transpar-
1691 ent (Fig. 8K). Most known species have the cephalic
1692 capsule uniformly colored in the first instar; species with
1693 state 0 vary from black to brown, whereas those with
1694 state 1 lack any dark pigmentation.

1695 13. *First instar with color of thoracic legs*: (0) dark
1696 (Fig. 8I); (1) pale to transparent (Fig. 8I).

1697 14. *First instar with subdorsal thoracic filaments*: (0)
1698 conspicuous stubs (Fig. 8I); (1) a slight swelling
1699 (Fig. 8J). In *Patricia* and *Athesis* the future position of
1700 the later instar thoracic filaments are marked only by a
1701 slight subdorsal swelling, whereas in remaining species
1702 that have these filaments in later instars short protuber-
1703 ances are clearly visible. Species that lack thoracic
1704 filaments are coded as not applicable.

1705 15. *First instar with entire transverse dark and light*
1706 *body “rings” extending to base of prolegs*: (0) present
1707 (Fig. 8I); (1) absent (Fig. 8J). Superficially similar rings
1708 are present in *Pteronymia inania* and *P. lonera*, but these
1709 extend only across the dorsum of the larvae, and are
1710 interpreted as non-homologous. These two species were
1711 therefore coded state 1.

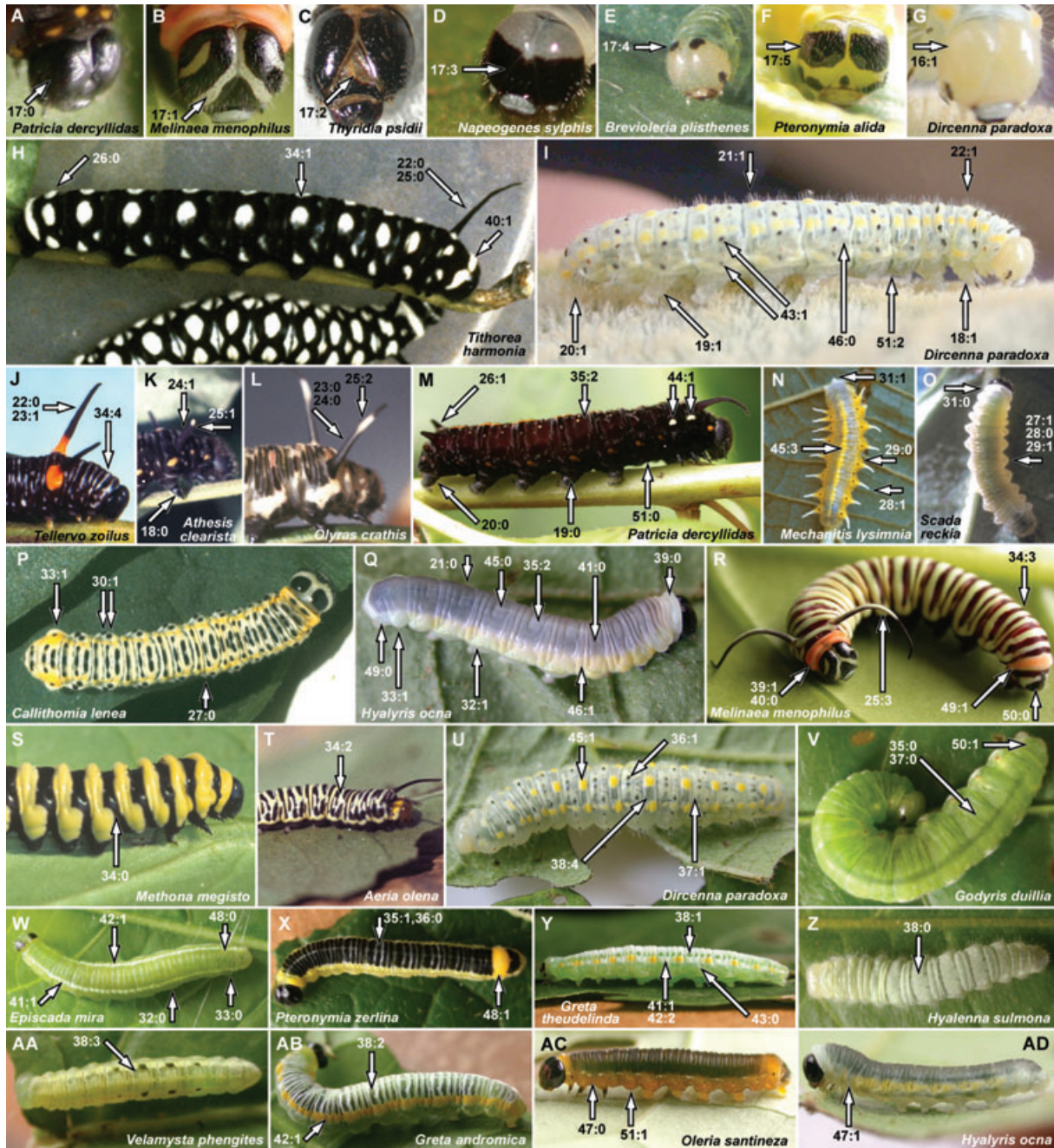


Fig. 9. Last instar larvae. Cephalic capsule, frontal view: (A) *Patricia derycillidas hazelea* (KRW-275), Ecuador; (B) *Melinaea menophilus zaneka* (KRW-186), Ecuador; (C) *Thyridia psidii*, Brazil; (D) *Napeogenes sylphis corena*, Ecuador; (E) *Brevioleria plisthenes*, Brazil; (F) *Pteronymia alida* ssp. n. (KRW-081-2), Ecuador; (G) *Dircenna paradoxa praestigiosa* (KRW-020), Ecuador. Lateral view: (H) *Tithorea harmonia*, Brazil; (I) *Dircenna paradoxa praestigiosa* (KRW-020), Ecuador. Thoracic tubercules: (J) *Tellervo zoilus*, Australia; (K) *Athesis c. clearista*, Venezuela; (L) *Olyras c. crathis*, Venezuela. (M) *Patricia derycillidas hazelea* (KRW-273), lateral view, Ecuador. Dorsal/dorsolateral view: (N) *Mechanitis l. lysimnia*, Brazil; (O) *Scada reckia theaphia*, Brazil; (P) *Callithomia lenea xantho*, Brazil; (Q) *Hyalyris ocna* ssp. n. (KRW-043), Ecuador; (R) *Melinaea menophilus zaneka* (KRW-186), Ecuador; (S) *Methona megisto*, Brazil; (T) *Aeria olena*, Brazil; (U) *Dircenna paradoxa praestigiosa* (KRW-110), Ecuador; (V) *Godyris duillia* (KRW-198), Ecuador; (W) *Episcada apuleia* (KRW-265), Ecuador; (X) *Pteronymia zerlina machay* (KRW-250), Ecuador; (Y) *Greta t. theudelinda* (KRW-224), Ecuador; (Z) *Hyalenna sulmona* ssp. n. (KRW-174), Ecuador; (AA) *Velamysta p. phengites* (KRW-238), Ecuador; (AB) *Greta andromica andania* (KRW-230), Ecuador; (AC) *Oleria santineza* ssp. n. (KRW-161), Ecuador; (AD) *Hyalyris ocna* ssp. n. (KRW-043), Ecuador.

Table 4
Taxon diversity in clades of Solanaceae plants and inferred Ithomiinae herbivores

Solanaceae clade	Plant species diversity	Plant generic diversity	Ithomiinae species diversity	Clade diversity	Notes
Datura	16	2	1	Nee (2001a)	
Capsicum	25	1	6	Nee (2001a)	
Brunfelsia	40	1	7	Nee (2001a)	
Solandra	52	9	18	Nee (2001a)	
Lycianthes	140	1	23	Nee (2001b, p. 109)	Plant species number an estimate, slightly smaller than <i>Cestrum</i>
<i>Withania</i> , etc. clade	202	15	28	Nee (2001a)	Half plant species diversity in single genus <i>Physalis</i> , with center of diversity in Mexico at limit of Ithomiinae range
<i>Cestrum</i>	150	1	66	Nee (2001b)	Plant species number an estimate, Hunziker (1979) estimates 250 species
<i>Solanum</i>	888	1	191	Nee (2001a)	Plant species number an estimate

1712 *Larva: last instar.* 16. *Last instar with dark pigmen-*
1713 *tation in cephalic capsule:* (0) present (e.g., Fig. 9F);
1714 (1) absent (Fig. 9G). Although most species that have
1715 a dark cephalic capsule in the first instar (Char. 12:0)
1716 retain some dark pigmentation in the fifth instar (but
1717 not allo, e.g., *Dircenna paradoxa*), there is consider-
1718 able variation as to whether dark pigmentation
1719 develops in later instars of species that have pale first
1720 instars.

1721 17. *If last instar cephalic capsule has dark pigmentation*
1722 *(Char. 16:0), then capsule:* (0) uniformly colored
1723 (Fig. 9A); (1) with a pale area at the edge of the vertex
1724 shaped like an inverted “v” (Fig. 9B); (2) with a pale
1725 area shaped like an inverted “v” inside the vertex, or
1726 vertex entirely pale (Fig. 9C); (3) with a frontal trans-
1727 verse black band (Fig. 9D); (4) with a dorsal black stripe
1728 or markings (Fig. 9E); (5) with two frontal transverse
1729 black bands, usually with much variation (Fig. 9F).

1730 18. *Last instar thoracic legs:* (0) black (Fig. 9K); (1)
1731 light, lacking dark pigmentation (Fig. 9I).

1732 19. *Last instar with an outer black plate on abdominal*
1733 *prolegs:* (0) present (Fig. 9M); (1) absent (Fig. 9I).

1734 20. *Last instar with black plate on anal prolegs:* (0)
1735 large (Fig. 9M); (1) reduced or absent (Fig. 9I).

1736 21. *Last instar with hairs on cuticle:* (0) short and
1737 sparse (Fig. 9Q); (1) long and dense (Fig. 9I). *Dircenna*,
1738 known *Hyalenna* and *Ceratinia neso* are distinctive in
1739 having the hairs on the cuticle notably denser and longer
1740 than in all other species.

1741 22. *Last instar with subdorsal filaments:* (0) present
1742 (Fig. 9H,J); (1) absent (Fig. 9I). Subdorsal, motile
1743 filaments occur throughout the Danainae and in primi-
1744 tive Ithomiinae.

1745 23. *If last instar has subdorsal filaments (Char. 22:0),*
1746 *then thoracic filaments are:* (0) on the mesothorax
1747 (Fig. 9L); (1) on the metathorax (Fig. 9J). Danainae
1748 show substantial variation in the position of filaments,
1749 which may occur on any thoracic or abdominal body

segment (Ackery and Vane-Wright, 1984). The thoracic
1750 filaments in *Tellervo* are on the metathorax, and in all
1751 Ithomiinae on the mesothorax. 1752

24. *If last instar has subdorsal filaments (Char. 22:0),*
1753 *then thoracic filaments are:* (0) longer than segment
1754 diameter (Fig. 9L); (1) shorter than segment diameter
1755 (Fig. 9K). State 1 occurs only in *Athesis clearista*. 1756

25. *If last instar has subdorsal filaments (Char. 22:0),*
1757 *then thoracic filaments are:* (0) entirely dark (Fig. 9H);
1758 (1) dark with a white tip (Fig. 9K); (2) dark with a white
1759 transverse band (Fig. 9L); (3) dark with a white dorsal
1760 area (Fig. 9R). 1761

26. *If last instar has subdorsal filaments (Char. 22:0),*
1762 *then these are:* (0) confined to thorax (Fig. 9H); (1) also
1763 present on eighth abdominal segment (Fig. 9M). 1764

27. *Last instar with lateral tubercles just above prolegs:*
1765 (0) absent (Fig. 9P); (1) present (Fig. 9O). 1766

28. *If last instar has lateral tubercles above prolegs*
1767 *(Char. 27:1), then they are:* (0) short (Fig. 9O); (1) long
1768 (Fig. 9N). 1769

29. *If last instar has lateral tubercles above prolegs*
1770 *(Char. 27:1), then they are:* (0) yellow (Fig. 9N); (1)
1771 same color as body (Fig. 9O). 1772

30. *Last instar with a pair of lateral swellings on each*
1773 *side of each segment:* (0) absent; (1) present (Fig. 9P).
1774 The upper swelling is positioned slightly dorsal to the
1775 lateral tubercles coded in Char. 27, while the ventral
1776 swelling is slightly dorsal to the sublateral swellings
1777 coded in Char. 32. 1778

31. *Last instar prothoracic segment with two dorsolat-*
1779 *eral protuberances:* (0) absent (Fig. 9O); (1) present
1780 (Fig. 9N). 1781

32. *Last instar with flattened, sublateral swellings,*
1782 *semicircular in dorsal view:* (0) absent (Fig. 9W); (1)
1783 present (Fig. 9Q). These slight swellings are positioned
1784 just below the spiracles and most easily observed in live
1785 larvae. 1786

- 1787 33. *Last instar with projecting lateral swellings on*
 1788 *eighth abdominal segment:* (0) absent (Fig. 9W); (1)
 1789 present (Fig. 9P,Q). This character is correlated almost
 1790 entirely with Char. 32 with the exception of *Callithomia*
 1791 *lenea* and *Pagyris cymothoe*; the former is coded 0,1 and
 1792 the latter 1,0. This swelling forms a blunt, cone-like
 1793 protuberance on which the spiracle sits, and merges with
 1794 the sublateral swelling (Char. 32:1) ventrally.
- 1795 34. *If last instar has transverse body rings (see Char.*
 1796 *15), then:* (0) rings occur singly in each segment
 1797 (Fig. 9S); (1) dark rings merge with one another
 1798 (Fig. 9H); (2) pale rings are irregular, disrupting black
 1799 rings (Fig. 9T); (3) each ring is finely divided (Fig. 9R);
 1800 (4) dark rings are merged to produce a uniform entire
 1801 purplish brown coloration (Fig. 9J).
- 1802 35. *If last instar lacks transverse body rings (see*
 1803 *Char. 15), then dark dorsal pigmentation:* (0) absent
 1804 (Fig. 9V); (1) present, forming a pattern above a pale
 1805 background (Fig. 9X); (2) entirely covering dorsum
 1806 (Fig. 9M,Q). There is a continuum between dorsal
 1807 colors of gray, dark green to olive green, darker
 1808 brown and black, so all these colors are considered to
 1809 represent dark pigmentation. All Napeogenini, Ithomi-
 1810 iini and Oleriini have almost uniform, dark dorsal
 1811 coloration of this kind (state 2), while all Godyridini
 1812 and Dircennini have pale green, largely translucent
 1813 bodies on which there may or may not be isolated
 1814 darker markings (states 0,1).
- 1815 36. *If last instar has patterned dark dorsal pigmentation*
 1816 *(Char. 35:1), it is expressed as:* (0) lines (Fig. 9X); (1)
 1817 spots and dashes (Fig. 9U).
- 1818 37. *If last instar has at least some area of dorsum*
 1819 *lacking dark pigmentation (Char. 35:0,1) then pale*
 1820 *green-white opaque markings are:* (0) absent (Fig. 9V);
 1821 (1) present (Fig. 9U). Larvae may be entirely translucent
 1822 green or also bear patches of opaque white, yellowish or
 1823 green coloration.
- 1824 38. *If last instar has pale green-white opaque markings*
 1825 *(Char. 37:1), then translucent unmarked areas:* (0) are
 1826 absent (i.e., entire dorsum is opaque) (Fig. 9Z); (1) form
 1827 a series of small spots, four to each segment, in a line
 1828 immediately dorsal of pale subdorsal line (Fig. 9Y); (2)
 1829 form transverse lines, four to each segment, crossing the
 1830 dorsum (these appear to represent expanded, joined
 1831 spots of state 2) (Fig. 9AB); (3) form a “U”-shaped
 1832 pattern in each segment, with the base of the “U” at the
 1833 dorsal edge of the pale subdorsal line (Fig. 9AA); (4) are
 1834 distributed in uneven patches (Fig. 9U); (5) are exten-
 1835 sive, leaving thin opaque lines in each segment
 1836 (Fig. 10D).
- 1837 39. *Last instar with contrasting colored “collar” on*
 1838 *prothorax:* (0) absent (Fig. 9Q); (1) present (Fig. 9R).
- 1839 40. *If last instar has a contrastingly colored prothoracic*
 1840 *“collar” (Char. 39:1), it is:* (0) yellow/orange (Fig. 9R);
 1841 (1) white (Fig. 9H).
41. *Last instar with a pair of subdorsal stripes:* (0) 1842
 absent (Fig. 9Q); (1) present (Fig. 9W,Y). State 1 is an 1843
 apparent synapomorphy for the Godyridini and Dir- 1844
 cennini. It is present in most known species and where it 1845
 is absent it has apparently been lost due to overall 1846
 reduction in body markings. 1847
42. *If last instar has a subdorsal stripe (Char. 41:1),* 1848
then it is: (0) uniform pale blue/green (Fig. 9W); (1) 1849
 uniform yellow (Fig. 9AB); (2) yellow in posterior end 1850
 (usually half) of each segment, and pale in the anterior 1851
 half (Fig. 9Y). 1852
43. *Last instar with a pair of lateral black dots (one* 1853
above, one below spiracle) in each segment: (0) absent 1854
 (Fig. 9Y); (1) present (Fig. 9I). 1855
44. *Last instar with two conspicuous pale yellow lateral* 1856
spots in segments 2A and 3A: (0) absent; (1) present 1857
 (Fig. 9M). 1858
45. *Last instar with pale mid-dorsal markings:* (0) 1859
 absent (Fig. 9Q); (1) a single pale yellow spot at 1860
 posterior edge of each segment (Fig. 9U); (2) three 1861
 orange spots on posterior 3 sections of each segment 1862
 (Fig. 10A); (3) a complete yellowish line on abdominal 1863
 segments only (Fig. 9N); (4) a complete, yellowish line 1864
 broken in the middle of each segment (Fig. 10C); (5) a 1865
 complete, pale greenish line (Fig. 10B). *Hypothyris* 1866
euclea apparently bears a mid-dorsal line, but this is 1867
 the black ground color visible between two subdorsal 1868
 bands of pale markings, not homologous with the pale 1869
 mid-dorsal lines coded here, which are green to 1870
 yellow. 1871
46. *Last instar with a colored lateral stripe (centred on* 1872
spiracles): (0) absent (Fig. 9I); (1) present (Fig. 9Q). 1873
 This stripe occurs in virtually all Mechanitini, Napeo- 1874
 genini, Ithomiini and Oleriini, but is absent elsewhere. 1875
47. *If last instar has a lateral stripe (Char. 46:1), then* 1876
it is: (0) complete (Fig. 9AC); (1) present on the 1877
 abdomen only (Fig. 9AD). 1878
48. *Last instar with subdorsal stripe expanded on eighth* 1879
abdominal segment to form a more or less complete dorsal 1880
band: (0) absent (Fig. 9W); (1) present (Fig. 9X). State 1 1881
 is an apparent synapomorphy for *Pteronymia*, occurring 1882
 in all known species. The yellow to yellow-green 1883
 subdorsal stripe is always broader in the eighth segment 1884
 than adjacent segments through dorsal expansion, and 1885
 varies from being slightly expanded (Fig. 10B) to 1886
 connecting across the segment and forming an entire 1887
 colored band (Fig. 9X). 1888
49. *Last instar with a conspicuous colored “ring” on the* 1889
ninth abdominal segment: (0) absent (Fig. 9Q); (1) 1890
 present (Fig. 9R). 1891
50. *Last instar with color of anal plate:* (0) mostly dark 1892
 (Fig. 9R); (1) other (with dark pigmentation very 1893
 reduced or absent) (Fig. 9V). 1894
51. *Last instar ventral color:* (0) dark (Fig. 9M); (1) 1895
 white to yellow (Fig. 9AC); (2) green (Fig. 9I). 1896



Fig. 10. Final instar larva, dorsal view: (A) *Patricia deryllidas* (KRW-273), Ecuador; (B) *Pteronymia alida* ssp. n. (KRW-81-2), Ecuador; (C) *Pteronymia euritea*, Brazil; (D) *Brevioleria plisthenes*, Brazil. Pupa, lateral view: (E) *Scada reckia theaphia*, Brazil; (F) *Oleria santineza* ssp. n. (KRW-161), Ecuador; (G) *Placidina euryanassa*, Brazil; (H) *Methona themisto*, Brazil; (I) *Greta andromica* (KRW060-2), Ecuador; (J) *Hyoscada anchiala* ssp. n., Ecuador (G.W. Beccaloni); (K) *Hyaliris ocna* ssp. n. (KRW-043), Ecuador; (L) *Episcada a. apuleia* (KRW-179), Ecuador; (M) *Tithorea harmonia gilbertii*, Peru (K.S. Brown). Pupa, dorsal view: (N) *Episcada a. apuleia* (KRW-215), Ecuador; (O) *Dircenna paradoxa praestigiosa* (KRW-129), Ecuador; (P) *Melinaea menophilus zaneka* (KRW-186), Ecuador; (Q) *Greta andromica andania* (KRW-060-2), Ecuador; (R) *Melinaea menophilus zaneka* (KRW-187), Ecuador; (S) *Ithomia t. terra* (KRW-269), Ecuador; (T) *Dircenna paradoxa praestigiosa*, as J; (U) *Hyaliris ocna* ssp. n. (KRW-058-1), Ecuador. Pupa, ventral view of abdomen tip and cremaster: (V) *Dircenna dero celtina*, Brazil; (W) *Melinaea menophilus zaneka* (KRW-187), Ecuador; (X) *Methona themisto*, Brazil; Eclosed pupa, lateral view: (Y) *Greta andromica andania* (KRW-60-2), Ecuador; (Z) *Episcada apuleia apuleia* (KRW-193), Ecuador. Final instar leaf shelter: (AA) *Dircenna adina lorica* (KRW-048), on *Solanum asperum*, Ecuador; (AB) *Dircenna adina lorica* (KRW-260), on *Solanum* sp. (sect. *torva*), Ecuador. Pharmacophagy: (AC) *Oleria tremona tremona*, male, feeding on Asteraceae flowers, Ecuador; (AD) various Ithomiinae and Danainae feeding at dried Boraginaceae bait, Brazil, Acre (1: *Melinaea menophilus*; 2: *Hypothyris semifulva*; 3: *Hypoleria lavinia*; 4: *Pteronymia tucuna*; 5: *Lycorea halia*, Danainae).

- 1897 52. *Last instar rests in a “J” posture*: (0) present 1953
 1898 (Fig. 9V); (1) absent (Fig. 9N). This characteristic 1954
 1899 resting posture occurs throughout the Ithomiinae with 1955
 1900 the exception of a handful of species in which it has 1956
 1901 apparently been lost.
- 1902 53. *Last instar leaf-shelter building behavior*: (0) absent 1957
 1903 (Fig. 9V); (1) a single leaf is bent (early instars) or rolled 1958
 1904 (later instars) and fastened loosely with silk (Fig. 10- 1959
 1905 AA,AB); (2) several leaves are loosely fastened together 1960
 1906 with silk. State 1 is an apparent synapomorphy for 1961
 1907 *Dircenna* + *Hyalenna*, while state 2 has been observed 1962
 1908 only in *Episcada clausina*. 1963
 1909 54. *Pupal angle*: (0) 180° (Fig. 10G); (1) 120° 1964
 1910 (Fig. 10E); (2) 90° (Fig. 10J). There is much variation 1965
 1911 between, but not within clades, in the extent to which the 1966
 1912 pupa is angled at the abdomen/thorax suture. Most of the 1967
 1913 more primitive species have a slight angle (state 1), most 1968
 1914 of the more derived species have a sharper angle (state 2), 1969
 1915 and small groups of species (*Methona*, some Mechanitini 1970
 1916 and *Placidina*) have a straight pupa (state 0). 1971
- 1917 55. *Dorsal edge of abdomen in posterior half to* 1972
 1918 *cremaster with a pronounced curve*: (0) absent (Fig. 10E); 1973
 1919 (1) present (Fig. 10H). 1974
- 1920 56. *Dorsal edge of abdomen at thorax/abdomen suture*: 1975
 1921 (0) slightly indented (120–180°) (Fig. 10E); (1) deeply 1976
 1922 indented (90°) (Fig. 10F). 1977
- 1923 57. *Abdominal segment 1 in comparison with segment* 1978
 1924 *2*: (0) of similar width (Fig. 10N); (1) constricted to half 1979
 1925 or less width (Fig. 10O); (2) absent (Fig. 10R). *Epityches* 1980
 1926 *eupompe* is difficult to evaluate because of fusion 1981
 1927 between abdominal segments, but segment 1 appears 1982
 1928 to be state 0. 1983
- 1929 58. *Protuberances at the base of the cremaster stalk in* 1984
 1930 *dorsal view*: (0) absent or vestigial (Fig. 10N); (1) 1985
 1931 conspicuous (Fig. 10O,P). 1986
- 1932 59. *Dorsal edge of abdomen at third abdominal* 1987
 1933 *segment*: (0) slightly protruding (Fig. 10M); (1) smooth 1988
 1934 (Fig. 10K). 1989
- 1935 60. *If dorsal edge of abdomen is protruding at third* 1990
 1936 *segment (Char. 59:0), then protrusion is*: (0) broad 1991
 1937 across the abdomen, like a “shelf” (Fig. 10M); (1) a 1992
 1938 bump at the middle of the abdomen only (Fig. 10J). 1993
- 1939 61. *Lateral tubercles at junction between wing base and* 1994
 1940 *posterior edge mesothorax*: (0) absent (Fig. 10Q); (1) 1995
 1941 present (Fig. 10R). In dorsal view, two (one each side) 1996
 1942 more or less pointed lateral projections are visible in all 1997
 1943 species near the junction of the wing base and anterior 1998
 1944 edge of the mesothorax. In a number of species an 1999
 1945 additional pair of tubercles (again one each side) are 2000
 1946 also present in a more posterior position at the posterior 2001
 1947 edge of the mesothorax. In *Dircenna dero* both pairs of 2002
 1948 tubercles are present, though the posterior pair is rather 2003
 1949 reduced. 2004
- 1950 62. *Ocular caps*: (0) rounded (Fig. 10R); (1) pointed 2005
 1951 (Fig. 10Q). The ocular caps are blunt, short projections 2006
 1952 that may either be rounded or pointed. 2007
 2008
63. *Ground color of pupa*: (0) yellow to greenish 1953
 (Fig. 10P); (1) light green (Fig. 10J); (2) strong green 1954
 (Fig. 10L); (3) cream white to light brown (Fig. 10K); 1955
 (4) dark brown (Fig. 10E); (5) orange (Fig. 10F). 1956
64. *Brown coloration in pupal skins after eclosion*: (0) 1957
 absent (Fig. 10Y); (1) present (Fig. 10Z). In the majority 1958
 of species the pupal cases after eclosion are colorless, 1959
 with the exception of black spots or markings. In some 1960
 species, notably in the Dircennini, there is an additional 1961
 brown coloration present, especially along the edges of 1962
 the wing cases, abdomen and cephalic region, sometimes 1963
 occurring over the entire pupa. 1964
65. *Reflective areas*: (0) absent (Fig. 10R); (1) small 1965
 stripes at edges of wing cases and wing veins (Fig. 10Q); 1966
 (2) covering most of wing case and abdomen (Fig. 10T); 1967
 (3) diffuse scattered areas throughout pupa (Fig. 10S); 1968
 (4) pupa totally reflective (Fig. 10M). Many ithomiine 1969
 pupae have areas that are brilliantly reflective gold, 1970
 silver or other colors. 1971
66. *Color of the cremaster stalk*: (0) black (Fig. 10P); 1972
 (1) red to pinkish (Fig. 10N); (2) colorless (Fig. 10O). 1973
67. *Central dorsal black spot on abdominal segment* 1974
3: (0) absent (Fig. 10S); (1) present (Fig. 10Q). This spot 1975
 is positioned on the abdominal segment 3 protrusion 1976
 (Char. 59:0), when that is present. 1977
68. *Paired dorso-lateral patterned bands on abdomen*: 1978
 (0) unmarked/same color as rest of pupa (Fig. 10T); 1979
 (1) with mottled brown pattern (Fig. 10S); (2) with an 1980
 even brown pattern (Fig. 10N); (3) absent except 1981
 single spot on segment 2 (Fig. 10R). Distinct dorso- 1982
 lateral bands are visible in most species, and in some 1983
 (e.g., *Episcada*) they merge to form a single dorsal 1984
 band. They may be marked with various darker colors 1985
 or be visible as distinct, unmarked ground color 1986
 between reflective areas. In *Melinaea menophilus* these 1987
 bands are absent except for a single mid-dorsal spot in 1988
 segment 2 formed by their fusion (inferred from 1989
 examination of other species in which fusion also 1990
 occurs, e.g., *Episcada*). 1991
69. *If paired dorso-lateral bands on abdomen have* 1992
mottled brown pattern present (Char. 68:1), then pattern: 1993
 (0) confined to bands (Fig. 10S); (1) spread as speckling 1994
 over abdomen (Fig. 10U); (2) broken into isolated spots 1995
 scattered over abdomen (Fig. 10G). 1996
70. *Lateral dark spot on abdominal segment 2 sur-* 1997
rounding or dorsal of spiracle: (0) absent (Fig. 10L); (1) 1998
 present (Fig. 10K). A number of species have brownish 1999
 coloration in this area and elsewhere on the pupa (see 2000
 Char. 64), but this is regarded as distinct from the black 2001
 spots coded here. 2002
71. *Lateral black spot in section between end of* 2003
abdominal segment 1 and wing margin: (0) absent 2004
 (Fig. 10L); (1) present (Fig. 10I). 2005
72. *Dorsal black stripe on suture between eighth and* 2006
ninth abdominal segments: (0) present (Fig. 10P); (1) 2007
 absent (Fig. 10Q). 2008

2009 73. *Dark markings on wing cases*: (0) large black
2010 spots (Fig. 10H); (1) parallel thin black lines
2011 (Fig. 10M); (2) two “v”-shaped discal marks, shading
2012 more or less along postdiscal veins and a line of
2013 submarginal dark spots (Fig. 10F); (3) fine, irregular
2014 lateral parallel lines (Fig. 10G); (4) diffuse irregular
2015 markings (Fig. 10K); (5) tiny black dots (Fig. 10I); (6)
2016 absent (Fig. 10L).

2017 74. *Exuvial holdfast tubercles (EHTs)*: (0) strongly
2018 sclerotized with black markings (Fig. 10W); (1)
2019 unmarked (Fig. 10V).

2020 75. *If EHTs are marked (Char. 74:0), then dark*
2021 *markings*: (0) cover EHTs only (Fig. 10W); (1) join the
2022 EHTs to one another and to the cremaster stalk
2023 (Fig. 10X).

2024 *Adult*

2025 *Ecology and chemistry*

2026 76. *Male attraction to pyrrolizidine alkaloid (PA)*
2027 *sources*: (0) absent/low; (1) high (Fig. 10AC,AD). PAs
2028 play a crucial role in the ecology of Danainae (for
2029 references see Ackery and Vane-Wright, 1984) and
2030 Ithomiinae, being the precursors for defensive chemicals
2031 (Brown, 1984) as well as male-disseminated sexual
2032 pheromones (Edgar et al., 1976). PAs are obtained by
2033 adults feeding at various sources (pharmacophagy),
2034 mainly Asteraceae flowers (Fig. 10AC) (and, rarely, leaf
2035 stems and/or branches) as well as dried or withered
2036 plants in the Boraginaceae (Fig. 10AD). In the Ithomi-
2037 iinae, species that show low attraction also tend to have
2038 females as well as males visiting PA sources; in species
2039 that have strong attraction it is almost exclusively males
2040 that visit such sources, because PAs are transferred to
2041 the female in the spermatophore (Brown, 1985). There-
2042 fore, although sexual dimorphism in pharmacophagy
2043 was initially coded as a character, it was excluded
2044 because it is strongly correlated with this character.
2045 Coding of this and the following character is based on
2046 several decades of field observations by KSB and
2047 AVLF, during which time baits of dried *Heliotropium*
2048 (Boraginaceae) were used extensively to attract ithomi-
2049 iines. Some additional Andean species are coded for this
2050 character based on observations of KRW of flower-
2051 feeding, but as baits were not used these species are
2052 coded as unknown for Char. 77.

2053 77. *If male attraction to PA sources is high (Char.*
2054 *76:1), then PA sources are*: (0) diverse, including
2055 Boraginaceae baits (Fig. 10AD); (1) mainly flowers of
2056 Eupatoriae (Fig. 10AC).

2057 78. *Level of PA storage in adults*: (0) low (< 1% dry
2058 weight); (1) high (1–20% dry weight). Basal Ithomiinae
2059 tend to store PAs from larval hostplants, and adults are
2060 generally not strongly attracted to PA sources, resulting
2061 in low levels of PA storage in adults (Brown, 1985; Trigo
2062 et al., 1996).

79. *3-OH-kynurenine in adults*: (0) absent; (1) present. 2063
The yellow pigment in the scales of many Ithomiinae is 2064
derived from 3-OH-kynurenine (Brown, 1967). 2065

80. *Male attraction to red flowers*: (0) frequent; (1) 2066
rare. Coding of this character is based mainly on 2067
extensive observations of ithomiine populations by 2068
KSB and AVLF in Brazil (São Paulo and other south- 2069
eastern states and Acre). The ecological significance of 2070
this behavior is unknown, but the lack of attraction to 2071
red flowers (unlike many other nymphalids) may be 2072
linked with the dependence of most species coded state 1 2073
on the predominantly white flowers of Asteraceae as a 2074
PA source. 2075

81. *Male attraction to rotting fish bait*: absent or very 2076
rare (0); common (1). A large proportion of all 2077
Nymphalidae are strongly attracted to baits of rotting 2078
carion, as well as to feces and damp sand or mud, 2079
especially when urine is present. These food substrates 2080
attract similar species and most likely provide sodium 2081
ions, among other possible nutrients (Arms et al., 1974). 2082
Feeding behavior is apparently related to adult mor- 2083
phology and ecology (Hall and Willmott, 2000), and 2084
very probably also to larval hostplants. Among the 2085
Ithomiinae only *Elzunia* and *Tithorea* are regularly 2086
attracted to rotting fish bait, based on 26 months of field 2087
work in Ecuador by KRW with extensive trapping in 2088
virtually all habitats where ithomiines occur. Outgroup 2089
behavior (*Tellervo*) is unknown, but species in the only 2090
neotropical forest danaine genus *Lycorea* Doubleday 2091
[1847] are also strongly attracted to fish baits. 2092

2093 *Male body*

2094 *Antenna*. The following two characters are based on 2094
an unpublished study by A. Brower (pers. comm.). 2095
There is substantial variation in the extent to which 2096
antennae are scaled, ranging from dense scales from the 2097
antennal base to the base of the club in some *Episcada* 2098
and *Aeria*, to only sparse scaling on the basal anten- 2099
nomeres in, for example, some *Oleria*. This variation is 2100
correlated to some extent with antennal color, with 2101
yellow antennae lacking scales, but not entirely, as 2102
Oleria antennae are black. There is also significant 2103
variation in the morphology of the carinae, the three 2104
ridges on the ventral surface of the antenna common to 2105
all Nymphalidae. These are almost absent in some 2106
Mechanitini, Ithomiini and Dircennini, and more 2107
marked in Oleriini. Some species (e.g., *Olyras* and 2108
Mechanitini) have more closely spaced carinae, with the 2109
lateral carinae about half way between the medial carina 2110
and antenna edge, while in others (e.g., Oleriini) the 2111
lateral carinae are placed at the distal edge of the 2112
antenna. Unfortunately, across the range of taxa studied 2113
here, it proved difficult to define character states and 2114
therefore to code much of this variation. 2115

82. *Sulci (ventral depressions containing sensory hairs)* 2116
on fourth from terminal antennomere of female antenna: 2117

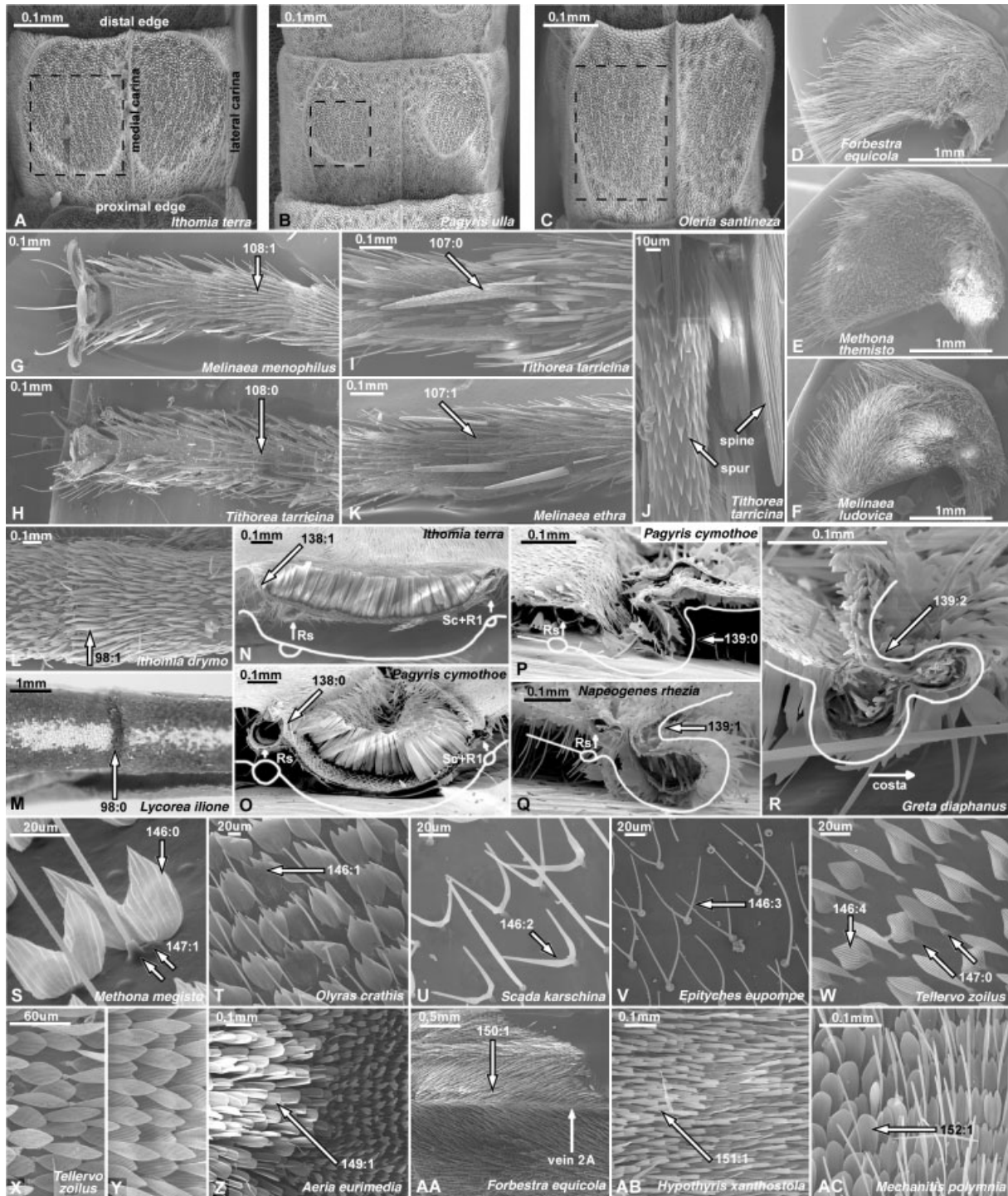


Fig. 11. Female antenna, fourth antennomere, ventral view (limits of sulci marked with dashed line): (A) *Ithomia t. terra*; (B) *Pagyris u. ulla*; (C) *Oleria s. santineza*. Male left tegula, lateral view: (D) *Forbestra e. equicola*; (E) *Methona themisto*; (F) *Melinaea l. ludovica*. Legs: (G) *Melinaea m. menophilus*, female mid-leg tarsus, ventral view; (H) *Tithorea tarricina pinthias*, same as G; (I) *Tithorea tarricina pinthias*, female mid-leg tibia and spurs; (J) same as I, tibial spur (left) and spine (right); (K) *Melinaea ethra*, female mid-leg tibia. Male ventral abdomen, junction tergites 2 (right) and 3 (left): (L) *Ithomia drymo*; (M) *Lycorea ilione*. Male hindwing anterior edge, cross-section through androconial scale patch between veins Sc + R1 and fRs, looking distally: (N) *Ithomia t. terra*; (O) *Pagyris cymothoe cymothoe*. Male hindwing anterior edge, cross-section through androconial scale patch between veins Sc + R1 and Rs, looking basally: (P) *Pagyris c. cymothoe*; (Q) *Napeogenes r. rhezia*; (R) *Greta diaphanus*. Wing scales: (S) *Methona megisto*, male DHW transparent area; (T) *Olyras c. crathis*, male DFW yellow tornal spot; (U) *Scada k. karschina*, male DFW translucent area; (V) *Epityches eupompe*, male DHW transparent area; (W) *Tellervo zoilus*, male DFW translucent white area. Androconial wing scales: (X) *Tellervo zoilus*, male DFW tornus, light basal area; (Y) as X, dark distal area; (Z) *Aeria eurimedia*, male DFW discal cell, androconial (left) and wing (right) scales; (AA) *Forbestra e. equicola*, male DFW elongate androconial scales lining vein 2A; (AB) *Hypothyris xanthostola*, male DHW cell 2A-Cu2, androconial (left) and non-androconial (right) scales; (AC) *Mechanitis p. polymnia*, male DHW anterior edge cell Cu1-M3, androconial (left) and nonandroconial (right) scales.

2118 (0) equidistant from medial and lateral carinae
 2119 (Fig. 11A); (1) nearer to lateral carinae (Fig. 11B).
 2120 There is variation in the size, depth, definition and
 2121 position of sulci among the Ithomiinae. Sulci range from
 2122 a shallow, smooth scoop in more primitive species (e.g.,
 2123 Melinaeini, *Tithorea*) to well-marked depressions (e.g.,
 2124 *Pteronymia*, *Episcada*, *Ceratinia*). Owing to continuous
 2125 variation, however, it proved difficult to code sulci
 2126 shape, and only two characters, based on sulci position,
 2127 were defined.

2128 83. *Sulci on fourth from terminal antennomere of*
 2129 *female antenna*: (0) equidistant from distal and proximal
 2130 edges of antennomere (Fig. 11A); (1) nearer proximal
 2131 edge of antennomere (Fig. 11C).

2132 *Labial palpus and head*. The third palpal segment is
 2133 variable in size, but due to continuous variation no
 2134 character was coded.

2135 84. *Labial palpus color in lateral view*: (0) black at tip
 2136 (segment 3) and on ventral half on segment 2 (dorsally
 2137 white) (Fig. 12B); (1) black at tip and extending
 2138 medially into segment 2 (Fig. 12A); (2) entirely black
 2139 (Fig. 12C).

2140 85. *Labial palpus with long blade and/or hair-like*
 2141 *scales ventrally*: (0) present (Fig. 12B); (1) absent
 2142 (Fig. 12A). These elongate scales are noticeably distinct
 2143 from the scales clothing the sides of the palpus.

2144 86. *Frons*: (0) black with ventrally tapering white
 2145 borders (Fig. 12E); (1) black with white border restric-
 2146 ted to dorsal half (Fig. 12F); (2) entirely black
 2147 (Fig. 12D).

2148 87. *Dorsal head with pale central marking*: (0) a small
 2149 dash posterior of antennae bases (Fig. 12H); (1) a line
 2150 extending from posterior edge of head to ventral edge of
 2151 frons (Fig. 12G).

2152 *Patagia, tegula, thorax and abdomen*. 88. *Patagia with*
 2153 *outer half of lobes*: (0) largely reddish orange (Fig. 12H);
 2154 (1) white to cream (Fig. 12I); (2) black (Fig. 12J); (3)
 2155 yellow (Fig. 12K).

2156 89. *Patagia with inner part of lobes, if different from*
 2157 *outer half*: (0) black (Fig. 12I); (1) white (Fig. 12J); (2)
 2158 reddish brown (Fig. 12L). Species with uniformly co-
 2159 lored patagia are coded as equivocal, to avoid duplica-
 2160 ting the previous character.

2161 90. *Anterior ventral projection of tegula*: (0) pale
 2162 yellow to white (Fig. 12N); (1) partially pale in center
 2163 (Fig. 12P); (2) dark brown/black (Fig. 12O); (3) reddish
 2164 brown (Fig. 12M).

2165 91. *Scale direction on tegula*: (0) posterior, except
 2166 more or less radiating from a postero-ventral point
 2167 (Figs 11D and 12M); (1) anticlockwise (right tegula)
 2168 around a central point (Figs 11E and 12P); (2) clockwise
 2169 (right tegula) and converging on center (Figs 11F and
 2170 12N). Scales typically lie flat against the tegula and all
 2171 point in a certain direction.

2172 92. *Pale continuous central band on tegula*: (0) absent
 2173 (Fig. 12O); (1) present (Fig. 12N).

93. *Dorsal thorax with pale midline*: (0) even in width 2174
 (Fig. 12Q); (1) tapering posteriorly (Fig. 12R); (2) 2175
 reduced to posterior third (Fig. 12S); (3) an elongate 2176
 central dash (Fig. 12T); (4) a small central spot 2177
 (Fig. 12U); (5) absent (Fig. 12V). Because this character 2178
 essentially codes reduction in the thoracic midline, 2179
 “absent” was logically included as a state rather than 2180
 a separate character. 2181

94. *Scales on dorsal metathorax pointing*: (0) anteriorly 2182
 (Fig. 13A); (1) anteriorly, except at apex where vertical 2183
 (Fig. 13B); (2) vertically, except anteriorly at posterior 2184
 edge (Fig. 13C); (3) vertically (Fig. 13D); (4) in circular 2185
 pattern on either side of thorax, pointing anteriorly in 2186
 center (Fig. 13E); (5) posteriorly, except anteriorly at 2187
 posterior edge (Fig. 13F); (6) in circular pattern on 2188
 either side of thorax, pointing posteriorly in center 2189
 (Fig. 13G). This character was occasionally difficult to 2190
 assess in museum specimens, especially as the metatho- 2191
 rax is often damaged by the pin and may have scales 2192
 rubbed off. Scales either lie flat against the metathorax 2193
 or nearly vertically. 2194

95. *Dorsal abdomen color*: (0) dark brown (Fig. 12W); 2195
 (1) orange-brown (Fig. 12X); (2) dark brown, yellow 2196
 laterally towards the base (Fig. 12Y); (3) dark brown 2197
 with lateral orange-brown smudges in the middle of 2198
 each tergite (Fig. 12Z); (4) dark brown, with the ventral 2199
 half of tergites white posteriorly (Fig. 12AA); (5) dark 2200
 brown with the edges of tergites lined with pale gray 2201
 (Fig. 12AB); (6) dark brown with white spots in the 2202
 middle of the posterior edge of each tergite (Fig. 12AC); 2203
 (7) dark brown with white spots at the anterior corner 2204
 ventral edge of tergites (Fig. 12AD); (8) dark brown 2205
 with white spots at posterior corner ventral edge of 2206
 tergites (Fig. 12AE); (9) black with white lateral spots at 2207
 the middle ventral edge of each tergite and a white 2208
 dorsal line of spots in the middle of each tergite 2209
 (Fig. 12AF); (A) dark brown with a pale, broken 2210
 dorsolateral line (Fig. 12AG); (B) dark brown with a 2211
 continuous pale dorsolateral line (Fig. 12AH). Like the 2212
 following two characters, the dorsal abdomen color 2213
 pattern is to some extent affected by mimicry. Never- 2214
 theless, despite often similar appearances, the precise 2215
 position of pattern elements with respect to body 2216
 sclerites provides evidence as to homology in pattern 2217
 development. 2218

96. *Ventral thorax pale stripes*: (0) continuous 2219
 from coxa to wing base on meso- and metathoraces 2220
 (Fig. 12AI); (1) broken at dorsal edge of meron 3 2221
 (Fig. 12AJ); (2) broken at meron 3 (Fig. 12AK); (3) 2222
 absent on meron 3 (Fig. 12AL); (4) broken on meron 2 2223
 and 3 (Fig. 12AM); (5) broken into white spots on 2224
 ventral edge of meron and between meron and epister- 2225
 num (Fig. 12AN); (6) broken into white spots at dorsal 2226
 edge of meron, episternum (Fig. 12AO). The ventral 2227
 thorax has lateral pale white to yellow stripes immedi- 2228
 ately basal of black stripes where the legs fold against 2229

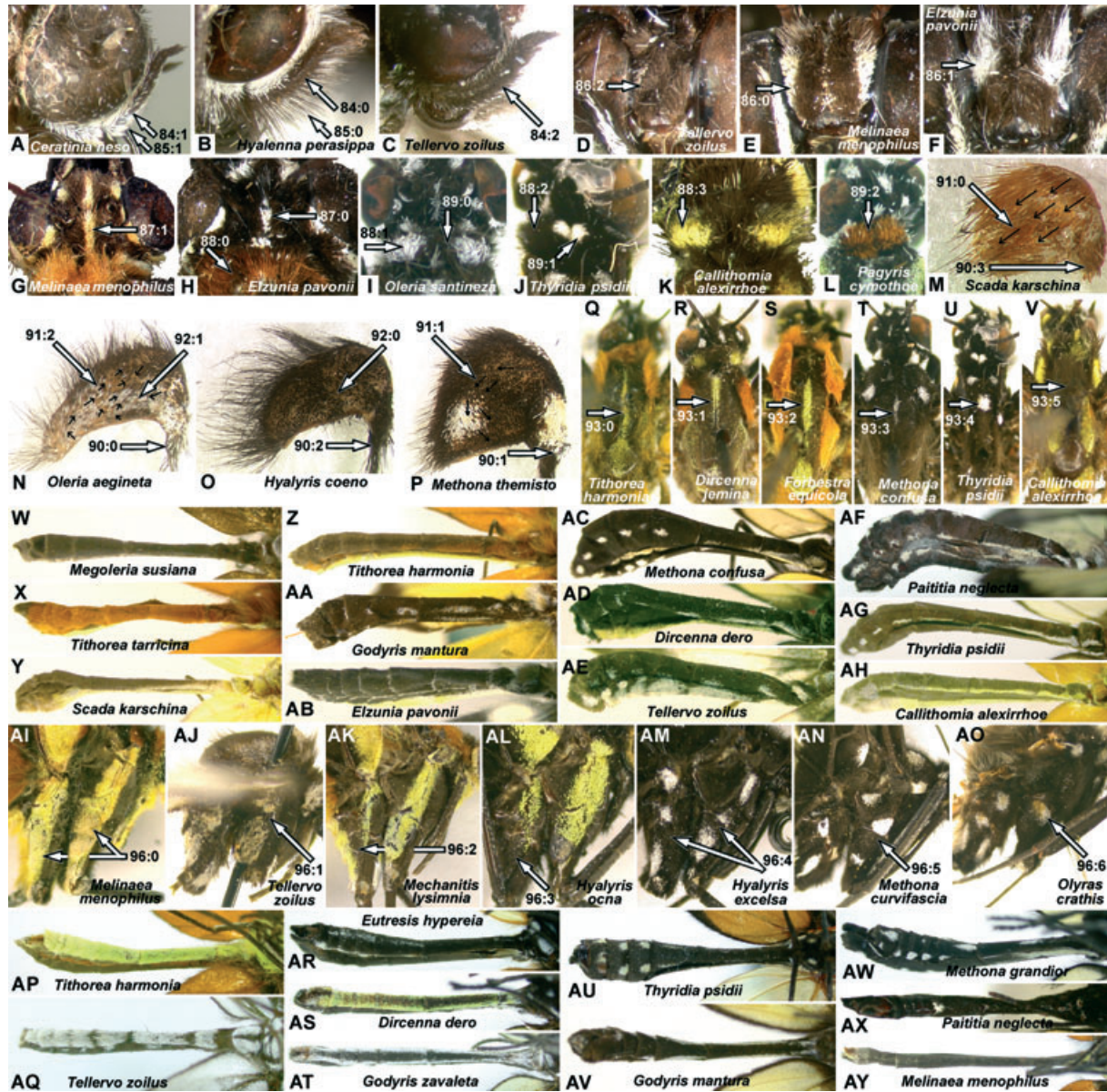


Fig. 12. Labial palpi: (A) *Ceratinia n. neso*; (B) *Hyalenna perasippa* ssp. n.; (C) *Tellervo z. zoilus*. Frons: D, *Tellervo z. zoilus*; (E) *Melinaea menophilus zaneka*; (F) *Elzunia pavonii*. Head and patagia, dorsal view: G, *Melinaea menophilus zaneka*; (H) *Elzunia pavonii*; (I) *Oleria s. santineza*; (J) *Thyridia psidii* aedesia; (K) *Callithomia alexirrhoe* butes; (L) *Pagyris cymothoe cymothoe*. Right tegula: M, *Scada k. karschina*; (N) *Oleria aegineta inelegans*; (O) *Hyalyris c. coeno*; (P) *Methona themisto*. Dorsal thorax: (Q) *Tithorea harmonia manabiana*; (R) *Dircenna jemina visina*; (S) *Forbestra equicola equicoloides*; (T) *Methona c. confusa*; (U) *Thyridia psidii* aedesia; (V) *Callithomia alexirrhoe* butes. Abdomen, dorsolateral view: (W) *Megolera s. susiana*; (X) *Tithorea tarricina bonita*; (Y) *Scada karschina*; (Z) *Tithorea harmonia hermas*; (AA) *Godyris mantura honrathi*; (AB) *Elzunia pavonii*; (AC) *Methona c. confusa*; (AD) *Dircenna dero* ssp. n.; (AE) *Tellervo z. zoilus*; (AF) *Paititia neglecta*; (AG) *Thyridia psidii* ino; (AH) *Mechanitis polymnia chimborazona*. Ventral thorax, lateral view: (AI) *Melinaea menophilus zaneka*; (AJ) *Tellervo z. zoilus*; (AK) *Mechanitis lysimnia menceles*; (AL) *Hyalyris ocna* ssp. n.; (AM) *Hyalyris excelsa* ssp. n.; (AN) *Methona c. curvifascia*; (AO) *Olyras c. crathis*. Abdomen, ventrolateral view: (AP) *Tithorea harmonia hermas*; (AQ) *Tellervo z. zoilus*; (AR) *Eutresis hyperaia banosana*; (AS) *Dircenna dero* ssp. n.; (AT) *Godyris zavaleta telesilla*; (AU) *Thyridia psidii* aedesia; (AV) *Godyris mantura honrathi*; (AW) *Methona grandior* ssp. n.; (AX) *Paititia neglecta*; (AY) *Melinaea menophilus zaneka*.

2230 the body. Among members of a mimicry ring containing
 2231 *Methona* and similar species, these stripes are usually
 2232 broken to form a similarly appearing pattern of a black
 2233 body with white dots.

97. Ventral abdomen and sides: (0) pale yellow to white 2234
 (Fig. 12AP); (1) white, with segment borders dark 2235
 brown (Fig. 12AQ); (2) dark brown with yellowish 2236
 white dorsal edges to sternites and a yellow-white 2237

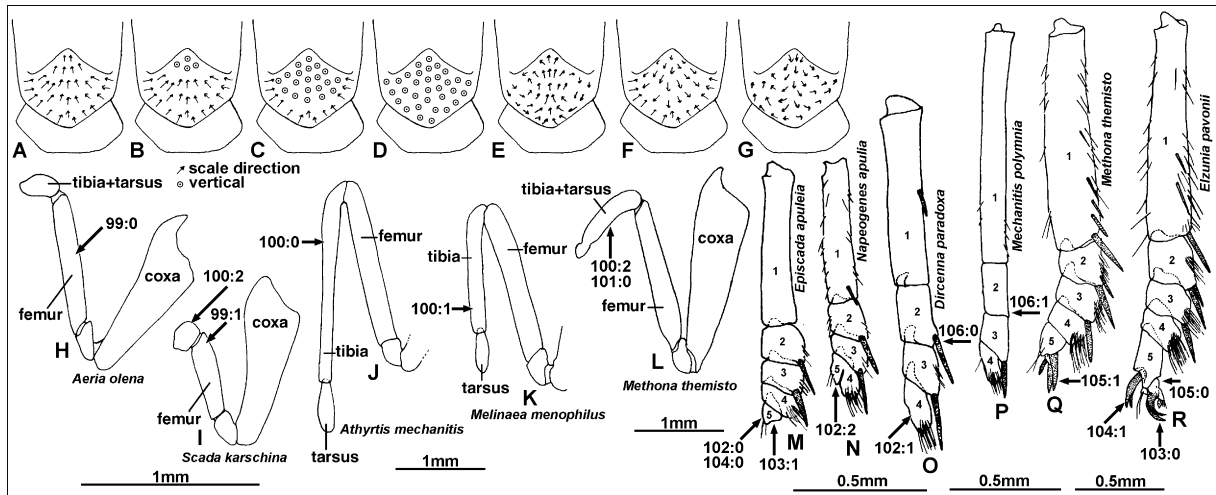


Fig. 13. Direction of scales on dorsal metathorax, representing Char. 95, states 0–6, respectively: (A–G). Male foreleg, lateral view: (H) *Aeria olenae*; (I) *Scada k. karschiana*; (J) *Athyrtis m. mechanitis*; (K) *Melinaea menophilus zaneka*; (L) *Methona themisto*. Female foreleg, lateral view: (M) *Episcada a. apuleia*; (N) *Napeogenes a. apulia*; (O) *Dirccenna paradoxa praestigiosa*; (P) *Mechanitis p. polymnia*; (Q) *Methona themisto*; (R) *Elzunia pavonii*.

2238 ventral midline in the posterior half (Fig. 12AR); (3)
 2239 yellow with a dark brown midline (Fig. 12AS); (4) white
 2240 with a dark brown midline (Fig. 12AT); (5) dark brown,
 2241 with a pale yellowish dorsolateral line broken at the
 2242 anterior edge of sternites (Fig. 12AU); (6) dark brown,
 2243 except white in the dorsal half posteriorly (Fig. 12AV);
 2244 (7) dark brown with a white midline and white spots at
 2245 dorso-posterior edge of sternites (Fig. 12AW); (8) black,
 2246 except for white spots at middle at posterior edge of
 2247 sternites, line of broken white dorso-lateral spots near
 2248 dorsal edge of sternite (Fig. 12AX); (9) dark brown
 2249 (Fig. 12AY).

2250 98. *Abdominal sternites with elongate scales at posterior*
 2251 *edge*: (0) absent (Fig. 11M); (1) present (Fig. 11L).
 2252 State 1 is an apparent synapomorphy for *Tellervo* +
 2253 *Ithomiinae*. In *Danainae* the scales at the posterior edges
 2254 of each sternite are similar morphologically to the rest of
 2255 the sternite, but in *Tellervo* and *Ithomiinae* they are
 2256 distinctly elongate.

2257 *Male foreleg*

2258 99. *Male foreleg with femur*: (0) equal or longer than
 2259 coxa (Fig. 13H); (1) shorter than coxa (Fig. 13I). Fox
 2260 and Real (1971) stated that *Napeogenini* had state 0 and
 2261 *Ithomiini* state 1 for this character. However, we found
 2262 the differences between these tribes to be very small, and
 2263 often difficult to see, if apparent at all. Only a small
 2264 number of primitive species show the femur substan-
 2265 tially shorter than the coxa, and only these were coded
 2266 state 1.

2267 100. *Male foreleg with tibia + tarsus*: (0) unfused,
 2268 longer than femur (Fig. 13J); (1) unfused, shorter or
 2269 equal to femur (Fig. 13K); (2) fused, shorter than femur
 2270 (Fig. 13L).

101. *If male foreleg tibia and tarsus are fused* (Char. 2271
 100:2), then they are: (0) elongate (Fig. 13L); (1) 2272
 rounded (Fig. 13I). The fused tibia and 2273
 tarsus is typically rounded or “pear”-like, except in *Methona* 2274
themisto. In *Episcada* and related genera the fused tibia 2275
 and tarsus may be flattened against the femur and so 2276
 triangular in outline, but given significant variation even 2277
 within species this character was not coded. 2278

Female legs

2279 More primitive species tend to have denser tarsal 2280
 trichoid sensillae. 2281

102. *Female foreleg fourth and fifth tarsal segments*: (0) 2282
 distinct (Fig. 13M); (1) fifth fused with fourth or absent 2283
 (Fig. 13O); (2) fifth partially fused with fourth, visible as 2284
 a bump (Fig. 13N). 2285

103. *Female foreleg fifth tarsal segment claws*: (0) 2286
 present (Fig. 13R); (1) absent (Fig. 13M). This and the 2287
 next two characters were coded as equivocal for species 2288
 where the fifth tarsal segment is absent or fused with the 2289
 fourth (Char. 102:1). 2290

104. *Female foreleg tarsus with paired “spurs” dorsally* 2291
on fifth segment: (0) absent (Fig. 13M); (1) present 2292
 (Fig. 13R). Spurs are elongate, articulating spine-like 2293
 projections, of similar color to other leg segments, 2294
 compared with the very dark brown, smaller and 2295
 morphologically distinct spines that are also present 2296
 on all legs (see Fig. 11J). 2297

105. *Female foreleg tarsus with paired “spurs” ventrally* 2298
on fifth segment: (0) absent (Fig. 13R); (1) present 2299
 (Fig. 13Q). 2300

106. *Female foreleg with paired spurs at ventral distal* 2301
edge of: (0) third, second (sometimes first) tarsal 2302
 segments (Fig. 13O); (1) third segment only (Fig. 13P). 2303

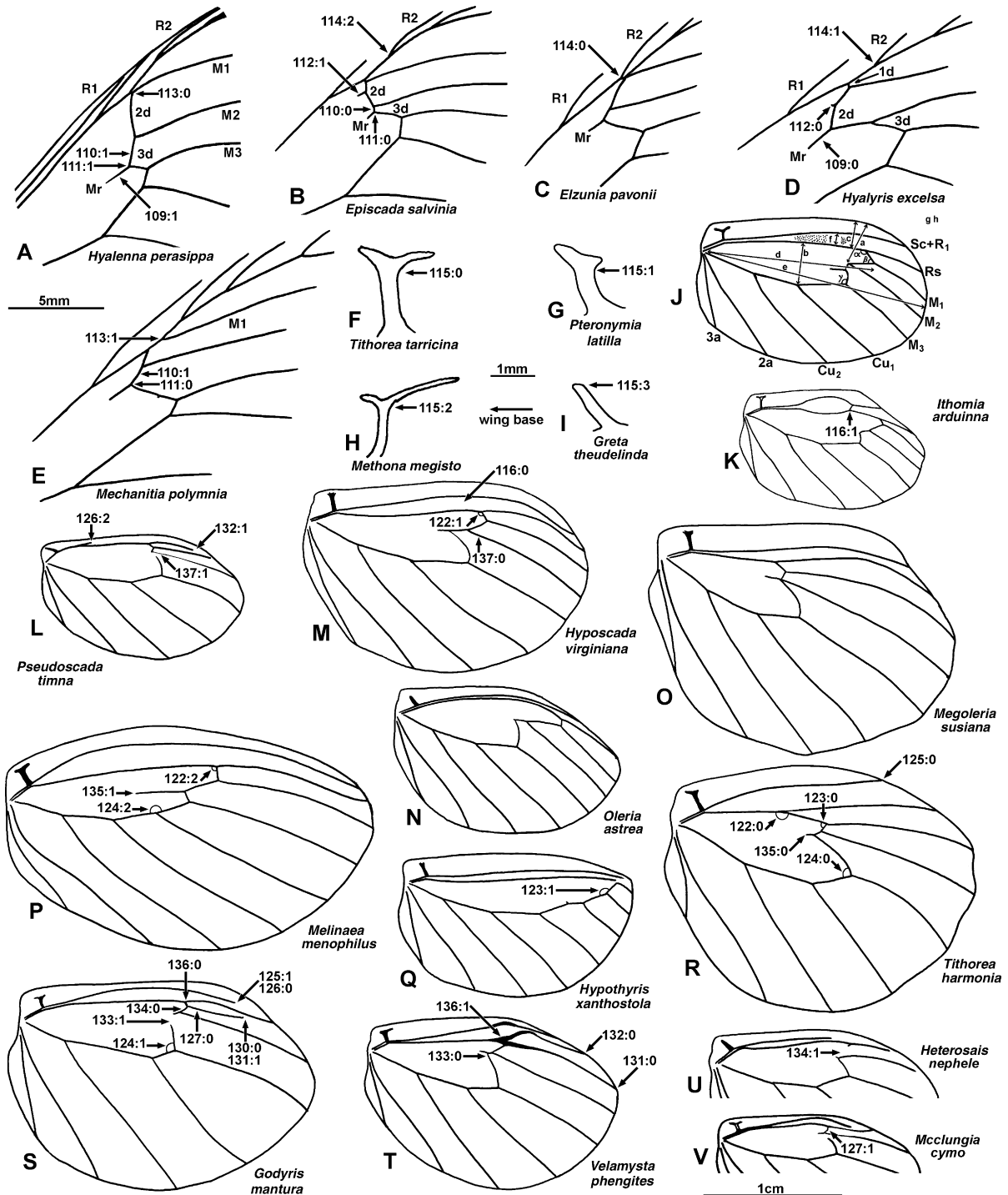


Fig. 14. Male forewing venation, discal area: (A) *Hyalenna perasippa* ssp. n.; (B) *Episcada s. salvinia*; (C) *Elzunia pavonii*; (D) *Hyaliris excelsa decumana*; (E) *Mechanitis p. polymnia*. Male VHW humeral vein: (F) *Tithorea tarricina duenna*; (G) *Pteronymia latilla fulvescens*; (H) *Methona megisto*; (I) *Greta t. theudelinda*. Male hindwing venation: (J) generalized diagram showing venation and measured shape variables; (K) *Ithomia a. arduinna*; (L) *Pseudoscada timna pusio*; (M) *Hyoscada virginiana adelphina*; (N) *Oleria astrea burchelli*; (O) *Megoleria s. susiana*; (P) *Melinaea m. menophilus*; (Q) *Hypothyris xanthostola*; (R) *Tithorea harmonia megara*; (S) *Godyrus mantura honrathi*; (T) *Velamysta p. phengites*; (U) *Heterosais n. nephele*; (V) *McClungia cymo salonina*.

- 2304 107. *Female mid- and hindleg tibial spurs*: (0) present
 2305 (Fig. 11I,J); (1) absent (Fig. 11K). Tibial spurs are
 2306 present absent in all Ithomiinae except *Tithorea* and
 2307 *Elzunia*. The distinction between spurs and spines is
 2308 discussed under Char. 104 and illustrated in Fig. 11(J).
- 2309 108. *Female foretarsus segment 4 ventral surface*: (0)
 2310 with sparse, thick spines similar to other segments
 2311 (Fig. 11H); (1) with dense, thin spines differing from
 2312 other segments (Fig. 11G). State 1 is a synapomorphy
 2313 for *Melinaea*.
- 2314 *Wing venation*
- 2315 109. *Male forewing. Male FW with medial recurrent*
 2316 *vein Mr on*: (0) 2d (Fig. 14D); (1) 3d (Fig. 14A).
- 2317 110. *If male FW with Mr on 3d (Char. 109:1), then*
 2318 *upper arm of 3d is*: (0) approximately half or less the
 2319 length of 2d (Fig. 14B); (1) about the same length as 2d,
 2320 or greater (Fig. 14A,E). In *Dircenna paradoxa* there is
 2321 geographic variation in the relative lengths of 3d and 2d.
 2322 Individuals from northern Ecuador and Colombia have
 2323 the upper arm of 3d similar in length to 2d, thus very
 2324 closely resembling the venation of *Hyalenna*, while
 2325 individuals from central and southern Ecuador to Peru
 2326 have state 0. There are no other morphological differ-
 2327 ences between individuals from these regions (Willmott
 2328 and Lamas, 2005).
- 2329 111. *If male FW with Mr on 3d (Char. 109:1), then Mr*
 2330 *positioned*: (0) nearer the base of vein M2 than M3
 2331 (Fig. 14B,E); (1) nearer the base of vein M3 than M2
 2332 (Fig. 14A). State 1 occurs exclusively in all *Hyalenna*.
- 2333 112. *Male FW with additional medial recurrent vein*
 2334 *anterior of Mr*: (0) absent or weak (about half size of
 2335 Mr) (Fig. 14D); (1) strong, about the same size as Mr
 2336 (Fig. 14B).
- 2337 113. *Male FW with M1 originating*: (0) at or on
 2338 discocellular veins (Fig. 14A); (1) distal of the discal cell
 2339 end (Fig. 14E). *Mechanitis lysimnia* shows significant
 2340 variation in forewing venation, even between wings of
 2341 the same individual. It was therefore coded as polymor-
 2342 phic.
- 2343 114. *Male FW with origin of vein R2*: (0) basal of
 2344 discal cell end (Fig. 14C); (1) distal of but near discal cell
 2345 end [ratio of cell end-R1/cell end-R2 > 1.3] (Fig. 14D);
 2346 (2) distal of and far from cell end (ratio of cell end-
 2347 R1/cell end-R2 < 1.3) (Fig. 14B).
- 2348 *Male hindwing. 115. Male hindwing humeral vein*: (0)
 2349 “forked” with distal and basal arms similar in length
 2350 (Fig. 14F); (1) forked with distal arm reduced to a bump
 2351 or absent (Fig. 14G); (2) forked with basal arm reduced
 2352 to a bump or absent (Fig. 14H); (3) unforked (both
 2353 arms apparently absent) (Fig. 14I). Fox (1940) placed a
 2354 great emphasis on whether or not the VHW humeral
 2355 vein was “forked” in his taxonomy. However, there is
 2356 substantial variation even within single individuals
 2357 (comparing both wings) in the extent of the “arms”
 2358 arising from the tip of the humeral vein, and as these
 fade gradually into the surrounding wing, assessing the
 shape of the vein is often rather subjective. The state
 “unforked” of Fox may arise either through loss of one
 or other of the arms at the tip or through loss of both (in
 which case a slight double bump is sometimes visible at
 the tip). These different possibilities have therefore been
 coded as distinct states.
116. *Male hindwing with cross-vein joining Sc + R1*
 and Rs: (0) absent (Fig. 14M); (1) present (Fig. 14K).
 State 1 is a synapomorphy for *Ithomia*.
117. *Male hindwing with ratio of distance between base*
 of vein M2 and costa/maximum discal cell width, r (= a/b ,
 Fig. 14J): (0) $r < 0.75$ (Fig. 14M); (1) $r > 0.75$
 (Fig. 14N). State 0 represents the discal cell being placed
 placed more anteriorly in the wing, nearer the costa, and
 occurs in most species in the tribes Godyridini and
 Dircennini.
118. *Male hindwing with ratio of distance between*
 costa and anterior edge discal cell opposite end of vein
 M2/distance between base of vein M2 and costa, r (= c/a ,
 Fig. 14J): (0) $r < 1.07$ (Fig. 14L); (1) $1.07 < r < 1.23$
 (Fig. 14K); (2) $1.23 < r$ (Fig. 14P). Higher numbered
 character states represent species in which the base of
 vein M2, which typically meets the discal cell near the
 medial recurrent vein, is positioned nearer the middle,
 rather than anterior edge, of the discal cell.
119. *Male hindwing with ratio of anterior cell length*
 (base of discal cell to base of vein M1 or Rs, whichever
 further)/maximum wing length, r (= d/e , Fig. 14J): (0)
 $r < 0.56$ (Fig. 14R); (1) $0.56 < r < 0.69$ (Fig. 14P); (2)
 $0.69 < r$ (Fig. 14Q). Species with higher numbered
 states have relatively longer discal cells in comparison
 with overall wing width, occurring especially in the
 Napeogenini and Oleriini.
120. *Male hindwing with ratio of maximum cell*
 width/anterior cell length (base of discal cell to base of
 vein M1 or Rs, whichever further), r (= b/d , Fig. 14J):
 (0) $r < 0.28$ (Fig. 14R); (1) $0.28 < r$ (Fig. 14Q).
 Species with state 0 have relatively narrower discal
 cells.
121. *Male hindwing with ratio of distance between*
 discal cell and Sc + R1 at maximum width of androco-
 nial scale patch/maximum cell width, r (= f/b , Fig. 14J):
 (0) $r < 0.2$ (Fig. 14N); (1) $0.2 < r < 0.3$ (Fig. 14O);
 (2) $0.3 < r$ (Fig. 14R). Species with higher numbered
 character states have a broader patch of androconial
 scales between veins Sc + R1 and Rs because these
 veins are further apart. Primitive species tend to have
 higher states. *Pseudoscada timma*, *P. erruca* and *P. florula*
 were coded as unknown because vein Sc + R1 does not
 extend to the broadest part of the androconial scale
 patch.
122. *Male hindwing with angle between veins Rs (in*
 discal cell) and Id (= α , Fig. 14J): (0) greater than 140°
 (Fig. 14R); (1) between 110 and 139° (Fig. 14M); (2) less
 than 110° (Fig. 14P).

- 2415 123. *Male hindwing with angle between veins 1d and 2d*
 2416 (= β , Fig. 14J): (0) acute or nearly right angle 2472
 2417 (Fig. 14R); (1) about 140° (Fig. 14Q). State 1 is an 2473
 2418 autapomorphy for *Hypothyris xanthostola*. 2474
- 2419 124. *Male hindwing with angle between veins 3d and*
 2420 *Cu1-M3* (= γ , Fig. 14J): (0) less than or equal to 90° 2475
 2421 (Fig. 14R); (1) between 90 and 145° (Fig. 14S); (2) 2476
 2422 greater than 145° (Fig. 14P). 2477
- 2423 125. *Male hindwing with vein Sc + R1*: (0) reaching 2478
 2424 margin (Fig. 14R); (1) not reaching margin (Fig. 14S). 2479
- 2425 126. *If male hindwing with vein Sc + R1 not reaching*
 2426 *margin (Char. 125:1)*: (0) Sc + R1 ends near or distal 2480
 2427 of cell end (Fig. 14S); (1) Sc + R1 ends about halfway 2481
 2428 along the cell (Fig. 15B); (2) Sc + R1 almost absent 2482
 2429 (Fig. 14L). 2483
- 2430 127. *Male hindwing with vein M1*: (0) present 2484
 2431 (Fig. 14S); (1) absent (Fig. 14V). State 1 occurs only in 2485
 2432 *Mcclungia cymo*, in which absence of M1 is inferred 2486
 2433 from the apparent presence of both 1d and 2d at the end 2487
 2434 of the discal cell, which lie anterior and posterior of the 2488
 2435 end of M1. Presence of both 1d and 2d is inferred from a 2489
 2436 kink in the discocellular vein lying between veins Rs and 2490
 2437 M2, which apparently represents the junction between 2491
 2438 these two veins. In the derived state of the following 2492
 2439 Char. 127:1, in contrast, the discocellular vein is straight 2493
 2440 between Rs and M2, suggesting the M1 and Rs are 2494
 2441 fused in species where only a single one of these veins is 2495
 2442 apparent. 2496
- 2443 128. *Male hindwing with veins M1 and Rs basally*:
 2444 (0) distinct (Fig. 15B); (1) fused (Fig. 15C). Fusion of 2497
 2445 these veins is inferred from the straight discocellular 2498
 2446 vein between veins Rs and M2, and related species in 2499
 2447 which the veins are partially fused. In *Heterosais* the 2500
 2448 discocellular vein attached to Rs is partially visible 2501
 2449 with the basal angle between it and vein Rs distinctly 2502
 2450 acute (Fig. 14U). As all other species in the Godyridi- 2503
 2451 ni have the angle between Rs and 1d greater than 2504
 2452 110° (Char. 122:0,1), the inference is that this vein 2505
 2453 represents vein 2d, in which case veins M1 and Rs are 2506
 2454 fused. 2507
- 2455 129. *If male hindwing with veins M1 and Rs basally*
 2456 *fused (Char. 128:1), remainder of veins are*: (0) 2508
 2457 partially fused (Fig. 15C); (1) entirely fused 2509
 2458 (Fig. 15A). 2510
- 2459 130. *Male hindwing with veins M1 and Rs distally*: (0) 2511
 2460 separate (Fig. 14S); (1) almost or actually touching at 2512
 2461 tip (Fig. 15B). Species with these veins entirely fused 2513
 2462 (Char. 129:1) are coded equivocal. 2514
- 2463 131. *Male hindwing with vein M1*: (0) reaching margin 2515
 2464 (Fig. 14T); (1) not reaching margin (Fig. 14S). Species 2516
 2465 with veins M1 and Rs entirely fused (Char. 129:1) are 2517
 2466 coded equivocal. 2518
- 2467 132. *Male hindwing with vein Rs*: (0) reaching margin 2519
 2468 (Fig. 14T); (1) not reaching margin (Fig. 14L). Species 2520
 2469 with veins M1 and Rs entirely fused (Char. 129:1) are 2521
 2470 coded equivocal. 2522
133. *Male hindwing with anterior tip of 3d*: (0) present 2471
 (Fig. 14T); (1) absent (Fig. 14S). State 1 is exclusive to 2472
 all Godyridini except for *Velamysta*, *Veladyris* and 2473
Heterosais. In the former two genera state 0 may be a 2474
 symplesiomorphy, in *Heterosais* it appears to be a 2475
 reversal and synapomorphy. 2476
134. *Male hindwing with vein 2d*: (0) complete 2477
 (Fig. 14S); (1) incomplete (Fig. 14U). This is a synapo- 2478
 morphy for *Heterosais*. 2479
135. *Male hindwing with vein Mr on*: (0) 3d (Fig. 14R); 2480
 (1) 2d (Fig. 14P). Species with Mr at the junction of 3d 2481
 and 2d are coded equivocal. Most Godyridini are also 2482
 coded equivocal as the anterior portion of 2d is absent 2483
 (Char. 134:1). 2484
136. *Male hindwing with base of veins M1, Rs and*
neighboring Sc + R1: (0) of similar width to rest of 2485
 vein (Fig. 14S); (1) swollen to about three times usual 2486
 width (Fig. 14T). State 1 is a synapomorphy for 2487
Velamysta. 2488
137. *Male hindwing with vein M2*: (0) of similar width 2490
 to other veins (Fig. 14M); (1) very narrow or absent 2491
 basally (Fig. 14L). 2492
138. *Male hindwing androconial scales beneath hair*
pencil: (0) on flat wing membrane or in a curved channel 2493
 running between Sc + R1 and Rs (Fig. 11O); (1) in a 2494
 curved channel extending posteriorly beyond vein Rs 2495
 (Fig. 11N). Most species have the wing membrane 2496
 beneath the androconial scales between veins Sc + R1 2497
 and Rs more or less curved to accommodate these 2498
 enlarged scales. In *Ithomia* this curved channel is of a 2499
 particular form, which extends posteriorly beyond vein 2500
 Rs. 2501
139. *Male hindwing fold in cell Sc + R1-Rs near*
margin: (0) absent or simple “U”-shape (Fig. 11P); (1) 2503
 “S”-shape (Fig. 11Q); (2) double “S”-shape (Fig. 11R). 2504
 A number of other species have the wing folded between 2505
 Sc + R1 and Rs to form a half-tube with parallel sides. 2506
 In species in several genera in the Napeogenini the wing 2507
 is even more strongly folded, so that vein Sc + R1 2508
 almost touches vein Rs (state 1), enclosing the andro- 2509
 conial scales between these two veins, while in *Greta* 2510
diaphanus it is doubly folded (state 2). 2511
- Female hindwing*. 140. *Female hindwing with vein*
Sc + R1: (0) meeting vein Rs at base of humeral vein 2513
 (Fig. 15G); (1) meeting and running alongside vein Rs 2514
 between humeral vein and point opposite base of vein 2515
 Cu2 (Fig. 15H); (2) meeting and running alongside vein 2516
 Rs distal of point opposite base of vein Cu2 (Fig. 15D); 2517
 (3) fused with vein Rs to distal of point opposite base of 2518
 vein Cu2 (Fig. 15F). 2519
141. *Female hindwing with cross-vein between vein*
Sc + R1 and discal cell: (0) absent (Fig. 15G); (1) 2521
 present (Fig. 15D). This cross-vein varies somewhat in 2522
 development, being a clear vein similar in thickness to 2523
 Sc + R1 in some species (e.g., *Hyalenna perasippa*) to 2524
 slight bumps, which just merge with one another, only 2525
 2526

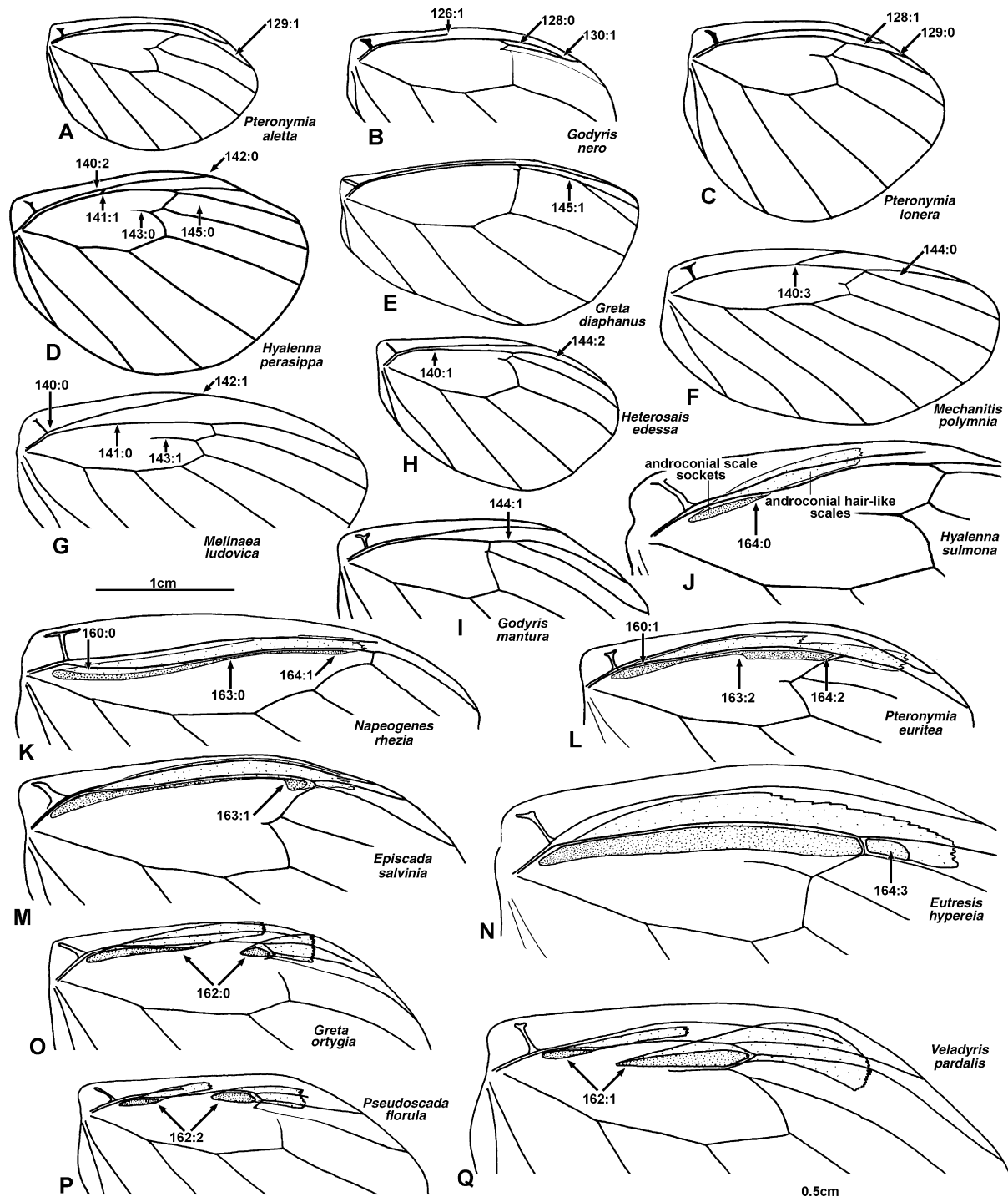


Fig. 15. Female hindwing venation: (A) *Pteronymia a. aletta*; (B) *Godyris nero*; (C) *Pteronymia lonera*; (D) *Hyalenna perasippa* ssp. n.; (E) *Greta diaphanus*; (F) *Mechanitis p. polymnia*; (G) *Melinaea l. ludovica*; (H) *Heterosais edessa*; (I) *Godyris mantura honrathi*. Male DHW discal cell, distribution of androconial hair-like scales ("hair pencil"): (J) *Hyalenna sulmona lobusa*; (K) *Napeogenes r. rhezia*; (L) *Pteronymia euritea*; (M) *Episcada s. salvinia*; (N) *Eutresis hypereia theope*; (O) *Greta o. ortygia*; (P) *Pseudoscada florula aureola*; (Q) *Veladyris p. pardalis*.

2527 visible in cleared specimens. A slight indentation in vein
2528 Sc + R1 usually indicates where the cross-vein originat-
2529 ates, if present.

142. Female hindwing with vein Sc + R1 ending at 2530
anal margin: (0) distal of cell end (1d) (Fig. 15D); (1) 2531
basal of cell end (Fig. 15G). If vein Sc + R1 is 2532

- 2533 incomplete (coded for males in Char. 125:1) then this
2534 character is coded as equivocal.
- 2535 143. *Female hindwing with vein Mr*: (0) on 3d
2536 (Fig. 15D); (1) 2d (Fig. 15G). Despite some correlation
2537 with Char. 135, sexes differ in the position of Mr in a
2538 number of species, and in most Godyradini males cannot
2539 be coded (see Discussion under Char. 135).
- 2540 144. *Female hindwing with veins M1 and Rs*: (0)
2541 distinct (Fig. 15F); (1) partially fused (Fig. 15I); (2)
2542 entirely fused (Fig. 15H).
- 2543 145. *Female hindwing with veins M2 and M1*: (0)
2544 separate (Fig. 15D); (1) partially fused (Fig. 15E).
- 2545 *Scales*
- 2546 *Main wing scales*. 146. *Transparent areas of wing with*
2547 *ground scales*: (0) flat crescents (Fig. 11S); (1) flat, leaf-
2548 shaped with multiple scalloped distal edge (Fig. 11T);
2549 (2) “U”-shaped hairs (Fig. 11U); (3) pitchfork-shaped
2550 hairs (Fig. 11V); (4) flat, leaf-shaped (Fig. 11W). Two
2551 types of scales are present on the main wing areas, one
2552 longer and narrower (cover scales) and the other shorter
2553 and broader (ground scales). Many ithomiines have
2554 areas of the wing translucent or transparent, through
2555 narrowing of both types of scale to reveal the transpar-
2556 ent wing membrane. Typically cover scales are hair-like,
2557 while ground scales occur in various different forms,
2558 coded here.
- 2559 147. *Wing with cover and ground scale bases*: (0)
2560 dispersed, or in lines (Fig. 11W); (1) almost touching
2561 (Fig. 11S). Cover and ground scales on the main wing
2562 areas (see Char. 146) are typically arranged in alternat-
2563 ing, irregular lines (e.g., Fig. 11Y) or more randomly
2564 dispersed. In *Athesis*, *Patricia* and *Methona* the scales
2565 are arranged in pairs, one of each type of scale in each,
2566 with the bases immediately adjacent.
- 2567 *Androconial scales (not DHW costal region)*. 148.
2568 *Male DFW with reduced scale density in a patch from*
2569 *anal margin to posterior edge discal cell*: (0) absent; (1)
2570 present (Fig. 11X,Y). State 1 is an autapomorphy for
2571 *Tellervo*. Examination of this part of the wing shows no
2572 evidence of modified, androconial scales, despite the
2573 sexual dimorphism in this character. The paler area on
2574 the male DFW results from slightly more dispersed and
2575 narrower wing scales.
- 2576 149. *Male DFW with patch of spatulate, silky black*
2577 *androconial scales in anterior half discal cell to base cells*
2578 *M3–M2 and M2–M1*: (0) absent; (1) present (Fig. 11Z).
2579 State 1 is an autapomorphy for *Aeria eurimedia*.
- 2580 150. *Male DFW with dense, elongate androconial*
2581 *scales lining vein 2A*: (0) absent; (1) present (Fig. 11AA).
2582 State 1 is a synapomorphy for *Forbestra* + *Mechanitis*.
- 2583 151. *Male DHW with dense, elongate triangular scales*
2584 *in discal area*: (0) absent; (1) present (Fig. 11AB). State 1
2585 is an autapomorphy for *Hypothyris xanthostola*.
- 2586 152. *Male DHW with dense, rounded androconial*
2587 *scales in postdiscal band*: (0) absent; (1) present
(Fig. 11AC). State 1 is an autapomorphy for *Mechanitis* 2588
polymnia. 2589
153. *If male DHW hair pencil present (Char. 156:1),* 2590
then VFW anal margin cell 2A–Cu2 is: (0) entirely 2591
covered with narrow hair-like to broader leaf-like scales 2592
(Fig. 17A); (1) devoid of scales in basal half of cell at 2593
anterior edge (Fig. 17C); (2) devoid of scales in an 2594
elongate patch in basal half of cell in middle (Fig. 17D); 2595
(3) devoid of scales in an elongate patch in basal half 2596
bordering on vein 2A (Fig. 17E); (4) devoid of scales in 2597
an ovoid patch in basal half extending across into anal 2598
margin-2 A (Fig. 17F); (5) devoid (or nearly so) of scales 2599
from near base to past base vein Cu2 (Fig. 17G). Cell 2600
2A–Cu2 on the VFW of male ithomiines is clothed with 2601
variously modified scales, the distribution of which is 2602
correlated with the position of androconial scales on the 2603
dorsal hindwing. *Tellervo* (the outgroup), which lacks 2604
hindwing androconial hair-like scales, is coded as 2605
equivocal. In some ithomiine species part of this cell is 2606
devoid of scales, or has only a very sparse scattering of 2607
needle-like scales. The extent of this bare area varies 2608
between genera and is coded here. State 5 is a synapo- 2609
morphy for Godyradini + Dircennini. 2610
154. *Male VFW cubital vein with elongate hairs* 2611
extending posteriorly: (0) absent (Fig. 16A); (1) present 2612
in basal half of vein only (Fig. 17E); (2) present 2613
throughout vein (Fig. 16B). 2614
155. *Male VFW with scales around vein 2A*: (0) absent 2615
or barely differentiated from scales in remainder of cell 2616
(Fig. 17C); (1) yellow, sparse, distinct from surrounding 2617
scales (Figs 16C and 17A); (2) yellow, very dense, 2618
elongate, distinct from surrounding scales (Figs 16D 2619
and 17B). 2620
- Male DHW androconial “hair pencil”*. 156. *Male* 2621
DHW with a linear band of androconial erectile, piliform 2622
scales (“hair pencil”) at anterior edge of discal cell: (0) 2623
absent (Fig. 17H); (1) present (Fig. 16E). State 1 is a 2624
universal synapomorphy for the Ithomiinae. The sockets 2625
are highly modified from usual scale sockets (see 2626
Fig. 16F) permitting the hairs to be raised in a fan- 2627
shape when pheromones are disseminated. 2628
157. *Male DHW hair pencil present*: (0) in males only; 2629
(1) in both sexes (Fig. 17O). State 1 occurs in several 2630
Methona species only. 2631
158. *Male DHW hair pencil scales*: (0) uniformly dense 2632
(Fig. 17I); (1) dense at base, much sparser towards cell 2633
end (Fig. 17K). 2634
159. *Male DHW hair pencil color*: (0) uniform 2635
(Fig. 17K); (1) darker at base, paler distally (Fig. 17L); 2636
(2) paler at base, darker distally (Fig. 17I). *Elzumia* is 2637
coded as equivocal as, in comparison with the morpho- 2638
logically similar and closely related *Tithorea*, it has 2639
apparently lost the distal hair pencil. 2640
160. *Male DHW hair pencil “footprint”*: (0) roughly 2641
equidistant from vein Rs throughout length (Fig. 15L); 2642
(1) displaced posteriorly from vein Rs towards base of 2643

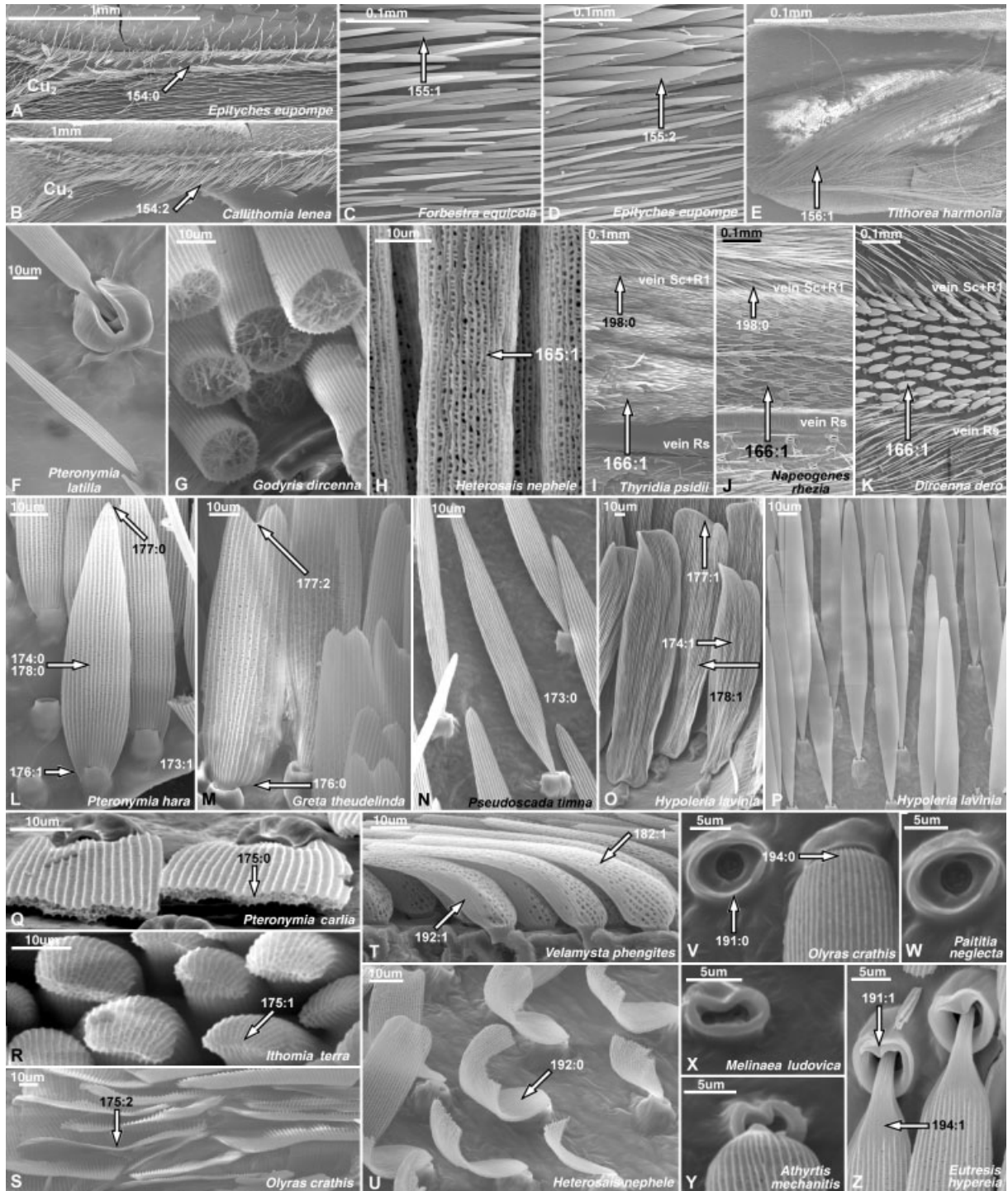


Fig. 16. Male androconial scales. VFW cubital vein: (A) *Epityches eupompe*; (B) *Callithomia lenea zelie*. VFW vein 2 A androconial (upper) and wing (lower) scales: C, *Forbestra e. equicola*; (D) *Epityches eupompe*. (E) *Tithorea harmonia megara*, male DHW androconial hair-like scales ("hair pencil") and underlying androconial scale patch. (F) *Pteronymia l. latilla*, DHW hair pencil scale and socket (upper), wing scale and socket (lower); (G) *Godyris dircenna*, cross-section through DHW hair pencil scales; (H) *Heterosais n. nephele*, thickened androconial hair-like scales underlying DHW hair pencil. DHW androconial scale patch between veins Sc + R1 and Rs: (I) *Thyridia psidii*; (J) *Napeogenes r. rhezia*; (K) *Dircenna dero celtina*. DHW androconial scales in cell Rs-Sc + R1, basal (B) and distal (D): (L) *Pteronymia h. hara* (B); (M) *Greta t. theudelinda* (B); (N) *Pseudoscada timna pusio* (B); (O) *Hypoleria lavinia riffarhi* (B); (P) *Hypoleria lavinia riffarhi* (D); (Q) *Pteronymia carlia* (B), cross-section; (R) *Ithomia t. terra* (B), scale tips; (S) *Olyras c. crathis* (B), scale tips; (T) *Velamysta p. phengites* (B), lateral view; (U) *Heterosais n. nephele* (B), torn scales underlying thickened hair pencil scales (H); (V) *Olyras c. crathis* (B), socket and base scale; (W) *Paititia neglecta* (B), socket; (X) *Melinaea l. ludovica* (B), socket; (Y) *Athyrtis mechanitis salvini* (B), socket and base scale; (Z) *Eutresis hypereia theope* (B), socket and base scale.



Fig. 17. Male wing androconia and markings. VFW anal margin: (A) *Forbestra equicola equicolides*, note androconial scales along vein 2A; (B) *Epityches eupompe*, note androconial scales along vein 2A; (C) *Paititia neglecta*; (D) *Aeria eurimedia agna*; (E) *Melinaea l. ludovica*; (F) *Tithorea tarricina duenna*; (G) *Callithomia lenea zelie*. DHW costa and discal cell: (H) *Tellervo z. zoilus*; (I) *Tithorea harmonia hippothous*; (J) *Aeria eurimedia agna*; (K) *Melinaea m. menophilus*; (L) *Epityches eupompe*; (M) *Pseudoscada florula aureola*; (N) *Hyalenna p. perasippa*; (O) *Methona themisto*; (P) *Episcada hemixanthe*; (Q) *Tithorea harmonia manabiana*; (R) *Pseudoscada t. timna*; (S) *Melinaea l. ludovica*; (T) *Elzunia pavonii*; (U) *Velamysta p. phengites*; (V) *Megoleria s. susiana*; (W) *Olyras c. crathis*; (X) *Pteronymia h. hara*. DHW androconial scales in cell Rs-Sc + R1: (Y) *Godyris mantura honrathi*, basal scales; (Z) as X, distal scales. VHW discal cell and costa: (AA) *Tithorea harmonia manabiana*; (AB) *Eutresis hypereia banosana*; (AC) *Paititia neglecta*; (AD) *Veladyris p. pardalis*.

wing (Fig. 15K). The sockets in which the androconial hair scales are inserted are enlarged and hemispherical, clearly visible on the wing membrane on cleared specimens and forming a distinct “footprint” where the hairs are attached. In most Ithomiinae the hairs are

attached in a band close to the edge of the discal cell (vein Rs) and parallel with this vein throughout the length of the hair pencil; in the Napeogenini the hair pencil is displaced away from vein Rs at the base of the hair pencil.

2649
2650
2651
2652
2653

2644
2645
2646
2647
2648

2654 161. *Male DHW hair pencil in a*: (0) single patch
 2655 (Fig. 17N); (1) double patch (Fig. 17K); (2) triple patch
 2656 (Fig. 17J). The hair pencil may be continuous or broken
 2657 into distinct patches. Most genera contain species with
 2658 both single and double hair pencils (only *Aeria eurime-*
 2659 *dia* has a third hair pencil). State 0 is either a result of
 2660 the hair pencil being unbroken (e.g., *Oleria*) or the loss
 2661 of the distal hair pencil (e.g., *Elzunia*), but no attempt
 2662 was made to distinguish between these origins due to
 2663 substantial variation in hair pencil extent.

2664 162. *When male DHW hair pencil is double* (Char.
 2665 161:1): (0) basal patch is larger than distal (Figs 15O
 2666 and 17L); (1) distal patch is larger than basal (Figs 15Q
 2667 and 17K); (2) both patches are equal in size (Figs 15P
 2668 and 17M).

2669 163. *Male DHW hair pencil "footprint"*: (0) even in
 2670 width or tapering distally (Fig. 15K); (1) tapering
 2671 distally then ending in an expanded circle (Fig. 15M);
 2672 (2) constricted in middle (Fig. 15L). If the hair pencil is
 2673 broken into distinct patches (Char. 161:2,3), then this
 2674 character is coded as equivocal.

2675 164. *Male DHW hair pencil "footprint"*: (0) less than
 2676 half width of discal cell (Fig. 15J); (1) not reaching end
 2677 of discal cell, but greater than half width of discal cell
 2678 (Fig. 15K); (2) reaching end of discal cell (Fig. 15L); (3)
 2679 greater than discal cell width, extending into cell M1-Rs
 2680 (Fig. 15N).

2681 165. *Male DHW hair pencil*: (0) of a single scale type
 2682 lying above scales and depression in cell Sc + R1-Rs
 2683 (Fig. 16E); (1) differentiated into paler dorsal hairs and
 2684 darker, thicker ventral hairs, latter lying within depres-
 2685 sion in cell Sc + R1-Rs (Fig. 16H). State 1 is a
 2686 synapomorphy for *Heterosais*. The thickened hairs have
 2687 a distinct ultrastructure, being strongly perforated with
 2688 the vanes sinuate (Fig. 16H), rather than unperforated
 2689 with parallel vanes (see Fig. 16G), and in all examined
 2690 specimens were loosely cemented together into a solid
 2691 mass. In several examined specimens of *Heterosais*
 2692 *nephele* these thickened hairs appeared to have abraded
 2693 the underlying androconial scales, curling them about
 2694 the lateral axis and bending them backwards at the
 2695 pedicel, and tearing a number of scales in half
 2696 (Fig. 16U).

2697 *Male DHW androconial scales beneath hair pen-*
 2698 *cil*. 166. *Male DHW androconial scales beneath hair*
 2699 *pencil*: (0) undifferentiated from those anterior of vein
 2700 Sc + R1; (1) differentiated from those anterior of vein
 2701 Sc + R1 (Fig. 16I–K). All male ithomiines have
 2702 modified, acicular or ovate lamellar androconial scales
 2703 in the distal half of the discal cell, surrounding the
 2704 sockets of the hair pencil, and extending anteriorly to
 2705 the costa. The scales that lie beneath the hair pencil
 2706 scales (when not erected) are further modified from
 2707 surrounding wing scales. In *Sais* and *Scada* veins
 2708 Sc + R1 and Rs are very close together with few
 2709 scales between these veins, but nevertheless those that

are present are slightly broader than those outside this
 area. In the following characters "androconial scales"
 refers to the modified androconial scales that underly
 the hair pencil only.

167. *Male DHW androconial scales* (Char. 166:1)
beneath hair pencil: (0) in cell Rs-Sc + R1 only
 (Fig. 17P); (1) in cell Rs-Sc + R1 and extending mid-
 way into cell M1-Rs (Fig. 17Q); (2) in cell Rs-Sc + R1
 and M1-Rs, reaching vein M1 (Fig. 17R); (3) in cells Rs-
 Sc + R1, M1-Rs, and reaching to vein M1, extending
 into anterior portion discal cell among bases of andro-
 conial hairs (Fig. 17S). In *Paititia*, *Olyras*, *Athyrtis* and
Melinaea there is a basal patch of androconial scales in
 cell Sc + R1-Rs, while the remainder of the cell
 contains a dense, tiny androconial scale. This type of
 scale further extends among the bases of the hair pencil
 scales in the discal cell, and into cell M1-Rs, a distinctive
 distribution. This type of scale apparently represents the
 usual modified scales that occur between veins Sc + R1
 and Rs, as in *Melinaea* it is confined in cell Sc + R1-Rs
 to a distal patch directly beneath the hair pencil. In
Godyris and relatives the androconial scales in cell M1-
 Rs represent an expansion of the scales usually in cell
 Sc + R1-Rs, and are distinct from scales in adjacent
 areas. *Brevioleria* and *Heterosais edessa* are coded
 equivocal as absence of androconial scales distally is
 believed correlated with absence of the distal portion of
 the hair pencil, coded in Char. 168.

168. *Male DHW androconial scales* (Char. 166:1)
beneath hair pencil: (0) present throughout (Fig. 17Q);
 (1) absent in basal area (Fig. 17U); (2) absent in distal
 area (Fig. 17T). The distribution of androconial scales
 varies between taxa, but in *Elzunia* and *Brevioleria* the
 absence of a distal hair pencil (inferred from comparison
 with close relatives in which it is present) is correlated
 with the absence of a distal patch of androconial scales,
 which are replaced by typical wing scales (state 2). In
Velamysta the basal area of Sc + R1-Rs contains
 apparently typical wing scales, similar to those anterior
 and posterior of this cell, and this species is thus coded
 1. In *Ithomia* a cross-vein closes cell Sc + R1-Rs
 immediately distal of the basal androconial scale patch
 and species were coded equivocal, as the wing area
 usually occupied by the distal part of the androconial
 scale patch is absent.

169. *Male DHW androconial scales* (Char. 166:1)
beneath hair pencil: (0) differentiated into patches of two
 distinct types of scale, one basal and one distal
 (Fig. 17Q); (1) undifferentiated, basal scale-type appar-
 ently absent (distal dominant) (Fig. 17P). The androco-
 nial scales beneath the DHW hair pencil may be uniform
 throughout, or differentiated, with those nearer the wing
 base different in color and/or morphology from those
 more distal (compare Figs 16O and Q, 18A and B, 18C
 and D). In species with a single type of scale this may
 result from the entire loss of the other patch (i.e., no

- 2766 androconial scales are present in part of the wing: Char.
2767 168) or from expansion of one or other patch at the
2768 expense of the other. Comparison of scale morphology
2769 in closely related species, where one bears differentiated
2770 scales and the other not, shows that in almost all cases
2771 the scales of the species with a single patch correspond
2772 to those of the distal patch in the other species. For
2773 *Methona* and *Mechanitini* there are no obvious close
2774 relatives, but the scales in most species more resemble
2775 the distal patch scales in other primitive ithomiines.
2776 Scales in species with only one type of scale were
2777 therefore coded as distal scales and basal scale charac-
2778 ters were left equivocal. This character was coded
2779 equivocal for species lacking part of the androconial
2780 patch (Char. 168) and for *Ithomia*, for the reasons
2781 discussed under Char. 168. Note that scales in *Heterosais*
2782 *edessa* are coded as distal patch scales even though
2783 the distal part of the androconial scale patch is absent,
2784 because scales are undifferentiated in the closely related
2785 *Heterosais nephele* and coded there as distal scales.
- 2786 170. *Male DHW androconial scale patch* (Char.
2787 166:1) *beneath hair pencil*: (0) continuous (Fig. 17P);
2788 (1) broken (Fig. 17Q). Species coded state 1 may have
2789 the two patches differing in scale morphology (e.g.,
2790 *Hypoleria lavinia*) or the same (e.g., *Episcada hymenaea*).
- 2791 171. *Male DHW basal androconial scale patch beneath*
2792 *hair pencil with distal border*: (0) approximately perpen-
2793 dicular to veins Sc + R1 and Rs or inclined with
2794 anterior edge more distal (Fig. 17S); (1) border much
2795 more distal posteriorly, with scale patch extending along
2796 posterior half of cell Sc + R1-Rs to just opposite
2797 discocellular veins (Fig. 17W). State 1 is a synapomor-
2798 phy for *Olyras* + *Paititia*. *Pteronymia hara* is coded
2799 equivocal as there is no clear boundary between basal
2800 and distal scale types.
- 2801 172. *Male DHW basal androconial patch scales*
2802 *beneath hair pencil*: (0) white (Fig. 17X); (1) whitish
2803 cream to gray buff (Fig. 17V); (2) brown (Fig. 17T); (3)
2804 mixed light and darker gray-brown (Fig. 17Y).
- 2805 173. *Male DHW basal androconial patch scales*
2806 *beneath hair pencil, density*: (0) sparse, with little overlap
2807 between adjacent scales, sockets of at least some scales
2808 visible (Fig. 16N); (1) dense, with much overlap
2809 (< 70%) between adjacent scales, sockets not visible
2810 (Fig. 16L); (2) very dense (> 70% overlap), sockets not
2811 visible, stacked almost vertically (Fig. 16O). Although
2812 occasionally basal and distal androconial patches share
2813 the same character state (for this and other following
2814 characters), in most cases this is not so, and no cases
2815 were found where a possible synapomorphy in the distal
2816 patch might be duplicated by coding the same feature in
2817 the basal patch.
- 2818 174. *Male DHW basal androconial patch scales*
2819 *beneath hair pencil*: (0) flat or lightly curving throughout
2820 scale (Fig. 16L); (1) curled longitudinally at edges and
2821 wrinkled (Fig. 16O).
175. *Male DHW basal androconial patch scales* 2822
beneath hair pencil, thickness: (0) similar in thickness to 2823
normal wing scales, width > 3 × height of vanes 2824
(Fig. 16Q); (1) very thin, similar width to height of 2825
vanes, translucent (Fig. 16R); (2) tubular, hollow in 2826
cross-section (Fig. 16S). 2827
176. *Male DHW basal androconial patch scales* 2828
beneath hair pencil, base of blade: (0) with shallow angle 2829
at pedicel (> 90°) (Fig. 16M); (1) “auriculate”, with 2830
sharp angle at pedicel (< 90°) (Fig. 16L). Species with 2831
rectangular scales (Char. 178:1) are coded state 0 and 2832
have an angle of approximately 90°. 2833
177. *Male DHW basal androconial patch scales* 2834
beneath hair pencil, tip: (0) tapering or rounded 2835
(Fig. 16L); (1) flat to indented (Fig. 16O); (2) bifurcate 2836
(Fig. 16M). 2837
178. *Male DHW basal androconial patch scales* 2838
beneath hair pencil, overall shape: (0) broader in basal 2839
half and tapering distally (Fig. 16L); (1) rectangular 2840
(Fig. 16O). 2841
179. *Male DHW distal androconial patch scales* 2842
beneath hair pencil, color: (0) white (Fig. 17U); (1) 2843
whitish cream to gray buff (Fig. 17V); (2) brown 2844
(Fig. 17Q); (3) whitish gray with brown tips (Fig. 17Z); 2845
(4) black. 2846
180. *Male DHW distal androconial patch scales* 2847
beneath hair pencil, density: (0) sparse, with little overlap 2848
between adjacent scales, sockets of at least some scales 2849
visible (Fig. 18B); (1) dense, with much overlap 2850
(< 70%) between adjacent scales, sockets not visible 2851
(Fig. 18F); (2) very dense (> 70% overlap), sockets not 2852
visible, stacked almost vertically (Fig. 18Q). 2853
181. *Male DHW distal androconial patch scales* 2854
beneath hair pencil: (0) straight about longitudinal axis 2855
(Fig. 18F); (1) curled at edges longitudinally (Fig. 18T). 2856
State 1 is a synapomorphy for *Forbestra* + *Mechanitis*. 2857
Coded equivocal for species with non-lamellar scales. 2858
182. *Male DHW distal androconial patch scales* 2859
beneath hair pencil in lateral view: (0) straight; (1) 2860
curving (Fig. 16T). State 1 is a synapomorphy for 2861
Velamysta. 2862
183. *If male DHW androconial scales beneath hair* 2863
pencil are differentiated (Char. 169:1), *patch with longer* 2864
scales is: (0) neither (equal in size) (Fig. 18C,D); (1) 2865
basal (< twice length of distal) (Fig. 16O,P); (2) basal 2866
(> twice length of distal) (Fig. 18A,B); (3) basal 2867
(> three times length of distal) (Fig. 18E,F); (4) distal 2868
(Figs 16M and 18N). 2869
184. *If male DHW androconial scales beneath hair* 2870
pencil are differentiated (Char. 169:1), *patch with* 2871
proportionally broader scales is: (0) neither (Fig. 18O,P); 2872
(1) basal (< twice width of distal) (Figs 16M and 18N); 2873
(2) basal (> twice width of distal) (Fig. 18C,D); (3) 2874
distal (Fig. 18A,B). 2875
185. *Male DHW distal androconial patch scales* 2876
beneath hair pencil, socket: (0) upright to reclining, 2877

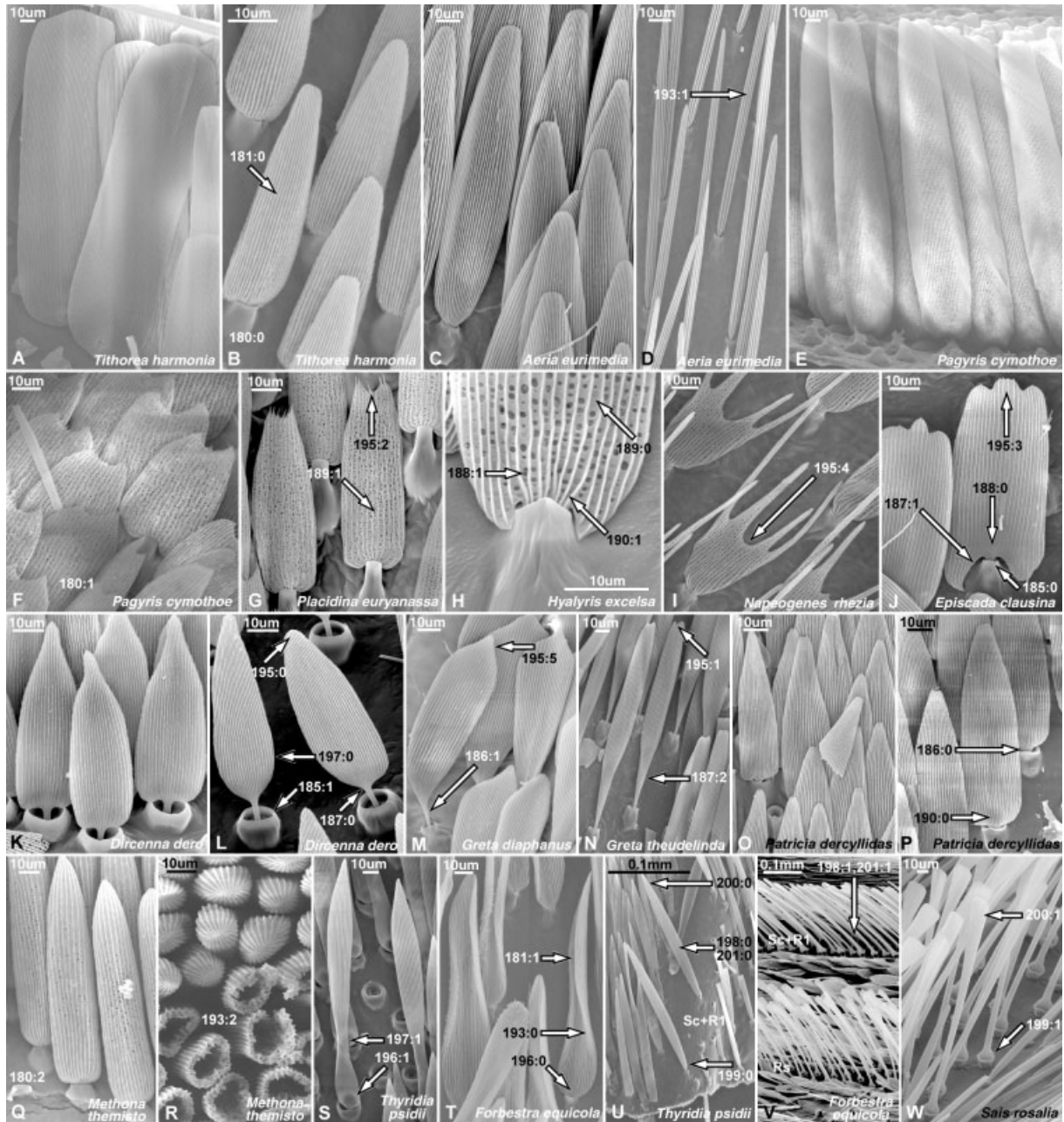


Fig. 18. Male DHW androconial scales in cell Rs-Sc + R1, basal (B), distal (D) or distal where undifferentiated (Du), homologous t; distal: (A) *Tithorea harmonia megara* (B); (B) *Tithorea harmonia megara* (D); (C) *Aeria e. eurimedia* (B); (D) *Aeria e. eurimedia* (D); (E) *Pagyris c. cymothoe* (B); (F) *Pagyris c. cymothoe* (D); (G) *Placidina euryanassa* (Du); (H) *Hyalyris e. excelsa* (Du), socket and base of scale; (I) *Napeogenes r. rhezia* (Du); (J) *Episcada clausina striposis* (Du); (K) *Dircenna dero* (B); (L) *Dircenna dero celtina* (D); (M) *Greta diaphanus* (Du); (N) *Greta t. theudelinda* (D); (O) *Patricia deryllidas hazelea* (B); (P) *Patricia deryllidas hazelea* (D); (Q) *Methona themisto* (Du); (R) *Methona themisto* (Du), cross-section and scale tips; (S) *Thyridia p. psidii* (Du); (T) *Forbestra e. equicola* (Du); (U) *Thyridia p. psidii*, scales lining vein Sc + R1; (V) *Forbestra e. equicola*, spatulate androconial scales lining veins Sc + R1 and Rs; (W) *Sais r. rosalia*, spatulate androconial scales lining vein Sc + R1.

2878 bottle-shape to short tube, with collar opening not
2879 greater than $3 \times$ pedicel width (Fig. 18J); (1) a short,
2880 rounded cup, collar opening approximately $5 \times$ pedicel
2881 width (Fig. 18L). There is substantial variation in the

morphology of androconial scale sockets, but only a 2882
single character state discrete from others could 2883
be defined. State 1 is a synapomorphy for *Dircenna* + 2884
Hyalenna, being lost in *H. perasippa*. 2885

- 2886 186. *Male DHW distal androconial patch scales*
 2887 *beneath hair pencil, pedicel*: (0) short, not extending
 2888 beyond collar (Fig. 18P); (1) elongate (Fig. 18M). Some
 2889 *Godyris* species have the pedicel and blade smoothly
 2890 merging, but the pedicel is still noticeably more elongate
 2891 than in all other species coded as state 0.
- 2892 187. *Male DHW distal androconial patch scales*
 2893 *beneath hair pencil base of blade*: (0) with shallow angle
 2894 at pedicel ($> 90^\circ$) (Fig. 18L); (1) auriculate, with sharp
 2895 angle at pedicel ($< 90^\circ$) (Fig. 18J); (2) flat, merging
 2896 smoothly with pedicel (Fig. 18N). A few species show
 2897 variation between scales, with some scales angled and
 2898 others auriculate, and were coded as dimorphic.
- 2899 188. *Male DHW distal androconial patch scales*
 2900 *beneath hair pencil, basal area of scale blade*: (0) smooth
 2901 or with windows reduced (Fig. 18J); (1) with windows
 2902 (Fig. 18H). In most species the androconial scale blade
 2903 is unperforated or perforated with windows mainly in
 2904 the distal portion. In the Ithomiini + Napeogenini the
 2905 blade has windows right to the very base (state 1).
- 2906 189. *Male DHW distal androconial patch scales*
 2907 *beneath hair pencil, ultrastructure*: (0) with flutes parallel
 2908 and not prominent (Fig. 18H); (1) with flutes prominent
 2909 and not parallel (Fig. 18G). Flutes are raised ridges
 2910 running across the channels between vanes, and are
 2911 typically less prominent than and oriented at right
 2912 angles or nearly so to vanes. State 1 occurs only in
 2913 *Pagyris* + *Placidina*, although this character could not
 2914 be coded for Ithomiini because the distal scales are
 2915 absent.
- 2916 190. *Male DHW distal androconial patch scales*
 2917 *beneath hair pencil, vanes at base of scale*: (0) parallel
 2918 or smoothly converging (Fig. 18P); (1) wrinkled
 2919 (Fig. 18H). In Ithomiini + Napeogenini the vanes are
 2920 distinctly pinched together and wrinkled at the base of
 2921 the scale, as if the scale has been constricted at this
 2922 point.
- 2923 191. *Male DHW distal androconial patch scales beneath*
 2924 *hair pencil, sockets*: (0) round (Fig. 16V,W); (1) “U”-
 2925 shaped (Fig. 16X–Z). State 1 occurs only in *Melinaea*,
 2926 *Athyrtis* and *Eutresis*.
- 2927 192. *Male DHW distal androconial patch scales*
 2928 *beneath hair pencil with vanes on lower surface*: (0)
 2929 similar to upper surface (Fig. 16U); (1) much reduced or
 2930 absent (Fig. 16T). Unlike most butterfly scales (Downey
 2931 and Allyn, 1975), but like those of some Danainae
 2932 (Ackery and Vane-Wright, 1984), almost all ithomiines
 2933 have scales with vanes on both surfaces of the blade,
 2934 except in *Velamysta* in which they are distinctly reduced
 2935 on the lower surface, probably because these scales seem
 2936 to be rigidly inserted into their sockets.
- 2937 193. *Male DHW distal androconial patch scales*
 2938 *beneath hair pencil*: (0) lamellar (Fig. 18T); (1) acicular
 2939 (Fig. 18D); (2) tubular (Fig. 18R).
- 2940 194. *Male DHW distal androconial patch scales*
 2941 *beneath hair pencil with basal area*: (0) with vanes
 (Fig. 16V); (1) lacking vanes (Fig. 16Z). This character
 was coded equivocal for most Godyridini, which lack
 vanes in the basal area because the pedicel is elongated,
 a character already coded elsewhere. The vanes are
 reduced in the middle of the scale towards the base in
 some Dircennini, but still present at the edges of the
 scale. In *Eutresis*, *Athyrtis* and *Melinaea* the vanes are
 absent across the entire scale in the basal part, and these
 taxa were coded state 1.
195. *Male DHW distal androconial patch scales*
beneath hair pencil, tip: (0) pointed to rounded to blunt
 (Fig. 18L); (1) indented (Fig. 18N); (2) bifurcate
 (Fig. 18G); (3) trifurcate (Fig. 18J); (4) deeply dentate
 (Fig. 18I); (5) pointed and attenuated at tip (Fig. 18M).
 State 4 is a synapomorphy for *Napeogenes*.
196. *Male DHW distal androconial patch scales*
beneath hair pencil, base: (0) tapering or similar width
 to rest of scale (Fig. 18T); (1) swollen (Fig. 18S).
197. *Male DHW distal androconial patch scales*
beneath hair pencil: (0) broadest at some point between
 base and tip (Fig. 18L); (1) constricted near base
 (Fig. 18S). Scales in most species broaden from the base
 then taper distally, except in *Thyridia*, in which they are
 medially constricted.
198. *Male DHW with differentiated scent scales lining*
veins Sc + R1 and Rs on DHW: (0) absent (Figs 16L,J
 and 18 U); (1) present (Fig. 18V). In most ithomiines
 the androconial scales lining vein Rs are similar in form
 to these scales anterior of this vein, while vein Sc + R1
 has very few or no scales. In *Sais*, *Scada*, *Forbestra* and
Mechanitis the scales on these veins are dense, strongly
 modified and distinct from surrounding areas. In *Thy-*
ridia the base of the androconial scales between veins
 Sc + R1 and Rs is swollen and the overall shape of the
 scale is spatulate, both characters of the scales lining
 veins Sc + R1 and Rs in remaining Mechanitini. Thus
 the latter may be homologous to the typical androconial
 scales between Sc + R1 and Rs, but given the different
 position on the wing, and presence of scales otherwise
 typical of primitive species between Sc + R1 and Rs, we
 code these two types of scale separately. State 1 is a
 synapomorphy for *Sais* + *Scada* + *Forbes-*
tra + *Mechanitis*.
199. *Male DHW androconial scales on veins Sc + R1*
and Rs with: (0) base tapering (Fig. 18U); (1) base
 sharply expanded (Fig. 18W). State 1 is a synapomor-
 phy for *Sais* + *Scada* + *Forbestra* + *Mechanitis*.
200. *Male DHW androconial scales on veins Sc + R1*
and Rs: (0) tapering distally (Fig. 18U); (1) spatulate
 (Fig. 18W). State 1 is a synapomorphy for *Sais* + *Sc-*
ada + *Forbestra* + *Mechanitis*.
201. *Male DHW androconial scales on veins Sc + R1*
and Rs: (0) lying flat against vein (Fig. 18U); (1) erect,
 pointing inwards to form a channel (Fig. 18V). State 1 is
 a synapomorphy for *Sais* + *Scada* + *Forbes-*
tra + *Mechanitis*.

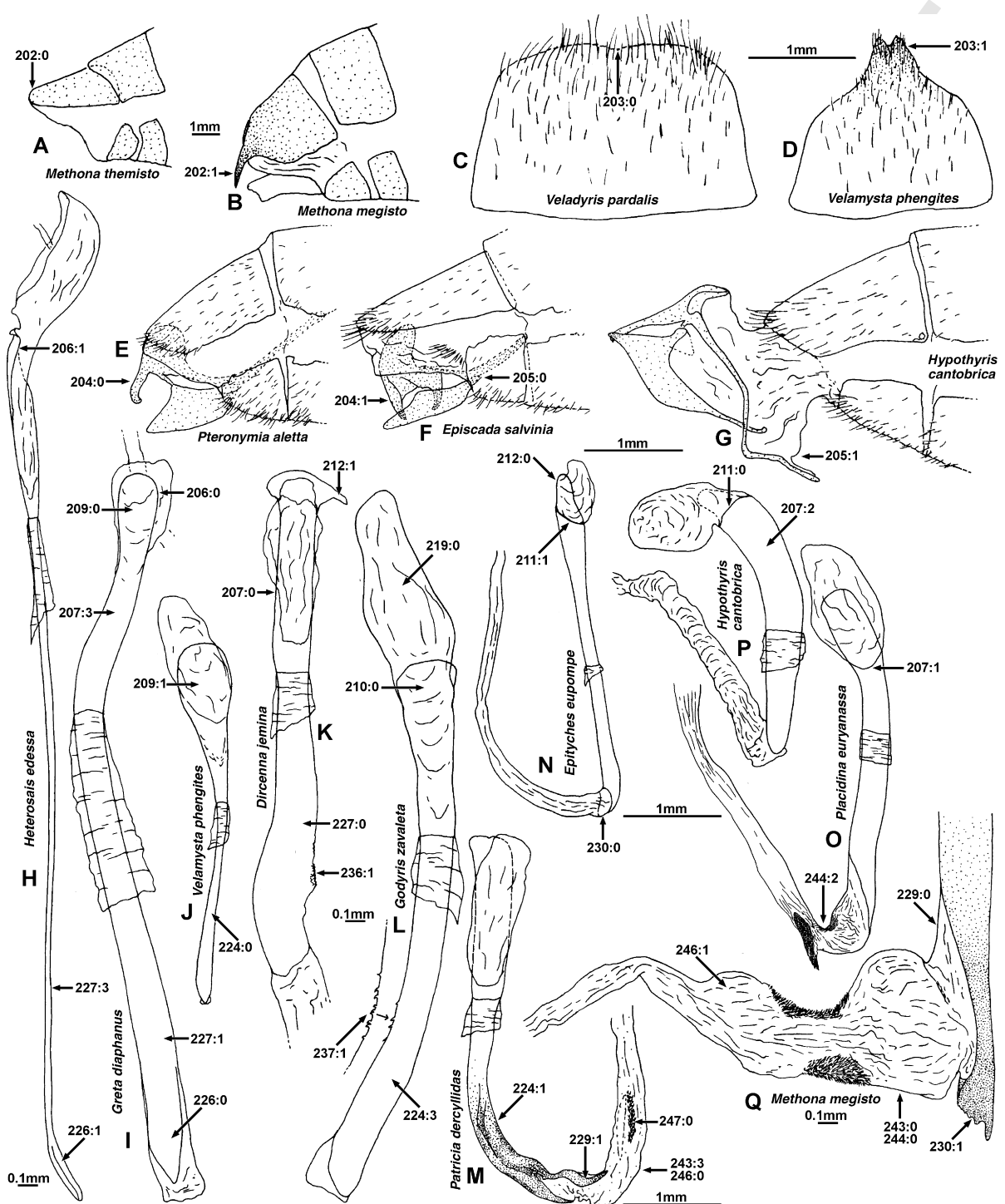


Fig. 19. Male genitalia and abdomen. Posterior abdomen tip, lateral view: (A) *Methona t. themisto*; (B) *Methona megisto*. Terminal (posterior) tergite, dorsal view: (C) *Veladyris p. pardalis*; (D) *Velamysta p. phengites*. Posterior abdomen tip, lateral view, genitalic capsule everted: (E) *Pteronymia a. aletta*; (F) *Episcada s. salvinia*; (G) *Hypothyris (Rhodussa) c. cantabrica*. Aedeagus, dorsal view: (H) *Heterosais edessa*; (I) *Greta diaphanus*; (J) *Velamysta p. phengites*; (K) *Dircenna j. jemina*; (L) *Godyris zavaleta rosata*. Aedeagus, dorsal view, vesica everted: (M) *Patricia d. dercyllidas*; (N) *Epityches eupompe*; (O) *Placidina euryanassa*; (P) *Hypothyris (Rhodussa) c. cantabrica*; (Q) *Methona t. themisto*, posterior tip only.

2998 *Male genitalia and abdomen*

2999 *Abdomen and genitalic capsule.* 202. *Male terminal*
3000 *tergite in lateral view:* (0) rounded or slightly lobed
3001 (Fig. 19A); (1) with pointed lateral projections
3002 (Fig. 19B). State 1 occurs only in *Eutresis hypereia*
3003 and *Methona megisto*.

3004 203. *Male terminal tergite in dorsal view:* (0) rounded
3005 or slightly indented in middle (Fig. 19C); (1) produced
3006 into a sclerotized “beak” with two prongs (Fig. 19D).
3007 State 1 is a synapomorphy for *Velamysta*.

3008 204. *Male genitalic capsule when extruded from*
3009 *abdomen:* (0) approximately horizontal (Fig. 19E); (1)
3010 vertical, with dorsal edge of uncus vertical (Fig. 19F).
3011 State 1 occurs in *Dircenna*, *Hyalenna*, *Ceratinia*, *Epis-*
3012 *cada* and related genera.

3013 205. *Base of vinculum when genitalic capsule everted*
3014 *from abdomen:* (0) remains inside/at edge last sternite
3015 (Fig. 19F); (1) completely everted (Fig. 19G). State 1 is an
3016 autapomorphy for *Tellervo* and *Hypothyris cantobrica*.

3017 *Aedeagus.* 206. *Anterior section of aedeagus (ductus*
3018 *ejaculatorius area) in dorsal view:* (0) straight (Fig. 19I);
3019 (1) rotated to right (Fig. 19H). State 1 is a synapomor-
3020 phy for *Heterosais*.

3021 207. *Anterior section of aedeagus in dorsal view,*
3022 *ignoring zone:* (0) straight (Fig. 19K); (1) bent sharply
3023 to left at ductus ejaculatorius (Fig. 19O); (2) curving
3024 evenly to left (Fig. 19P); (3) kinked slightly right then
3025 left (Fig. 19I). Initial attempts to code overall aedeagus
3026 shape produced so many character states that resultant
3027 coding contained little phylogenetic information. How-
3028 ever, much of the variation between species occurs
3029 through the aedeagus being bent at the zone. This
3030 variation was therefore disregarded, thus greatly redu-
3031 cing the number of coded states.

3032 208. *Aedeagus ventral edge below ductus ejaculatorius*
3033 *in lateral view:* (0) straight (Fig. 20L); (1) angled at
3034 middle (Fig. 20G).

3035 209. *Aedeagus width in anterior section in dorsal view:*
3036 (0) approximately even throughout or broadening ante-
3037 riorly to up to twice width (Fig. 19I); (1) broadening
3038 anteriorly to four times width (Fig. 19J). State 1 is an
3039 synapomorphy for *Velamysta*.

3040 210. *Aedeagus anterior section in dorsal view:* (0) of
3041 even width or gradually broadening throughout anteri-
3042 orly (Fig. 19L); (1) abruptly broadening at anterior tip
3043 like a mallet (Fig. 20E).

3044 211. *Dorsal junction of aedeagus with posterior edge of*
3045 *ductus ejaculatorius in dorsal view:* (0) symmetrical
3046 (Fig. 19P); (1) asymmetrical (Fig. 19N). State 1 is an
3047 autapomorphy for *Epityches*.

3048 212. *Aedeagus with lateral projections at anterior tip:*
3049 (0) absent (Fig. 19N); (1) present (Fig. 19K).

3050 213. *Aedeagus base with paired, broad rounded*
3051 *lateral lobes:* (0) absent (Fig. 20C); (1) present
3052 (Fig. 20A). State 1 is an autapomorphy for *Hyposcada*
3053 *virginiana*.

214. *Anterior dorsal edge of aedeagus forming a* 3054
support for ductus ejaculatorius: (0) absent (Fig. 21A); 3055
(1) present (Fig. 21G). State 1 is an autapomorphy for 3056
Pteronymia hara. 3057

215. *Aedeagus base with anterior edge of ductus* 3058
ejaculatorius located on a forward fold: (0) absent 3059
(Fig. 20I); (1) present (Fig. 20J). State 1 is an 3060
autapomorphy for *Hyposcada virginiana*. 3061

216. *Anterior end of aedeagus:* (0) opening dorsally 3062
(Fig. 21G); (1) opening to right-hand side (Fig. 21D); 3063
(2) opening ventrally (Fig. 21B). In most species the 3064
anterior section of the aedeagus opens dorsally into the 3065
ductus ejaculatorius. In *Hypoleria adasa*, *Mcclungia*, 3066
Brevioleria and *Godyris mantura* the aedeagus is rotated 3067
to the right 90° and opens into the ductus ejaculatorius 3068
to the right, and in *Callithomia* it is rotated 180° and 3069
thus opens ventrally. 3070

217. *Anterior end of aedeagus opening into ductus* 3071
ejaculatorius: (0) vertically, with anterior tip of aede- 3072
agus forming a sclerotized rounded lobe equal in 3073
height to remainder of aedeagus (Fig. 20G); (1) 3074
subvertically, similar to state 0 but with sclerotized 3075
lobe at anterior tip absent (Fig. 20O); (2) subhorizon- 3076
tally, with no sclerotized anterior lobe and broad, 3077
semisclerotized edges basal of ductus ejaculatorius 3078
(Fig. 20K); (3) horizontally, with no sclerotized anter- 3079
ior lobe and ventral edge of aedeagus and ductus 3080
ejaculatorius making a straight line (Fig. 20M). In 3081
more primitive species the ductus ejaculatorius arises 3082
vertically from the anterior section of the aedeagus 3083
but posterior of the tip (state 0). In a number of more 3084
derived species it is shifted anteriorly so that the 3085
sclerotized anterior tip of the aedeagus is absent and 3086
the ductus ejaculatorius opens subhorizontally. 3087

218. *Ductus ejaculatorius:* (0) unsclerotized, soft tissue 3088
(Fig. 20J); (1) semisclerotized (Fig. 20H). State 1 is a 3089
synapomorphy for *Haenschia* also occurring in *Hypole-* 3090
ria adasa. 3091

219. *Ductus ejaculatorius:* (0) lying in a flat plane 3092
(Fig. 19K); (1) bent and twisted to right (Fig. 20G); (2) 3093
twisted to left in dorsal view (Fig. 20C). This character 3094
refers to the shape of the ductus ejaculatorius, whereas 3095
Char. 220 refers to its orientation with respect to the 3096
aedeagus base. 3097

220. *Ductus ejaculatorius emerging:* (0) perpendicu- 3098
larly from aedeagus (Fig. 20C); (1) rotated to the right 3099
to lie flat against aedeagus (Fig. 20E). State 1 is a 3100
synapomorphy for *Hypoleria adasa*, *Mcclungia*, *Brevi-* 3101
oleria and *Godyris mantura*. The ductus ejaculatorius is 3102
similar in shape to related species but is rotated 90° so to 3103
lie flat against the aedeagus, opening to the left. 3104

221. *Extension of ductus ejaculatorius anteriorly* 3105
beyond aedeagus: (0) shorter than anterior section of 3106
aedeagus (Fig. 20F); (1) longer than anterior extension 3107
of aedeagus (Fig. 20M). State 1 is a synapomorphy for 3108
Haenschia, also occurring in some *Hypothyris*. 3109

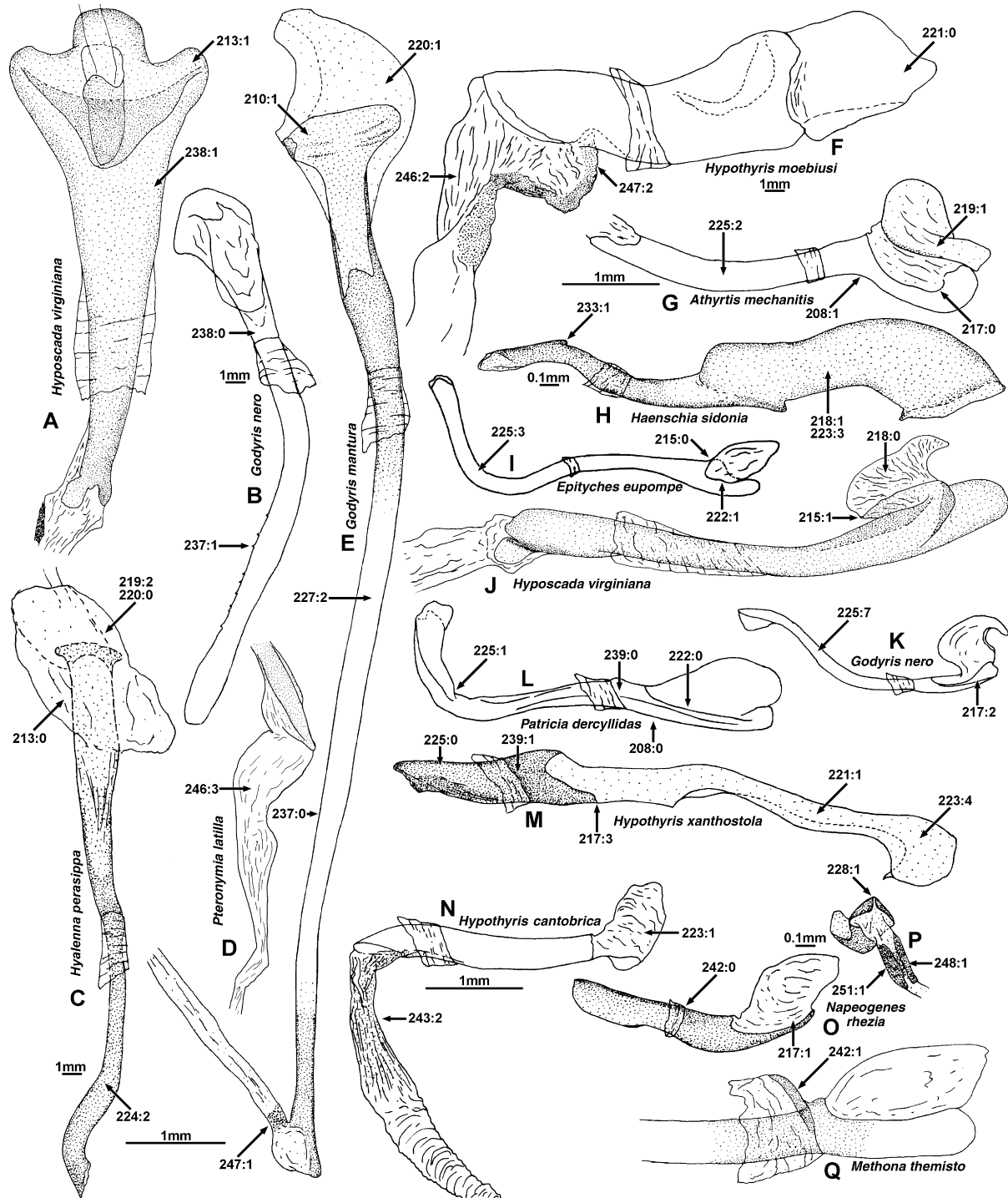


Fig. 20. Male genitalia. Aedeagus, dorsal view: (A) *Hyoscada* versus *virginiana*, vesica everted; (B) *Godyris nero*; (C) *Hyalenna p. perasippa*; (D) *Pteronymia l. latilla*, tip only, vesica everted; (E) *Godyris mantura honrathi*, vesica everted. Aedeagus, lateral view: (F) *Hypothesis m. moebiusi*, vesica everted; (G) *Athyrtis mechanitis salvini*; (H) *Haenschia sidonia*; (I) *Epityches eupompe*; (J) *Hyoscada* versus *virginiana*, vesica everted; (K) *Godyris nero*; (L) *Patricia d. deryllidas*; (M) *Hypothesis (Garsauritis) x. xanthostola*; (N) *Hypothesis (Rhodussa) c. cantobrica*, vesica everted; (O) *Napeogenes rhezia cyrianassa*. (P) *Napeogenes rhezia cyrianassa*, posterior view, vesica everted. (Q) *Methona t. themisto*, lateral view of basal section.

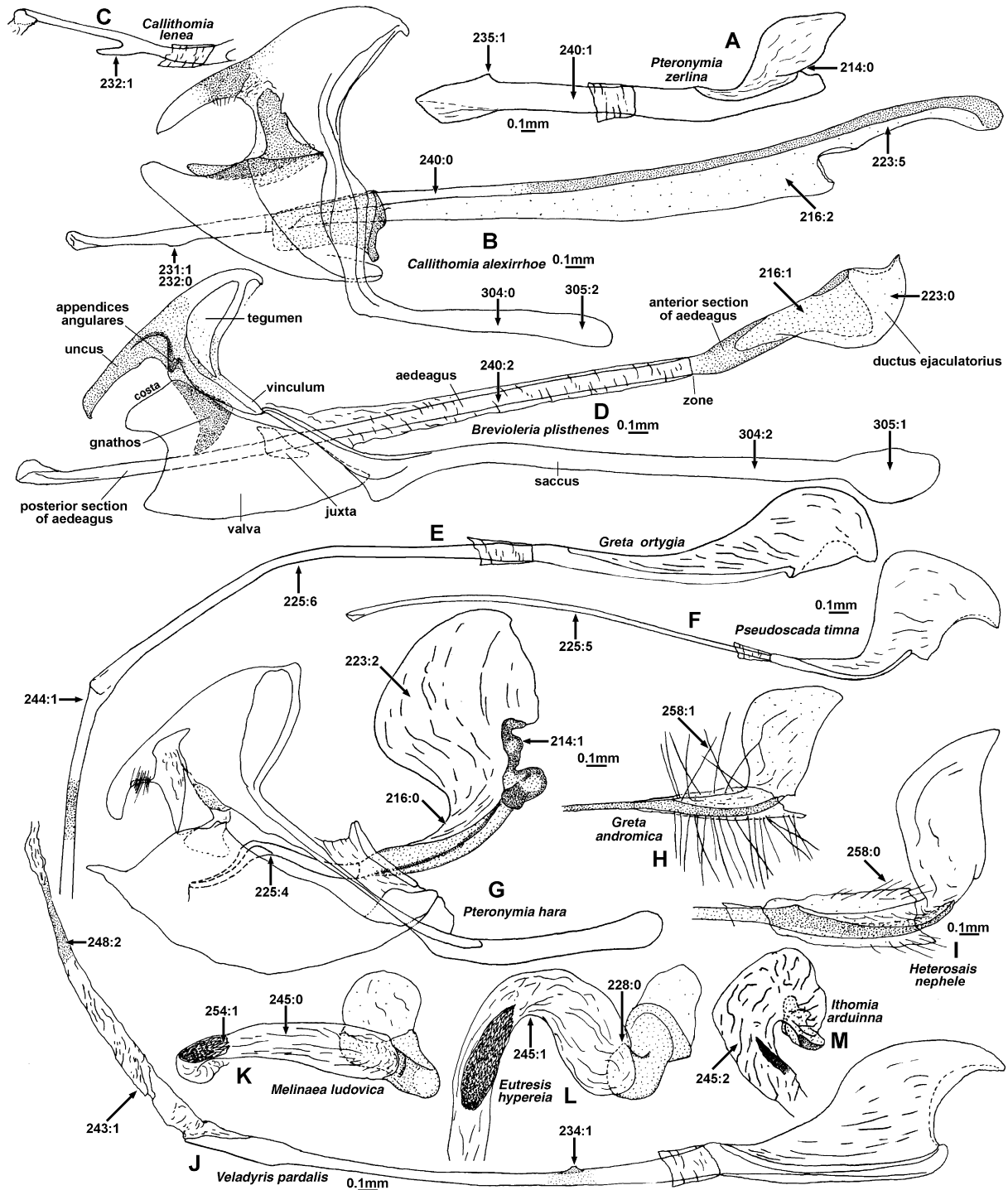
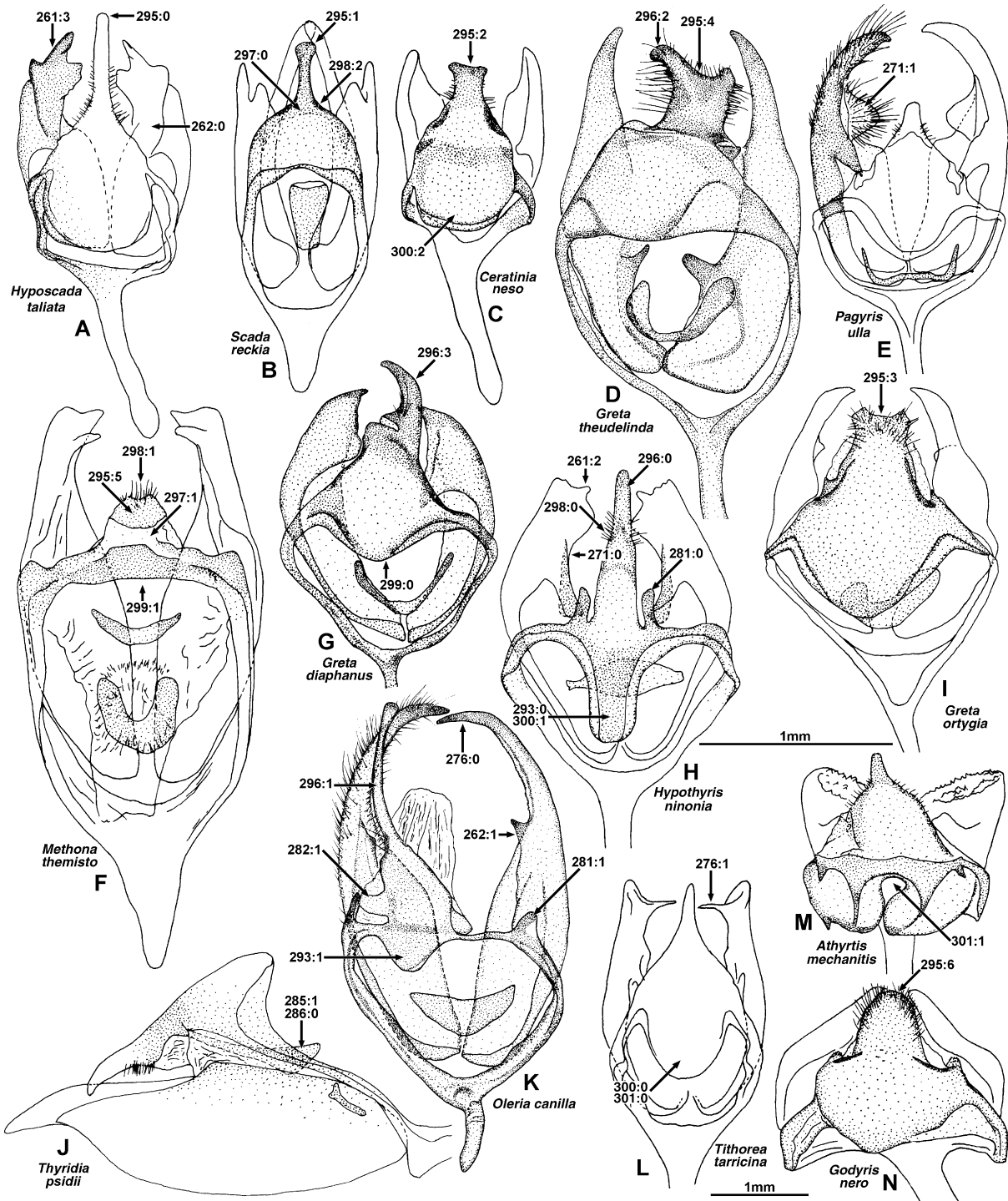


Fig. 21. Male genitalia. (A) *Pteronymia z. zerlina*, aedeagus, lateral view. (B) *Callithomia alexirrhoe zeuxippe*; (C) *Callithomia lenea zelia*, aedeagus posterior tip, lateral view; (D) *Brevioleria plisthenes*; (E) *Greta o. ortygia*, aedeagus, lateral view, vesica everted; (F) *Pseudoscada timna pusio*, aedeagus, lateral view; (G) *Pteronymia h. hara*; (H) *Greta andromica andania*, aedeagus, lateral view of basal section; (I) *Heterosais nephele*, aedeagus, lateral view of basal section; (J) *Veladyris p. pardalis*, aedeagus, lateral view, vesica everted; (K) *Melinaea l. ludovica*; (L) *Eutresis h. hypereia*; (M) *Ithomia a. arduinna*.

- 3110 222. *Ductus ejaculatorius* opening into aedeagus: (0)
3111 just slightly less to about half length of anterior section
3112 (Fig. 20L); (1) less than half length of anterior section
3113 (Fig. 20I).
- 3114 223. *Ductus ejaculatorius* shape: (0) a simple “hood”,
3115 greater or equal in width to height (Fig. 21D); (1) a
3116 vertically expanded “hood”, height greater than width
3117 (Fig. 20N); (2) a vertically expanded “hood” wider
3118 dorsally than at base (Fig. 21G); (3) a tube, greatly
3119 elongated anteriorly (Fig. 20H); (4) an anteriorly elon-
3120 gated sickle shape (Fig. 20M); (5) elongate with small
3121 opening posterior of anterior end of aedeagus
3122 (Fig. 21B). In all states except 4 and 5 the ductus
3123 ejaculatorius opens at its anterior edge; in 4 it opens
3124 ventrally and in 5 dorsally but in the middle of the
3125 ductus ejaculatorius.
- 3126 224. *Posterior section of aedeagus in dorsal view,*
3127 *ignoring zone:* (0) straight (Fig. 19J); (1) bent to right
3128 near tip (Fig. 19M); (2) bent to left near tip (Fig. 20C);
3129 (3) evenly curving to left (Fig. 19L). See Discussion
3130 under Char. 207.
- 3131 225. *Posterior section of aedeagus in lateral view,*
3132 *ignoring zone:* (0) straight (Fig. 20M); (1) curving
3133 upwards near tip (Fig. 20L); (2) curving slightly and
3134 evenly upwards (Fig. 20G); (3) curving sharply upwards
3135 (Fig. 20I); (4) bent downwards near tip (Fig. 21G); (5)
3136 curving evenly downwards (Fig. 21F); (6) bent down-
3137 wards at middle (Fig. 21E); (7) kinked up near middle
3138 then down at tip (Fig. 20K).
- 3139 226. *Aedeagus posterior section:* (0) of even width
3140 (Fig. 19I); (1) broadening at posterior tip (Fig. 19J).
- 3141 227. *Ratio of length of posterior section of aedeagus*
3142 *divided by minimum width of posterior section, r:* (0)
3143 $r < 13$ (Fig. 19K); (1) $13 < r < 34$ (Fig. 19I); (2)
3144 $34 < r < 67$ (Fig. 20E); (3) $67 < r$ (Fig. 19H). If the
3145 aedeagus is evenly tapering throughout, the average
3146 width was measured. Higher states indicate a relatively
3147 longer and thinner aedeagus.
- 3148 228. *Aedeagus posterior tip in posterior view:* (0)
3149 rounded in cross-section (Fig. 21L); (1) with a dorsal
3150 “peak” (Fig. 20P). State 1 is a synapomorphy for
3151 *Napeogenes*.
- 3152 229. *Aedeagus posterior tip with a sclerotized “ribbon”*
3153 *on right side extending on to base of vesica:* (0) absent
3154 (Fig. 19Q); (1) present (Fig. 19M). State 1 is a synapo-
3155 morphy for *Athesis* + *Patricia*.
- 3156 230. *Aedeagus posterior tip with a flat, serrate heavily*
3157 *sclerotized flange:* (0) absent (Fig. 19N); (1) present
3158 (Fig. 19Q). State 1 is a synapomorphy for *Methona*.
- 3159 231. *Aedeagus with dorsolateral projection on left side*
3160 *near middle posterior section:* (0) absent; (1) present
3161 (Fig. 21B). State 1 is a synapomorphy for *Callithomia*.
- 3162 232. If aedeagus has a dorsolateral projection on left
3163 side near middle posterior section (Char. 231:1), then
3164 projection is: (0) a bump (Fig. 21B); (1) a spine
3165 (Fig. 21C).
233. *Aedeagus posterior tip with a rounded, anteriorly* 3166
curved and posteriorly straight projection: (0) absent; (1) 3167
present (Fig. 20H). State 1 is a synapomorphy for 3168
Haenschia. 3169
234. *Aedeagus with small dorsal flange about a quarter* 3170
way along posterior section: (0) absent; (1) present 3171
(Fig. 21J). State 1 is an autapomorphy for *Veladyris* 3172
pardalis. 3173
235. *Aedeagus with flat, pointed dorsal projection near* 3174
posterior tip: (0) absent; (1) present (Fig. 21A). State 1 3175
occurs here only in *P. zerlina*, but is a synapomorphy for 3176
a clade of eight *Pteronymia* species. 3177
236. *Aedeagus with serrate right lateral edge near* 3178
posterior tip: (0) absent; (1) present (Fig. 19K). State 1 is 3179
a synapomorphy for *Dircenna* (excluding *D. paradoxa*). 3180
237. *Aedeagus posterior tip with line of small teeth* 3181
along left lateral edge near tip: (0) absent (Fig. 20E); (1) 3182
present (Figs 19L and 20B). State 1 is a synapomorphy 3183
for *Godyris* (excluding *G. mantura* and relatives). 3184
238. *Aedeagus in dorsal view:* (0) even in width or 3185
broadening in part of anterior or posterior section only 3186
(Fig. 20B); (1) broadening evenly throughout 3187
(Fig. 20A). State 1 is an autapomorphy for *Hyposcada* 3188
virginiana. 3189
239. *Aedeagus in lateral view:* (0) little varying in width 3190
(Fig. 20L); (1) tapering continuously from anterior to 3191
posterior tip (Fig. 20M). 3192
240. *Ratio of length of posterior section of aedeagus to* 3193
anterior section, r: (0) $r < 0.5$ (Fig. 21B); (1) 3194
 $0.5 < r < 1.58$ (Fig. 21A); (2) $1.58 < r$ (Fig. 21D). 3195
State 0 indicates posterior section much shorter than 3196
anterior; state 1 indicates posterior and anterior sections 3197
more or less equal in length; state 2 indicates posterior 3198
section much longer than anterior. 3199
241. *Total length of aedeagus divided by genitalic* 3200
capsule height, r: (0) $r < 1.22$ (Fig. 21G); (1) 3201
 $1.22 < r < 1.8$; (2) $1.8 < r < 3$; (3) $3 < r$ (Fig. 21B). 3202
Genitalic capsule height is the distance from the top of 3203
the tegumen to the middle of the saccus, measured along 3204
the vinculum. 3205
242. *Aedeagus with dorsal projection at base junction of* 3206
anterior and posterior sections: (0) absent (Fig. 20O); (1) 3207
present (Fig. 20Q). State 1 is a synapomorphy for 3208
Methona. 3209
- Vesica and cornuti.* 243. *With aedeagus anterior* 3210
opening directly dorsally (“midnight”), vesica everts in 3211
posterior view: (0) at 9–10.30 pm (to left) (Fig. 19Q); (1) 3212
at midnight (dorsally) (Fig. 21J); (2) at 6–7.30 pm 3213
(ventrally) (Fig. 20N); (3) at 3 pm (to right) (Fig. 19M). 3214
The vesica usually everts at an angle to the aedeagus, 3215
and the direction in which it everts varies between 3216
genera and species. To control for the rotation of the 3217
aedeagus with respect to the genitalic capsule in some 3218
species (Char. 216:1,2) the direction in which the vesica 3219
everts is measured relative to the anterior opening of the 3220
aedeagus into the ductus ejaculatorius. In species in 3221

- 3222 which this opening is horizontal (Char. 217:3), the edge
3223 of the sclerotized part of the aedeagus at the junction to
3224 the ductus ejaculatorius in lateral view is inclined,
3225 indicating the vertical sense in which the ductus ejacu-
3226 latorius opened in ancestors. Some species coded state 1
3227 for Char. 244, in which the vesica everts in a direct line
3228 with the aedeagus, could still be coded for this character
3229 based on a slight angle between vesica and aedeagus.
- 3230 244. *Vesica everting*: (0) at an angle to aedeagus
3231 (Fig. 19Q); (1) in a direct line with aedeagus (Fig. 21E);
3232 (2) recurved back towards anterior end of aedeagus
3233 (Fig. 19O). In many species the vesica is slightly curved
3234 back anteriorly throughout its length, but in species
3235 coded state 2 this curvature is sharp and occurs near the
3236 cornuti.
- 3237 245. *Vesica in posterior view*: (0) straight (Fig. 21K);
3238 (1) curved with concave side down (Fig. 21L); (2) curved
3239 into a spiral (Fig. 21M).
- 3240 246. *Base of vesica*: (0) of even width (Fig. 19M); (1)
3241 expanded then contracting (Fig. 19Q); (2) expanded into
3242 a parallelogram shape then narrowing (Fig. 20F); (3)
3243 expanded with a central constriction (Fig. 20D).
- 3244 247. *Patches of cornuti placed*: (0) near middle of
3245 vesica (Fig. 19M); (1) near base (distance between
3246 cornuti and aedeagus much less than size of cornutus)
3247 (Fig. 20E); (2) extending into soft tissue in mouth of
3248 aedeagus (Fig. 20F); (3) right inside soft tissue in mouth
3249 of aedeagus (Fig. 25E). Because one or other of the two
3250 (primitive) patches of cornuti is sometime absent, and
3251 because these patches are placed more or less opposite
3252 one another, this character refers to the position of
3253 either or both of the patches of cornuti.
- 3254 248. *Cornuti*: (0) in two distinct patches or on one side
3255 of aedeagus only (Fig. 25C); (1) in two distinct patches
3256 partially fused into a band (Fig. 20P); (2) completely
3257 fused into a uniform band (Fig. 21J).
- 3258 249. *Patches of cornuti*: (0) directly opposite
3259 (Fig. 25C); (1) with outer patch at distal edge of inner
3260 patch (Fig. 25A). In most species the vesica everts at an
3261 angle to the aedeagus, with one patch of cornuti on the
3262 side nearer the aedeagus (anterior) and the other on the
3263 farther side (posterior). These patches are referred to as
3264 the “inner” and “outer” patches, respectively. In almost
3265 all species the posterior tip of the aedeagus is more
3266 strongly sclerotized and distally extended on one side,
3267 with this corresponding directly to the “outer” side of
3268 the vesica. The position of the patches of cornuti with
3269 respect to the aedeagus tip is thus used to infer whether
3270 patches are inner or outer in species where the vesica
3271 everts in a direct line with the aedeagus (Char. 244:1).
- 3272 250. *Cornuti of inner patch* (see Discussion for Char.
3273 249): (0) distinct, large spines (Fig. 25C); (1) tiny spines
3274 to faint heavier sclerotization (Fig. 25F); (2) absent
3275 (Fig. 25B).
- 3276 251. *Cornuti of outer patch* (see Discussion for Char.
3277 249): (0) distinct, large spines (Fig. 25C); (1) tiny spines
to faint heavier sclerotization (Fig. 20P); (2) absent
(Fig. 25D); (3) very elongate spines (Fig. 25H). If the
two patches of cornuti are fused completely into a band
(Char. 248:2), then this character is coded as equivocal,
as both patches of cornuti are morphologically the same
and Char. 227 would otherwise be duplicated.
252. *Cornuti of inner patch* (see Discussion for Char.
249) forming: (0) a V-shape (Fig. 25C); (1) oval to
thin line (Fig. 25E); (2) two parallel narrow bands
(Fig. 25G); (3) a broad rectangular band (Fig. 25F). If
the two patches of cornuti are fused completely into a
band (Char. 248:2), this character is coded as equivocal.
253. *Cornuti of outer patch* (see Discussion for Char.
249) forming: (0) an approximate oval or rounded
rectangle (Fig. 25C); (1) a thin line (Fig. 25H). If the
two patches of cornuti are fused completely into a band
(Char. 248:2), this character is coded as equivocal.
254. *Cornuti of outer patch* (see Discussion for Char.
249): (0) even (Fig. 25H); (1) strongly differentiated
with basal cornuti much larger than distal (Fig. 21K).
- Juxta*. 255. *Juxta*: (0) present (sclerotized) (Fig. 23C);
(1) absent (unsclerotized) (Fig. 23D). State 1 is an
autapomorphy for *Ithomia drymo*.
256. *In lateral view juxta placed*: (0) about level with
vinculum (Fig. 25M); (1) level with posterior edge of
valvae (Fig. 25N). State 1 is a synapomorphy for
Godyris dircenna and *G. nero*.
257. *Juxta*: (0) varying from a “U”- to “V”-shaped
strip to plate in ventral view, straight and narrow or
moderately (no more so than juxta height) broad in
lateral view (Fig. 24E); (1) a narrow strip with dorsal
tips curved posteriorly in lateral view (Fig. 25O); (2) a
small round plate in ventral view (Fig. 24G); (3) a highly
elongate plate in ventral view (Fig. 24A); (4) an elongate
tube rectangular in lateral and ventral view (twice as
long as wide) (Fig. 24I). There is substantial variation in
juxta shape but much of this proved too continuous to
be coded, with the exception of several particularly
distinctive morphologies.
258. *Manica*: (0) with or without hairs (Fig. 21I); (1)
with very long hairs (Fig. 21H). The manica is the
membrane folded around and connected to the aedeagus
at the zone, the junction between the basal and distal
sections. In most species there are scattered hairs on the
inside surface of this membrane, visible when the aede-
agus is extruded. In *Pseudoscada* and certain *Greta* these
hairs are substantially longer than in all other species.
- Valvae*. 259. *Valvae*: (0) meeting at very base only
(Fig. 24A); (1) partially joined in base by soft tissue
(Fig. 24H); (2) closely appressed/fused at base
(Fig. 23L); (3) fused entirely at base and with soft tissue
in middle (Fig. 24B).
260. *Inner faces of valvae*: (0) approximately parallel
when valvae are closed (Fig. 24A); (1) divergent
(Fig. 24B). State 1 is an autapomorphy for *Athyrtis*.



18 Fig. 22. Male genitalia, dorsal view, aedeagus removed, setae on valvae omitted except on right valva E and K. (A) *Hyposcada taliata*; (B) *Scada reckia theaphia*; (C) *Ceratinia n. neso*; (D) *Greta t. theudelinda*; (E) *Pagyris u. ulla*; (F) *Methona t. themisto*; (G) *Greta diaphanus*; (H) *Hypothyris n. ninonia*; (I) *Greta o. ortygia*; (J) *Thyridia p. psidii*; (K) *Oleria canilla*; (L) *Tithorea tarricina parola*; (M) *Athyrtis mechanitis salvini*; (N) *Godyris nero*.

3334 261. *Valva posterior tip*: (0) ending in a smoothly
 3335 rounded point or lobe (that may be bifurcate at very tip,
 3336 as in *Hyposcada anchiala*) (Fig. 25I); (1) with a single

dorso-lateral, inner lobe or projection (Fig. 25J); (2) 3337
 tripartite (Fig. 22H); (3) with a lobe and a “cup” 3338
 (Fig. 22A). Most primitive species of Ithomiinae have 3339

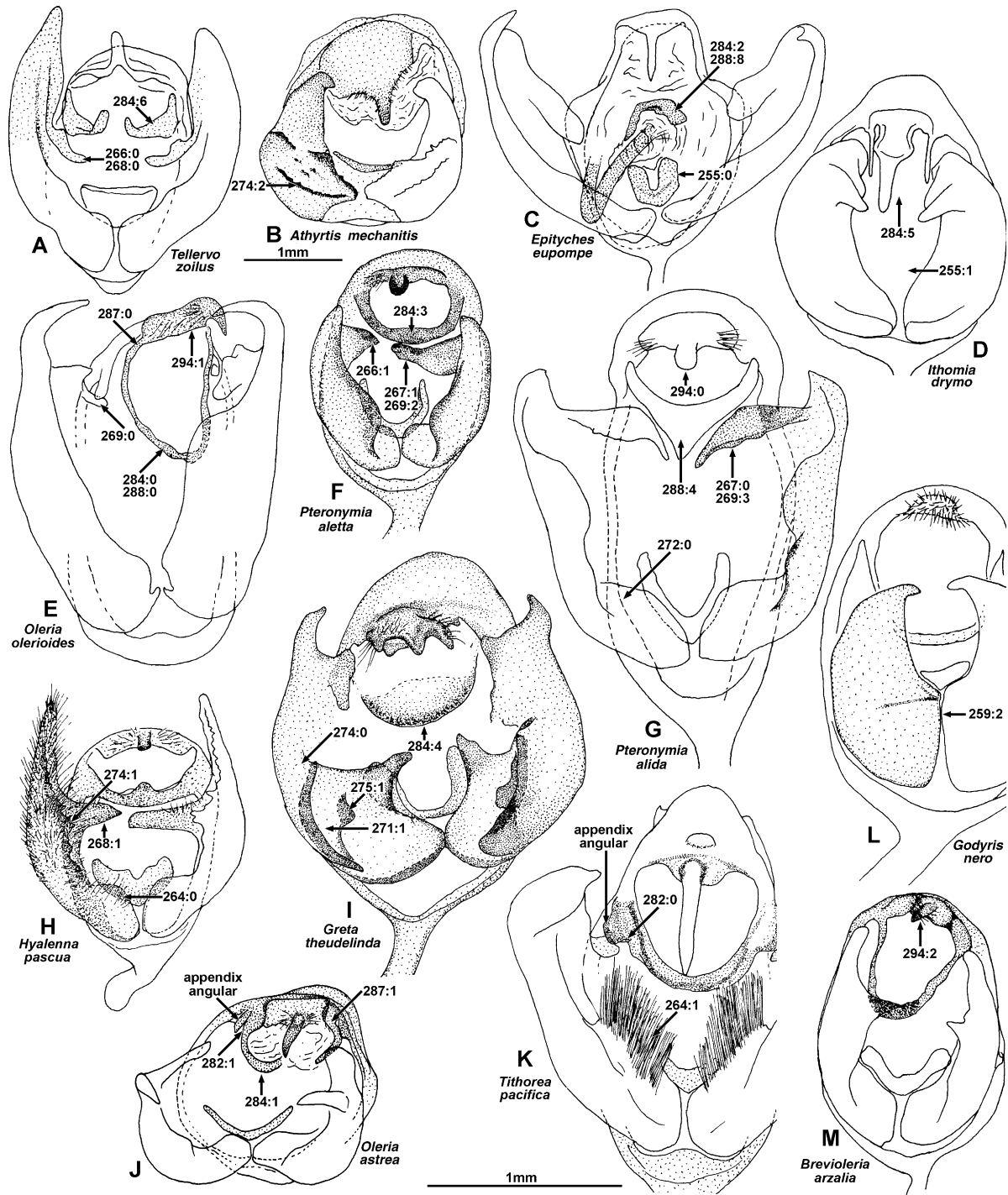
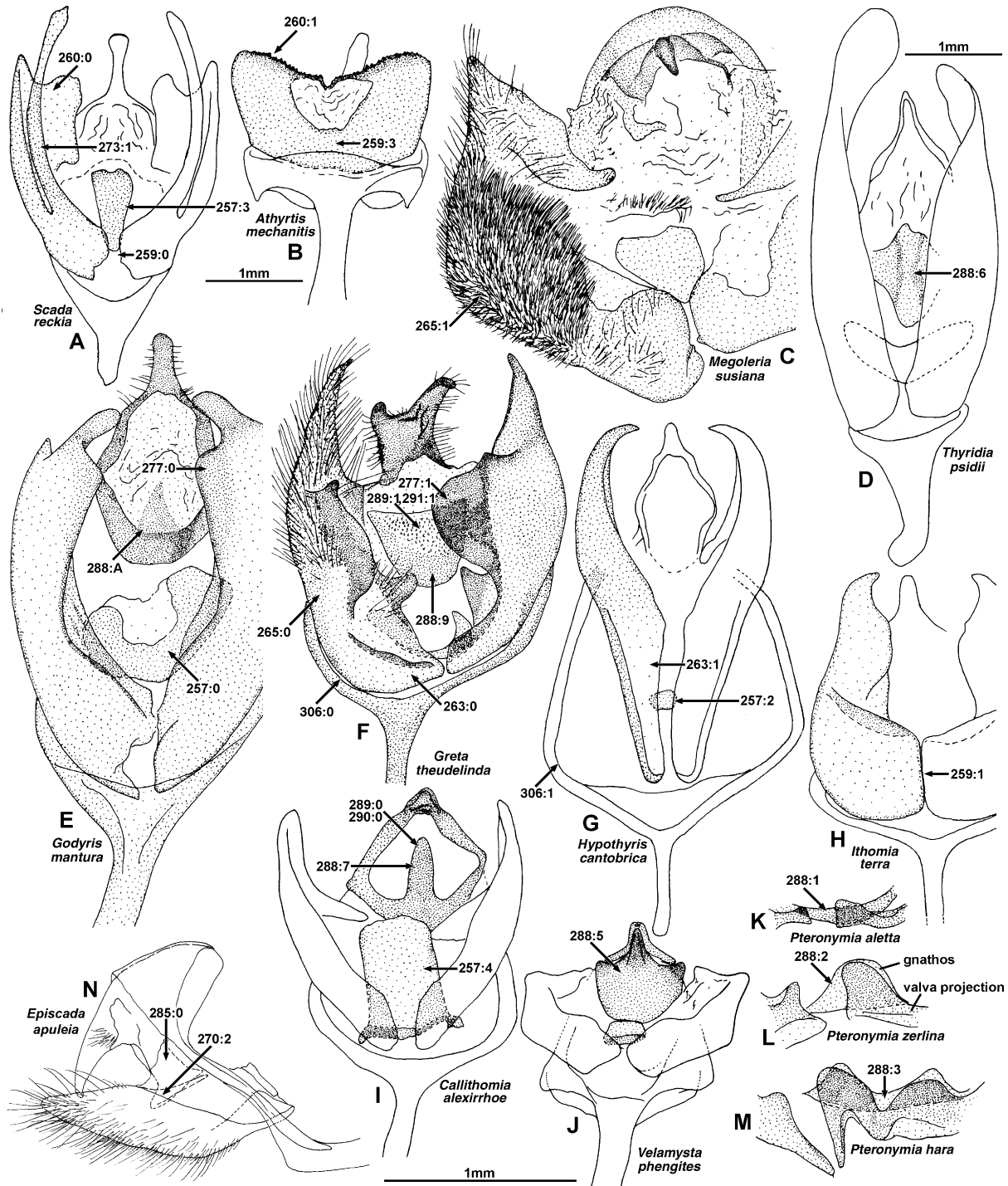


Fig. 23. Male genitalia, posterior view, aedeagus removed except C, setae on valvae omitted except on right valva H. (A) *Tellervo z. zoilus*; (B) *Athyrtis mechanitis salvini*; (C) *Epityches eupompe*; (D) *Ithomia drymo*; (E) *Oleria olerioides*; (F) *Pteronymia a. aletta*; (G) *Pteronymia a. alida*; (H) *Hyalenna pascua*; (I) *Greta t. theudelinda*; (J) *Oleria astrea burchelli*; (K) *Tithorea p. pacifica* Willmott & Lamas, 2004; (L) *Godyris nero*; (M) *Brevioleria arzalia* ssp. n.

3340 the posterior section of the valvae bifurcate, although
 3341 the upper projection (state 1) is variously modified,
 3342 forming an inner ridge in *Tithorea* (Char. 276:1). It is

possible that the “tripartite” posterior tip in some 3343
 Napeogenini also represents a similar state to 1, but as 3344
 this is rather unclear and primitive Napeogenini have a 3345



19 Fig. 24. Male genitalia, ventral view (except C, N), aedeagus removed, setae on valvae omitted except on right valva C and F. (A) *Scada reckia theaphia*; (B) *Athyrtis mechanitis salvini*; (C) *Megoleria s. susiana*, posterior view; (D) *Thyridia p. psidii*; (E) *Godyrnis mantura honrathi*; (F) *Greta t. theudelinda*; (G) *Hypothyris (Rhodussa) c. cantobrica*; (H) *Ithomia t. terra*; (I) *Callithomia alexirrhoe zeuxippe*; (J) *Velamysta p. phengites*. Gnathos and inner dorsal projection from costa of valva, ventral view: (K) *Pteronymia a. aletta*; (L) *Pteronymia z. zerlina*; (M) *Pteronymia h. hara*. Lateral view: (N) *Episcada a. apuleia*.

3346 simple valva (state 0) it was coded as a distinct state.
 3347 Similarly, it also seems possible (but less likely) that the
 3348 projecting dorsal, basal edge of the valva (Char. 262:1)

3349 may be homologous with Char. 261:1, but because of
 3350 the different position (only *Scada* is ambiguous) it is
 3351 coded as a distinct character.

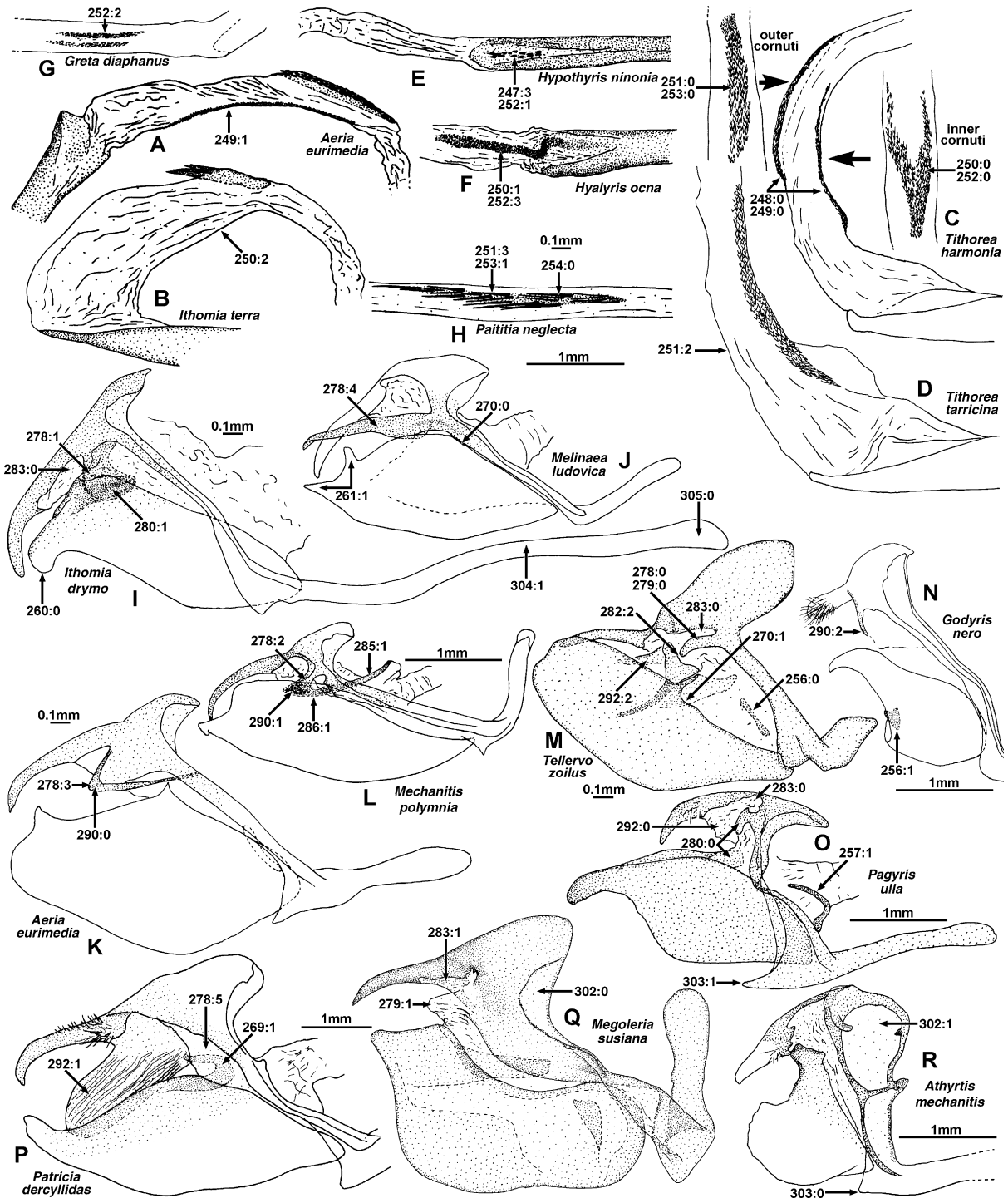


Fig. 25. Male genitalia. Aedeagus posterior tip and everted vesica, dorsal view: (A) *Aeria e. eurimedia*; (B) *Ithomia t. terra*; (C) *Tithorea harmonia manabiana*; (D) *Tithorea tarricina parola*. Aedeagus tip and everted vesica, view perpendicular t; cornuti: (E) *Hypothyris n. ninonia*; (F) *Hyalyris ocna* ssp. n. Vesica, view perpendicular t; cornuti: (G) *Greta diaphanus*; (H) *Paititia neglecta*. Male genitalia, lateral view: (I) *Ithomia drymo*; (J) *Melinaea l. ludovica*; (K) *Aeria eurimedia negricola*; (L) *Mechanitis p. polymnia*; (M) *Tellervo z. zoilus*; (N) *Godyris nero*; (O) *Pagyris u. ulla*; (P) *Patricia d. deryllidas*; (Q) *Megoleria s. susiana*; (R) *Athyrtis mechanitis salvini*.

- 3352 262. *Valva basal costa in dorso-lateral view*: (0) rounded, not projecting inwards beyond rest of valva (Fig. 22A); (1) a smooth plate, projecting inwards and sometimes posteriorly (Fig. 22K). See Discussion under Char. 261; although *Scada* are coded 1 and appear similar to *Oleria*, the state is independently derived and in *Scada* may represent a modification of Char. 261:1. This is the dorsal edge of the valva, not the inner, dorso-basal portion that articulates with the vinculum (Char. 266–269).
- 3353 263. *Basal portion of valva*: (0) similarly sclerotized to remainder of valva (Fig. 24F); (1) very elongate and weakly sclerotized (Fig. 24G). State 1 is an autapomorphy for *Hypothyris cantobrica*.
- 3354 264. *Thick, long, dense hairs on inner basal edge of valva*: (0) absent (Fig. 23H); (1) present (Fig. 23K).
- 3355 265. *Thick, short, dense hairs on ventral posterior part of valva*: (0) absent (Fig. 24F); (1) present (Fig. 24C). State 1 is a synapomorphy for *Megoleria*.
- 3356 266. *Valva dorsal inner projection from costa (articulating with vinculum) sclerotized*: (0) similar to rest of valva (Fig. 23A); (1) more heavily than rest of valva (Fig. 23F).
- 3357 267. *Valvae dorsal inner projections from costa (Char. 266)*: (0) approximately even in size (Fig. 23G); (1) larger on right-hand side (Fig. 23F).
- 3358 268. *Valva dorsal inner projection from costa (Char. 266)*: (0) in line with more posterior valva edge (Fig. 23A); (1) angled inwards (Fig. 23H).
- 3359 269. *Shape of valvae dorsal inner projections from costa (Char. 266)*: (0) varying from smoothly rounded to a slightly elongate, even lobe (Fig. 23E); (1) curving inwards and ending in an expanded rounded lobe (Fig. 25P); (2) right projection is a vertically broad then horizontally broad plate (Fig. 23F); (3) pointed, downward curving plate (Fig. 23G). State 2 occurs only in some *Pteronymia* and *Haenschia*. In *Haenschia* the right projection is a plate twisted through 90°, so that it is vertical at the base and horizontal at the tip. The right projection is similar in some *Pteronymia* except the tip is more heavily sclerotized and rounded, and the states in both these genera are interpreted as homologous.
- 3360 270. *Valvae with ratio of distance between anterior edge and vinculum in line with dorsal edge of valva, and valva maximum height, r*: (0) $r < 0.55$ (Fig. 25J); (1) $0.55 < r < 1.1$ (Fig. 25M); (2) $r > 1.1$ (Fig. 24N). Species with higher states have the anterior edge of the valva further from the vinculum (relative to the valva width), resulting in valvae that can be opened to a greater extent.
- 3361 271. *Broad, rounded, flat, weakly sclerotized lobe on dorsal inner edge of valva*: (0) absent (Fig. 22H); (1) present (Fig. 22E). State 1 occurs only in *Placidina* and *Pagyris*, and is either a synapomorphy for these two genera or has been subsequently lost in *Ithomia*.
- 3362 272. *Inner face of valva in basal half with a broad, curving concavity*: (0) absent (Fig. 23G); (1) present (Fig. 23I). This concavity is shaped like a “suction cup” on the inner face of the valva, producing a notch or cleft at its dorsal edge around the middle of the valva, visible in posterior view.
- 3363 273. *Valva ventral base with a very elongate, narrow projection extending posteriorly beyond valva*: (0) absent; (1) present (Fig. 24A). State 1 occurs only in several *Scada* species.
- 3364 274. *Inner face of valva*: (0) smooth (Fig. 23I); (1) with spiny projections along the middle of the ventral edge (Fig. 23H); (2) with spiny projections in lines across the basal half of the valva (Fig. 23B). State 1 occurs here in *H. pascua* and is a synapomorphy for four *Hyalenna* species. State 2 is an autapomorphy for *Athyrtis*. In *Haenschia*, and to a lesser extent some other species (e.g., *Dircenna paradoxa*), the inner face of the valva is marked with numerous small “warts” which represent the expanded bases of hairs in states 1 and 2 the projections do not terminate in hairs.
- 3365 275. *Inner face of valva with small ridges near base*: (0) absent; (1) present (Fig. 23I).
- 3366 276. *Valva with a vertical ridge on inner face just anterior of tip*: (0) absent (Fig. 22K); (1) present (Fig. 22L).
- 3367 277. *Valvae ventral projections*: (0) symmetrical (Fig. 24E); (1) strongly asymmetrical (Fig. 24F). The ventral base of the valvae in a number of species, especially in the Godyridini, has various flat or elongate projections, which may be more or less symmetrical or strongly asymmetrical.
- 3368 *Gnathos and appendices angulares*. 278. *Appendices angulares*: (0) moderately sized projection on vinculum (similar in size to vinculum thickness) (Fig. 25M); (1) curved, vertical plates (Fig. 25I); (2) moderately posteriorly elongate projections (Fig. 25L); (3) large, triangular projections (Fig. 25K); (4) long, hollow tubes similar in length to valvae (Fig. 25J); (5) absent or tiny bumps on vinculum (Fig. 25P).
- 3369 279. *Appendices angulares*: (0) sclerotized (Fig. 25M); (1) unsclerotized (Fig. 25Q). State 1 occurs only in *Megoleria susiana*, in which the appendices angulares are visible as unsclerotized projections.
- 3370 280. *Appendices angulares*: (0) do not overlap in lateral view with valva dorsal inner projections (Char. 266) (Fig. 25O); (1) do overlap (Fig. 25I). The appendices angulares are usually dorsal of the dorsal edge of the valva and inner dorsal projections, but in a number of Napeogenini they extend ventrally to lie close beside these projections. If the appendices angulares are absent (some species coded 278:6) then this character is coded as equivocal.
- 3371 281. *Appendices angulares positioned with respect to tegumen*: (0) equidistant (Fig. 22H); (1) further away on left side (Fig. 22K). Some species coded 278:6 were

- 3464 coded for this character if some trace of the appendices
 3465 angulares was visible. In the Godyridini some species
 3466 have the edge of the vinculum produced posteriorly into
 3467 a slight fold immediately adjacent to the gnathos, and
 3468 this represents the appendices angulares.
- 3469 282. *Gnathos*: (0) attached to uncus and appendices
 3470 angulares (Fig. 23J); (1) attached to uncus only
 3471 (Figs 22K and 23J); (2) attached to uncus and tegumen
 3472 by unsclerotized tissue (Fig. 25M). The “gnathos” refers
 3473 to any sclerotized band or ring that encircles the tuba
 3474 analis and extends from near the junction of the
 3475 vinculum and base of the uncus. The gnathos is highly
 3476 variable in form and in many cases these different forms
 3477 are not anatomically homologous. However, because of
 3478 substantial variation between these forms, and because
 3479 most seem to serve a similar purpose (supporting the
 3480 tuba analis), for simplicity they are coded as single
 3481 characters. In most Ithomiinae the gnathos attaches to
 3482 the base of the uncus and the appendices angulares,
 3483 which themselves arise from the upper part of the
 3484 vinculum. In the Oleriini (*Megoleria*, *Hyposcada* and
 3485 *Oleria*), the gnathos is attached to the base of the uncus
 3486 only, and quite distinct from the appendices angulares.
- 3487 283. *Appendices angulares and expanded base of uncus*:
 3488 (0) separated by soft tissue (Fig. 25I,M,O); (1) fused
 3489 with semi or sclerotized tissue (Fig. 25Q). The uncus in
 3490 primitive species consists of a tapering, pointed tube that
 3491 broadens towards the base, where it usually bears lateral
 3492 hairs, then narrows distinctly (in lateral view) before its
 3493 connection with the tegumen. The narrow area lies
 3494 dorsal of weakly sclerotized region between the appen-
 3495 dices angulares/vinculum and the broad base of the
 3496 uncus. In *Scada*, Oleriini, Dircennini and Godyridini,
 3497 this intermediate region is also semi or completely
 3498 sclerotized, forming the dorsal part of the gnathos
 3499 (which is isolated from the appendices angulares in
 3500 Oleriini, but fused to these in the remainder). This
 3501 character is coded equivocal if the appendices angulares
 3502 are absent.
- 3503 284. *Gnathos form of sclerotization*: (0) a narrow,
 3504 entire, weakly sclerotized strip (Fig. 23E); (1) a scler-
 3505 otized strip near vinculum only, not complete
 3506 (Fig. 23J); (2) a sclerotized strip above aedeagus only
 3507 (Fig. 23C); (3) a very heavily sclerotized continuous
 3508 band (Fig. 23F); (4) a heavily sclerotized scoop
 3509 isolated from vinculum (Fig. 23I); (5) absent
 3510 (Fig. 23D); (6) strongly sclerotized, posteriorly point-
 3511 ing tubes, not complete (Fig. 23A). Absent is included
 3512 as a state of this character as other states involve
 3513 reduction in the gnathos.
- 3514 285. *Gnathos*: (0) more or less parallel to vinculum
 3515 (Fig. 24N); (1) projecting anteriorly (Figs 22J and 25L).
 3516 In most species in which the outline of the gnathos is
 3517 visible in lateral view it is more or less parallel with the
 3518 vinculum. In *Aeria* and the Mechanitini the gnathos is
 3519 directed anteriorly, at a sharp angle to the vinculum.
286. *If gnathos arms in lateral view are projecting* 3520
anteriorly (Char. 285:1), then arms are: (0) straight 3521
 (Fig. 22J); (1) bent at right angles near base (Fig. 25L). 3522
287. *If gnathos is attached to uncus only (Char. 237:1),* 3523
then base of gnathos arms in posterior view: (0) evenly 3524
 curving (Fig. 23E); (1) kinked (Fig. 23J). State 1 is a 3525
 synapomorphy for *Oleria*. 3526
288. *Gnathos ventral portion*: (0) of similar width to 3527
 the base of gnathos arms or slightly broader 3528
 (Fig. 23E); (1) about twice width of base of gnathos 3529
 arms (Fig. 24K); (2) broadening posteriorly into a 3530
 smooth projection (not narrow projection like state 7) 3531
 (Fig. 24L); (3) with two posterior projections 3532
 (Fig. 24M); (4) with a posterior broad, slight projec- 3533
 tion and larger broad, anterior projection (broader 3534
 and shorter projections than 6) (Fig. 23G); (5) with 3535
 long central posterior and broad anterior projection (6 3536
 has short posterior projection, 7 has short anterior 3537
 projection) (Fig. 24J); (6) with a short central poster- 3538
 ior and long anterior projection (Fig. 24D); (7) with a 3539
 posteriorly pointing central projection (Fig. 24I); (8) 3540
 slightly broader and concave ventrally forming a 3541
 “hood” (Fig. 23C); (9) greatly broadened into a 3542
 square shape (Fig. 24F); (A) a rectangular sclerotized 3543
 band with a posteriorly pointing semisclerotized projec- 3544
 tion (Fig. 24E). If the gnathos is absent ventrally, 3545
 this character is coded equivocal. 3546
289. *Gnathos ventrally*: (0) uniformly sclerotized 3547
 (Fig. 24I); (1) becoming less sclerotized posteriorly 3548
 (Fig. 24F). State 1 is a synapomorphy for Godyridini 3549
 excluding *Veladyris* and *Velamysta*, apparently being lost 3550
 in *Hypoleria adasa*. 3551
290. *Base of gnathos/appendices angulares*: (0) smooth 3552
 (Fig. 25K); (1) with rounded bumps (Fig. 25L); (2) with 3553
 tiny spines (Fig. 25N). 3554
291. *Gnathos with tiny bumps at posterior edge in* 3555
ventral view: (0) absent (Fig. 24I); (1) present (Fig. 24F). 3556
 State 1 is a synapomorphy for Godyridini excluding 3557
Veladyris and *Velamysta*, apparently being lost in 3558
Hypoleria adasa. 3559
- Tuba analis*. 292. *Male genitalia with tuba analis*: (0) 3560
 weakly sclerotized (except for gnathos, if present) 3561
 (Fig. 25O); (1) a sclerotized, wrinkled tube (Fig. 25P); 3562
 (2) a semisclerotized flat plate (Fig. 25M). State 1 occurs 3563
 only in *Patricia*, state 2 only in *Tellervo*. 3564
- Uncus and tegumen*. 293. *Uncus and tegumen in dorsal* 3565
view: (0) symmetrical (Fig. 22H); (1) strongly asymmet- 3566
 rical, with tegumen displaced to right (Fig. 22K). 3567
294. *Uncus in posterior view*: (0) horizontal (Fig. 23G); 3568
 (1) rotated slightly anticlockwise (Fig. 23E); (2) rotated 3569
 slightly clockwise (Fig. 23M). 3570
295. *Uncus in dorsal view*: (0) tapering to a single point 3571
 (Fig. 22A); (1) slightly flared and bifid at tip (Fig. 22B); 3572
 (2) broad and shallowly bifid at tip (Fig. 22C); (3) broad 3573
 and deeply bifid at tip, flaring slightly laterally 3574
 (Fig. 22I); (4) asymmetrical, bifid, right projection 3575

3576 longer than left (Fig. 22D); (5) short, blunt, flat or
3577 slightly bifid at tip (Fig. 22F); (6) broad and rounded
3578 (Fig. 22N).

3579 296. *Uncus in dorsal view perpendicular to base of*
3580 *uncus*: (0) straight (Fig. 22H); (1) curved to left near
3581 base of narrow distal portion (Fig. 22K); (2) bent at
3582 base to left (Fig. 22D); (3) curved to right (Fig. 22G). A
3583 straight uncus can appear bent or curved in dorsal view,
3584 if the entire uncus and tegumen are rotated in posterior
3585 view (Char. 294:1,2).

3586 297. *Uncus*: (0) continuously connected to tegumen by
3587 sclerotized tissue (Fig. 22B); (1) isolated from tegumen
3588 by unsclerotized tissue at base (Fig. 22F). State 1 is an
3589 synapomorphy for *Methona*.

3590 298. *Uncus with lateral hairs*: (0) near base and at sides
3591 only (Fig. 22H); (1) near base, at sides and extending on
3592 to tip (Fig. 22F); (2) lacking hairs (Fig. 22B).

3593 299. *Tegumen*: (0) present (Fig. 22G); (1) absent
3594 (Fig. 22F). State 1 is an synapomorphy for *Methona*.

3595 300. *Ratio of width of tegumen to length uncus + teg-*
3596 *umen*, r : (0) $0.3 < r < 0.55$ (Fig. 22L); (1) $r < 0.3$
3597 (Fig. 22H); (2) $r > 0.55$ (Fig. 22C). State 1 indicates a
3598 relatively narrow tegumen, state 2 indicates a relatively
3599 broad tegumen, in dorsal view.

3600 301. *Tegumen*: (0) a rounded lobe (Fig. 22L); (1) deeply
3601 cleft (Fig. 22M). State 1 is an autapomorphy for *Athyrtis*.

3602 302. *Weakly sclerotized tissue on antero-ventral edge*
3603 *of tegumen in lateral view*: (0) equal or less in size than
3604 sclerotized dorsal portion (Fig. 25Q); (1) greatly expan-
3605 ded (Fig. 25R). State 1 is an autapomorphy for *Athyrtis*.

3606 303. *Saccus posterior edge protruding*: (0) not
3607 much beyond vinculum (Fig. 25R); (1) substantially
3608 beyond vinculum (Fig. 25O).

3609 304. *Ratio of saccus length to length of uncus + teg-*
3610 *umen*, r : (0) $r < 1.25$ (Fig. 21B); (1) $1.25 < r < 2.1$
3611 (Fig. 25I); (2) $2.1 < r$ (Fig. 21D). Higher states indicate
3612 a relatively longer saccus. Saccus length is measured
3613 from the anterior tip to the midpoint of the saccus where
3614 it intersects a line parallel to and passing through the
3615 middle of the vinculum.

3616 305. *Saccus width*: (0) approximately even through-
3617 out (ratio maximum width/minimum width, $r < 2.25$)
3618 (Fig. 25I); (1) broadening near anterior tip (ratio
3619 maximum width/minimum width, $r > 2.25$)
3620 (Fig. 21D); (2) broadening gradually throughout,
3621 towards anterior tip (ratio maximum width/minimum
3622 width, $r > 2.25$) (Fig. 21B). Most species have the
3623 saccus of even width, while many species in the
3624 Godyridini and *Callithomia* have the saccus enlarged
3625 at the anterior tip. The maximum saccus width
3626 therefore refers to the maximum width in the anterior
3627 portion of the saccus. In a few cases the saccus evenly
3628 tapers anteriorly, in which case a single average width
3629 was used for both maximum and minimum saccus
3630 width. In the Godyridini the saccus broadens notice-

ably only near the anterior tip, whereas in *Callithomia* 3631
it broadens gradually throughout its length. 3632

Vinculum. 306. *Vinculum*: (0) running close to or 3633
outside antero-ventral portion of valvae (Fig. 24F); (1) 3634
far outside antero-ventral portion of valvae (Fig. 24G). 3635
State 1 is an autapomorphy for *Hypothyris cantobrica*. 3636

Female genitalia and abdomen 3637

External. 307. *Terminal (eighth) tergite in dorsal* 3638
view: (0) entirely sclerotized or with small unsclerotized 3639
area at indentation at middle of posterior edge 3640
(Fig. 26A); (1) like state 0, but with anterior half also 3641
weakly sclerotized (Fig. 26B); (2) with sclerotized halves 3642
medially divided by unsclerotized tissue (Fig. 26C). 3643

308. *Pleural tissue connecting terminal (eighth) and* 3644
penultimate (seventh) tergites: (0) similar in width to 3645
tissue between other tergites (Fig. 26D); (1) much 3646
narrower than between adjacent tergites, with tergite 3647
edges adjacent (Fig. 26F). 3648

309. *Eighth sternite*: (0) present (Fig. 26F); (1) absent, 3649
terminal tergite of similar height to remaining tergites 3650
(Fig. 26G); (2) absent, terminal tergite elongate ven- 3651
trally (Fig. 26I). Character 320 codes the form of the 3652
eighth sternite, also known as the lamella postvaginalis, 3653
which is usually present as a pair of distinct, separate or 3654
fused plates ventral of the terminal (eighth) tergite. In 3655
some species these plates are visibly fused to the ventral 3656
edge of the terminal tergite (see Discussion under Char. 3657
320), and in others they are apparently absent. This 3658
absence may be the result of loss of the eighth sternite or 3659
fusion with the terminal tergite; some species (e.g., 3660
Tithorea tarricina) have the terminal tergite similar in 3661
size to remaining tergites, suggesting that the eighth 3662
sternite has simply been lost, whereas others have the 3663
terminal tergite elongated (e.g., *Napeogenes*), suggesting 3664
fusion with the eighth sternite. To avoid unnecessary 3665
inferences about whether or not the eighth sternite is 3666
present and fused or absent, we therefore coded instead 3667
the shape of the terminal tergite when the eighth sternite 3668
is apparently absent. Species coded for this character 3669
were therefore coded as equivocal for Char. 320. 3670

310. *Penultimate (seventh) tergite*: (0) approximately 3671
same width as terminal (eighth) tergite, or larger 3672
(Fig. 27B); (1) about half the width of terminal tergite 3673
(Fig. 27A). 3674

311. *Posterior edge of penultimate (seventh) tergite*: 3675
(0) straight (Fig. 26D); (1) weakly curved around 3676
spiracle (Fig. 26G); (2) strongly curved around spiracle 3677
(Fig. 26H). 3678

312. *Ventral edge of penultimate (seventh) tergite*: (0) 3679
smooth and uniformly sclerotized (Fig. 26G); (1) wrin- 3680
kled and heavily sclerotized (Fig. 26E). 3681

313. *Seventh sternite and terminal (eighth) tergite*: (0) 3682
distinct, separated by soft pleural tissue (Fig. 27C); (1) 3683
almost fused with semisclerotized intervening pleural 3684

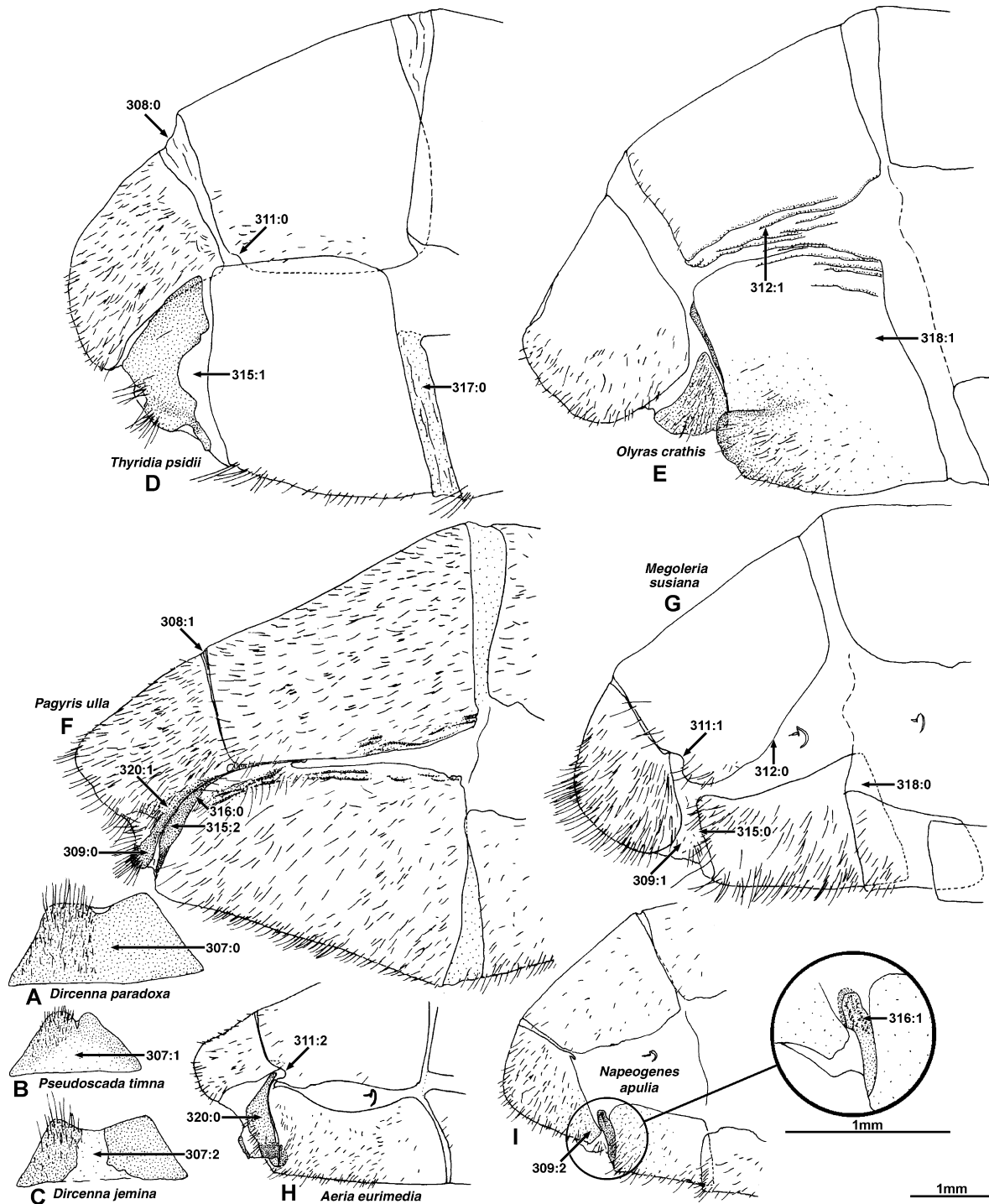


Fig. 26. Female abdomen. Terminal (posterior) tergite, dorsal view: (A) *Dircenna paradoxa praestigiosa*; (B) *Pseudoscada timna* ssp. n.; (C) *Dircenna j. jemina*. Abdomen posterior tip, lateral view: (D) *Thyridia p. psidii*; (E) *Olyras c. crathis*; (F) *Pagyris u. ulla*; (G) *Megoleria s. susiana*; (H) *Aeria e. eurimedia*; (I) *Napeogenes apulia* ssp. n.

3685 tissue (Fig. 27A). State 1 is a synapomorphy for
3686 *Aremfoxia* + *Epityches*.

3687 314. Pleural tissue between right-hand penultimate
3688 (seventh) tergite and seventh sternite with a large,

irregular, heavily sclerotized mass: (0) absent (Fig. 27C); 3689
(1) present (Fig. 27B). State 1 is an autapomorphy for 3690
Oleria santineza. 3691

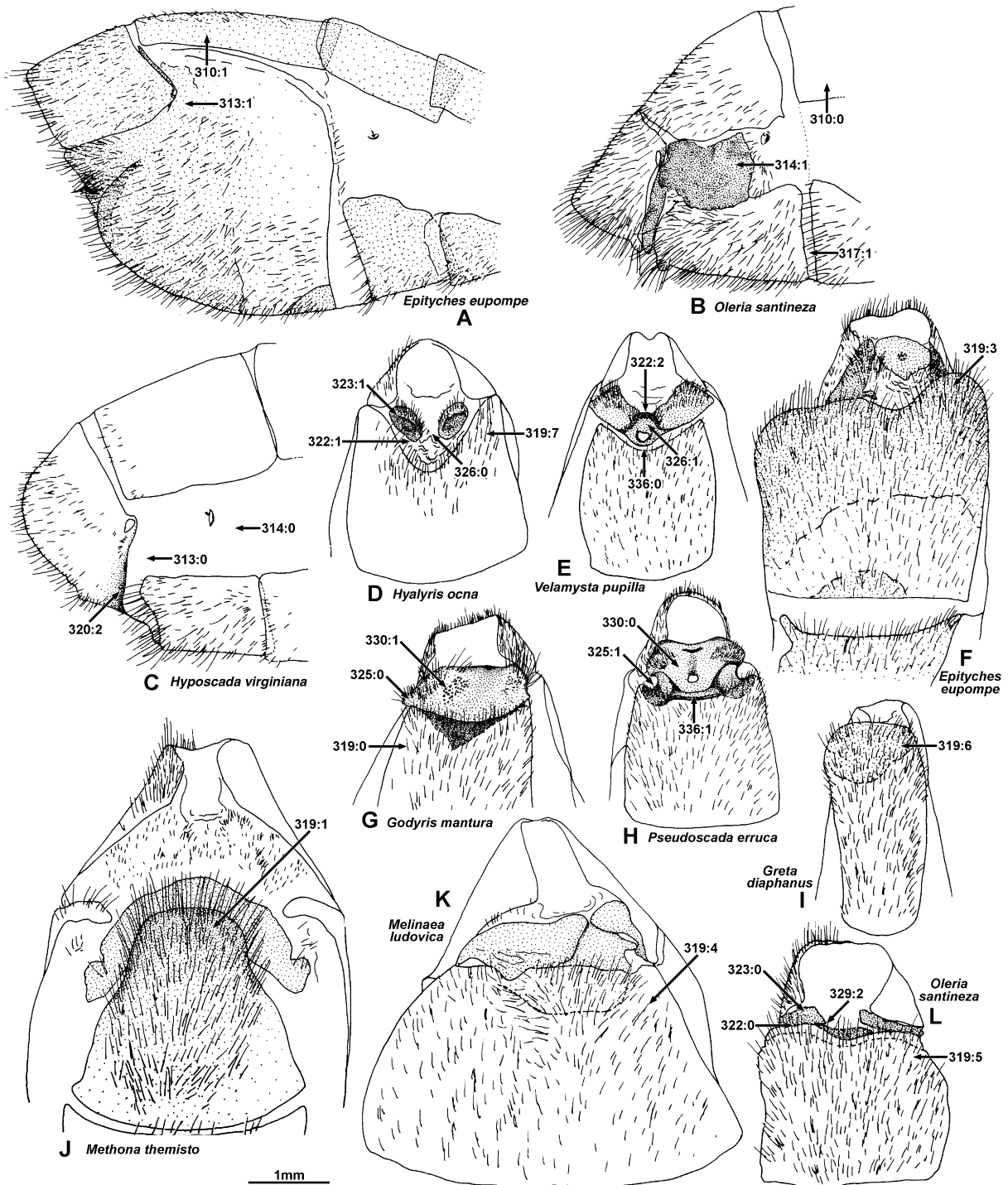


Fig. 27. Female abdomen. Abdomen posterior tip, lateral view: (A) *Epityches eupompe*; (B) *Oleria santineza* ssp. n.; (C) *Hyoscada virginiana evanides*. Abdomen posterior tip, ventral view: (D) *Hyaliris ocna* ssp. n.; (E) *Velamysta pupilla cruxifera* (Hewitson, 1877); (F) *Epityches eupompe*; (G) *Godyris mantura honrathi*; (H) *Pseudoscada erruca*; (I) *Greta diaphanus*; (J) *Methona t. themisto*; (K) *Melinaea l. ludovica*; (L) *Oleria santineza* ssp. n.

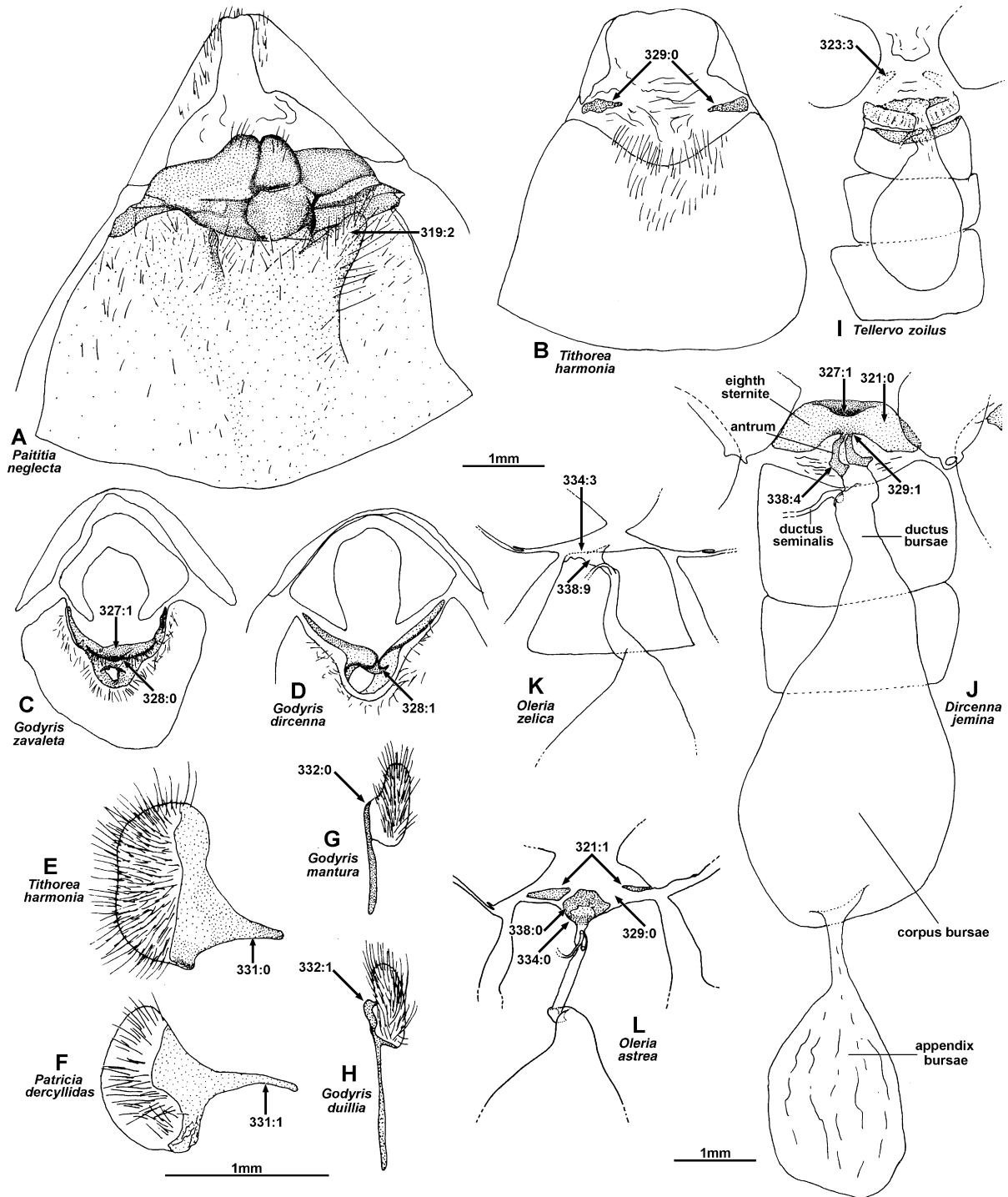


Fig. 28. Female abdomen and genitalia. Abdomen posterior tip, ventral view: (A) *Paititia neglecta*; (B) *Tithorea harmonia megara*. Abdomen posterior tip, posterior view: (C) *Godyris zavaleta telesilla*; (D) *Godyris dircenna*. Papilla analis, lateral view: E, *Tithorea harmonia megara*; (F) *Patricia d. dercyllidas*. Papilla analis, dorsal view: (G) *Godyris mantura honrathi*; (H) *Godyris duillia*. Genitalia, dorsal view: (I) *Tellervo z. zoilus*; (J) *Dircenna j. jemina*; (K) *Oleria z. zelica*; (L) *Oleria astrea burchelli*.

- 3692 315. *Pleural tissue at lateral posterior edge of seventh*
 3693 *sternite*: (0) weakly sclerotized (Fig. 26G); (1) semiscler- 3748
 3694 rotized (Fig. 26D); (2) strongly sclerotized, forming a 3749
 3695 broad, smooth band (Fig. 26F). slightly protruding lobes. 3750
- 3696 316. *Sclerotized pleural tissue at lateral posterior edge*
 3697 *of seventh sternite (Char. 315:1)*: (0) smooth (Fig. 26F); 3751
 3698 (1) with tiny studs (Fig. 26I). State 1 is a synapomorphy 3752
 3699 for *Napeogenes*. 3753
- 3700 317. *Pleural tissue between seventh and sixth sternites*
 3701 *sclerotized*: (0) weakly (Fig. 27B); (1) strongly 3754
 3702 (Fig. 26D). 3755
- 3703 318. *Seventh sternite*: (0) similar in width to sixth 3756
 3704 (Fig. 26G); (1) about twice width (Fig. 26E). 3757
- 3705 319. *Seventh sternite overall shape*: (0) slightly inden- 3758
 3706 ted or straight, smooth, uniformly sclerotized 3759
 3707 (Fig. 27G); (1) heavily sclerotized forming a rounded 3760
 3708 “keel” (Fig. 27J); (2) with a more heavily sclerotized, 3761
 3709 shallow, rounded projection on the right-hand side only 3762
 3710 (Fig. 28A); (3) asymmetrical, swollen, extended posteri- 3763
 3711 orly on right side (Fig. 27F); (4) asymmetrical and 3764
 3712 folded inwards at posterior right end (Fig. 27K); (5) 3765
 3713 symmetrical and folded inwards with a heavily sclero- 3766
 3714 tized lip (Fig. 27L); (6) elongate, rounded and folded 3767
 3715 inwards at posterior tip (Fig. 27I); (7) deeply invaginat- 3768
 3716 ed at posterior edge forming a “U” shape in ventral 3769
 3717 view, as broad anteriorly as laterally (Fig. 27D). 3770
- 3718 320. *Eighth sternite lateral plates*: (0) distinct or fused 3771
 3719 to terminal (eighth) tergite only at spiracular opening 3772
 3720 (Fig. 26H); (1) fused to terminal (eighth) tergite in basal 3773
 3721 half (Fig. 26F); (2) entirely fused to terminal tergite 3774
 3722 (Fig. 27C). Entire fusion with the terminal tergite (state 3775
 3723 2) is inferred from the ventral edge of the tergite being 3776
 3724 elongate, distinctly more heavily sclerotized and lacking 3777
 3725 in hairs than the remaining tergite, and/or with a notch 3778
 3726 at the posterior edge where the sternite and tergite are 3779
 3727 joined. If there is no such evidence of the eighth sternite 3780
 3728 plates the character is coded equivocal (and these species 3781
 3729 are coded 309:1,2). 3782
- 3730 321. *Basal attachment of eighth sternite plates*: (0) 3783
 3731 symmetrical (Fig. 28J); (1) asymmetrical, with left plate 3784
 3732 attached near base of tergite and right side more ventral 3785
 3733 (Fig. 28L). 3786
- 3734 322. *Eighth sternite lateral plates in ventral view with*
 3735 *anterior edge*: (0) near or posterior of posterior edge of 3787
 3736 terminal sternite (Fig. 27L); (1) extending far anteriorly 3788
 3737 past posterior edge terminal sternite (Fig. 27D). State 1 3789
 3738 is a synapomorphy for *Hypothyris* and *Hyalyris*, also 3790
 3739 recurring in *Methona megisto*. 3791
- 3740 323. *Shape of eighth sternite lateral plates*: (0) flat or 3792
 3741 concave plates (Fig. 27L); (1) slightly convex, wrinkled 3793
 3742 dish-like plates (Fig. 27D); (2) double curved plates, 3794
 3743 forming a protruding “snout” above ostium bursae 3795
 3744 (Fig. 27E); (3) slightly protruding rounded lobes 3796
 3745 (Fig. 28I). Many Godyridini have the eighth sternite 3797
 3746 plates pinched inwards just before the ostium bursae, 3798
 3747 then flared outwards to form a slightly protruding 3799
 “snout” above the ostium bursae. In *Tellervo* the eighth 3800
 sternite plates are visible only as weakly sclerotized, 3801
 slightly protruding lobes. 3802
324. *Edges of eighth sternite lateral plates*: (0) flat or 3751
 lightly curved (Fig. 30D); (1) with ventro-inner edge 3752
 recurved, forming a pouch from inside view (Fig. 30A). 3753
 State 1 is a synapomorphy for Mechanitini excluding 3754
Thyridia. 3755
325. *Anterior edge of eighth sternite plates*: (0) flat or 3756
 convex (Fig. 27G); (1) formed into a broad, concave 3757
 half-tube (Fig. 27H). 3758
326. *Eighth sternite lateral plates*: (0) separate 3759
 (Fig. 27D); (1) fused at ventral inner edges into a band 3760
 (independent of whether or not also fused with antrum) 3761
 (Fig. 27E). 3762
327. *Tissue at ventral edge of mouth of oviduct, above*
eighth sternite plates: (0) flat and unsclerotized 3763
 (Fig. 30D); (1) a pouch, sclerotized on ventral edge 3764
 (Fig. 28C,J). State 1 is a synapomorphy for Godyrid- 3765
 ini + Dircennini. 3766
328. *Eighth sternite lateral plate edges*: (0) not pinched 3767
 together forming an “x”-pattern in ventral view 3768
 (Fig. 28C); (1) pinched together forming an “x”-pattern 3769
 in ventral view (Fig. 28D). State 1 is a synapomorphy 3770
 for *Godyris dircenna* + *G. nero*. 3771
329. *Eighth sternite lateral plates*: (0) distinct from 3772
 antrum (Fig. 28B,L); (1) fused to antrum (Fig. 28J); (2) 3773
 fused on right side only (Fig. 27L). If the antrum is 3774
 completely unsclerotized, this character is coded equi- 3775
 vocal. 3776
330. *Inside edge of antrum near dorsal edge*: (0) smooth 3777
 (Fig. 27H); (1) heavily studded (Fig. 27G). State 1 is an 3778
 autapomorphy for *Godyris mantura*. 3779
- Internal.* 331. *Anterior apophysis of papilla analis*: (0) 3780
 short (Fig. 28E); (1) long (Fig. 28F). There is some 3781
 variation in the length and shape of the anterior 3782
 apophysis, but in *Tellervo*, *Tithorea*, *Elzunia* and *Meth-*
ona it is distinctly shorter than in other species. 3783
332. *Papillae anales in dorsal view with outer edge of*
sclerotized basal part: (0) contiguous with unsclerotized 3784
 distal part (Fig. 28G); (1) forming a distinct “step” 3785
 (Fig. 28H). 3786
333. *Anterior edge of eighth sternite plates*: (0) no more 3787
 heavily sclerotized than rest of plates (Fig. 29D); (1) 3788
 more heavily sclerotized, forming a distinct band 3789
 (Fig. 29H). 3790
334. *Ostium bursae position on last sternite*: (0) central 3791
 (Fig. 28L); (1) right-central (Fig. 30C); (2) left central 3792
 (Fig. 31D); (3) on right corner (Fig. 28K). 3793
335. *Dorsal edge of antrum plate*: (0) flat (Fig. 30C); 3794
 (1) recurved anteriorly (Fig. 30B). The antrum is usually 3795
 tubular or broadens posteriorly to form a flat plate. In 3796
Scada the dorsal edge of this flat plate is recurved 3797
 anteriorly. 3798
336. Flat, posteriorly protruding sclerotized plate 3801
 between posterior edge seventh sternite and ostium 3802

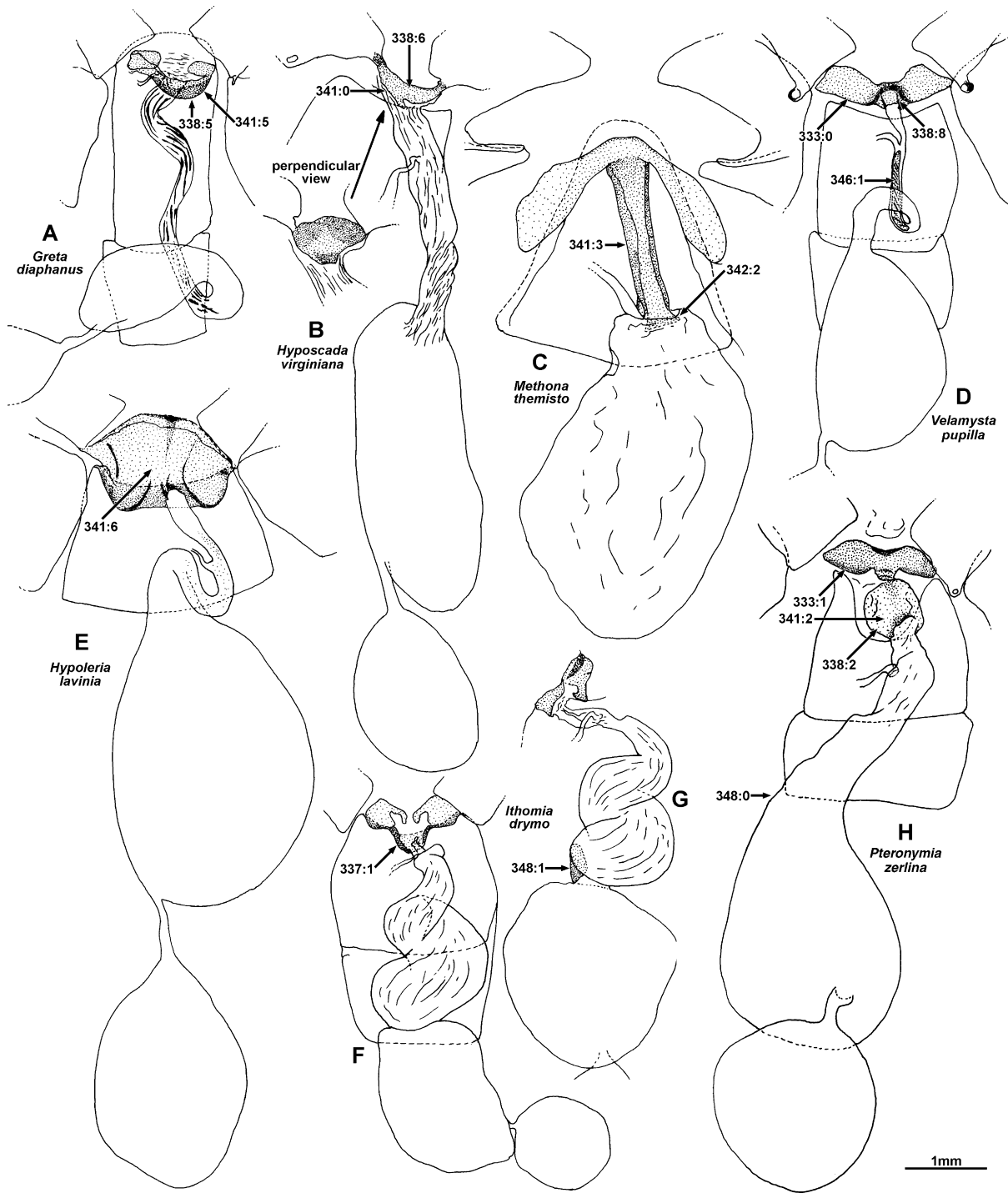


Fig. 29. Female genitalia, dorsal view (except G). (A) *Greta diaphanus*; (B) *Hyposcada virginiana evanides*; (C) *Methona t. themisto*; (D) *Velamysta pupilla cruxifera*; (E) *Hypoleria lavinia libera* Godman & Salvin, 1879; (F) *Ithomia drymo*; (G) *Ithomia drymo*, lateral view antrum, ductus bursae and corpus bursae; (H) *Pteronymia zerlina machay*.

3804 bursae: (0) absent (Fig. 27E); (1) present (Fig. 27H).
 3805 State 1 occurs here only in four *Pseudoscada* species. In
 3806 most species the ostium bursae is at the posterior edge of
 3807 the seventh sternite, whereas in state 1 there is a distinct,

sclerotized plate between the posterior edge and the
 ostium bursae, possibly formed of the pleural tissue at
 the edge of this sternite.

3808
 3809
 3810

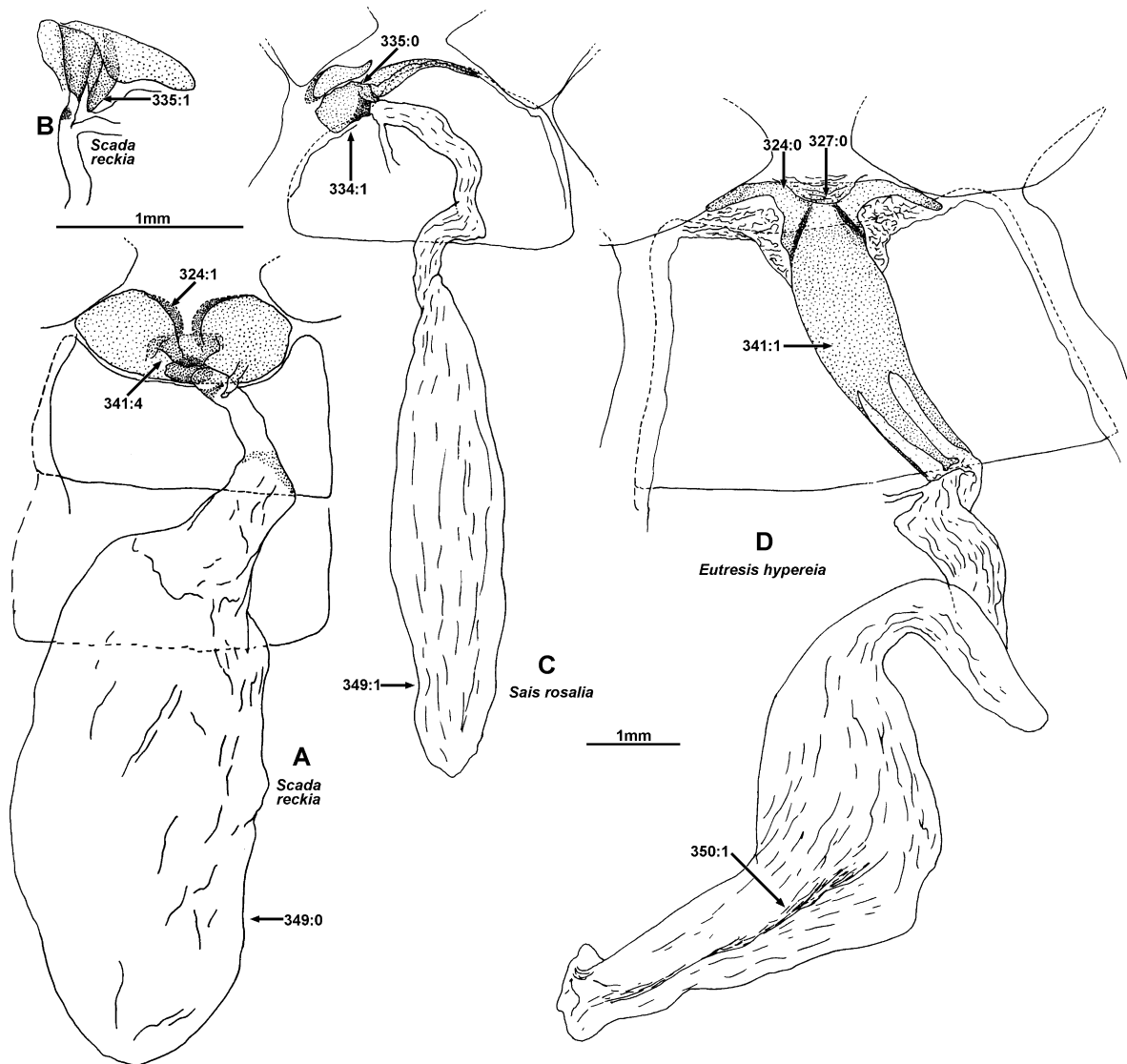


Fig. 30. Female genitalia, dorsal view. (A) *Scada reckia theaphia*; (B) *Scada reckia theaphia*, antrum and entrance ductus bursae, lateral view; (C) *Sais r. rosalia*; (D) *Eutresis h. hypereia*.

3811 337. *Antrum ventrally*: (0) unsupported (Fig. 31A); (1)
 3812 supported by a sclerotized “lip” (Figs 29F and 31G).
 3813 The sclerotized “lip” in state 1 may be the posterior edge
 3814 of the last sternite or part of the antrum, but in *Placidina*
 3815 (Fig. 31G) and *Pagyris* it is present and there is also a
 3816 sclerotized patch immediately anterior that appears to
 3817 represent the actual antrum (see also discussion under
 3818 Char. 338).

3819 338. *Antrum sclerotization*: (0) a completely sclero-
 3820 tized tube (Fig. 28L); (1) sclerotized except in a dorsal
 3821 band (Fig. 31A); (2) sclerotized except for a more
 3822 weakly sclerotized ventral band (Fig. 29H); (3) semi-
 3823 sclerotized (Fig. 31B); (4) sclerotized dorsally, more so
 3824 in two parallel longitudinal bands (Fig. 28J); (5) sclero-
 3825 tized in a broad dorsal band only (Fig. 29A); (6)

sclerotized in a dorsal plate only (Fig. 29B); (7) a
 3826 ventral round sclerotized patch only (Fig. 31G); (8) a
 3827 thin sclerotized ring (Fig. 29D); (9) unsclerotized
 3828 (Fig. 28K). The antrum is usually a sclerotized ring or
 3829 tube between the ductus bursae and ostium bursae. In
 3830 primitive Ithomiinae, such as *Tithorea* (and other
 3831 nymphalids, e.g., the limenitidine genus *Adelpha*), the
 3832 antrum is a thickened half tube which is dorsally
 3833 grooved. A similar form of antrum also occurs in
 3834 *Methona* (Char. 341:3), which is entirely sclerotized,
 3835 among other species, as well as *Pagyris* and *Placidina*, in
 3836 which it is sclerotized in a small ventral patch only (state
 3837 7). In most other species the antrum is more or less
 3838 flattened tube, which is assumed to be homologous to
 3839 the half tube in *Tithorea*, etc. Species coded state 8 have
 3840

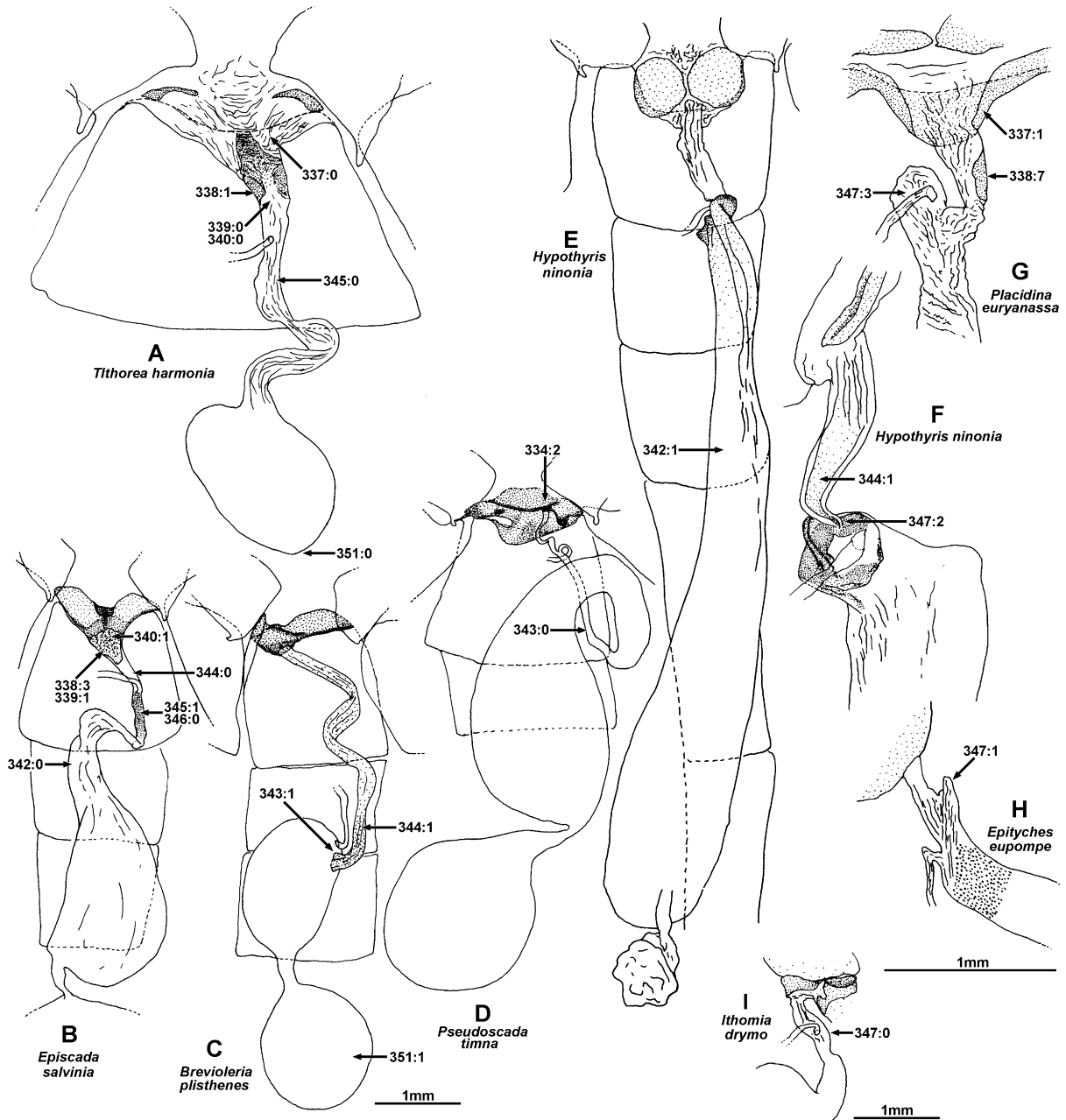


Fig. 31. Female genitalia. Dorsal view: (A) *Tithorea harmonia megara*; (B) *Episcada s. salvinia*; (C) *Brevioleria plisthenes*; (D) *Pseudoscada timna* ssp. n.; (E) *Hypothyris n. ninonia*. Antrum and base of ductus bursae: (F) *Hypothyris n. ninonia*, lateral view; (G) *Placidina euryanassa*, dorsal view; (H) *Epityches eupompe*, lateral view; (I) *Ithomia drymo*, lateral view.

3841 the ductus bursae almost completely unsclerotized, but a
 3842 more heavily sclerotized ring surrounding its mouth,
 3843 usually extending on to the fused eighth sternite plates
 3844 and inset into the posterior edge of the seventh sternite,
 3845 is inferred to be the antrum.

3846 339. *Antrum with a faint, internal sclerotized triangular*
 3847 *patch*: (0) absent (Fig. 31A); (1) present (Fig. 31B). This
 3848 character is coded equivocal if the antrum is heavily
 3849 sclerotized.

3850 340. *Antrum inner walls*: (0) smooth (Fig. 31A); (1)
 3851 studded (Fig. 31B). State 1 is a synapomorphy for
 3852 *Ceratinia* + *Episcada*.

3853 341. *Shape of antrum*: (0) gradual funnel or tube
 3854 similar in width to ductus bursae (Fig. 29B); (1) a large
 3855 funnel (Fig. 30D); (2) a long, broad (3 × width ductus
 3856 bursae), tube of almost even width (Fig. 29H); (3) a very
 3857 long, narrow, dorsally grooved tube (Fig. 29C); (4) a
 3858 tube broadening into a flat, perpendicular plate

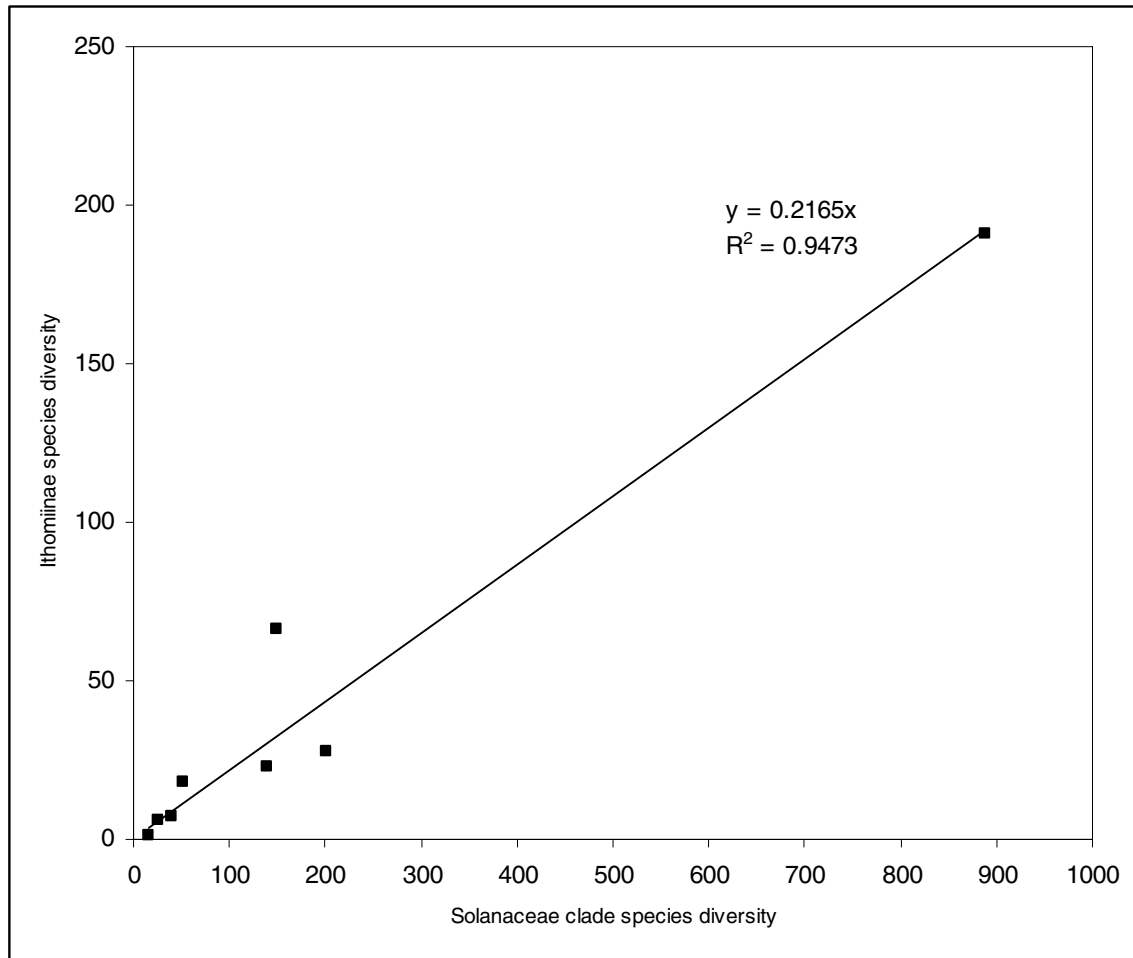


Fig. 32. Relationship between Solanaceae clade diversity and associated ithomiine herbivore diversity.

3859 (Fig. 30A); (5) a very broad, shallow, “cup” curving at
 3860 edges (Fig. 29A); (6) a semicylindrical plate (Fig. 29E).
 3861 In *Methona* (state 3), the sclerotized tube connecting the
 3862 corpus bursae to the eighth sternite plates is similar in
 3863 morphology to the antrum in primitive species like
 3864 *Tithorea* (see Discussion under Char. 338), and is
 3865 therefore inferred to represent the antrum. State 5 is
 3866 an autapomorphy for *Greta diaphanus*, state 6 is an
 3867 autapomorphy for *Hypoleria lavinia*.

3868 342. *Ductus bursae*: (0) medium or short [extending
 3869 one to two tergites from ostium bursae] (Fig. 31B); (1)
 3870 long [extending more than three tergites from the ostium
 3871 bursae] (Fig. 31E); (2) absent (Fig. 29C). Reasons for
 3872 considering the sclerotized tube connecting the corpus
 3873 bursae to the eighth sternite in *Methona* to be the
 3874 antrum, rather than the ductus bursae, are discussed
 3875 under Char. 341.

3876 343. *Ductus bursae* portion anterior of ductus seminalis:
 3877 (0) present (Fig. 31D); (1) absent (ductus seminalis
 3878 arises from corpus bursae) (Fig. 31C). State 1 is a
 3879 synapomorphy for *Hypoleria adasa* + *Mcclun-*
 3880 *gia* + *Brevioleria* + *Godyris mantura*. *Methona* is

3881 coded equivocal because the ductus bursae is inferred
 3882 to be absent (see Char. 342).

3883 344. *Ductus bursae* just posterior of ductus seminalis
 3884 with sclerotization fading posteriorly: (0) absent
 3885 (Fig. 31B); (1) present (Fig. 31C,F).

3886 345. *Ductus bursae* anterior of ductus seminalis with
 3887 sclerotization fading anteriorly: (0) absent (Fig. 31A); (1)
 3888 present (Fig. 31B).

3889 346. If ductus bursae anterior of ductus seminalis has
 3890 sclerotization fading anteriorly (Char. 345:1), then
 3891 sclerotization is: (0) evenly fading (Fig. 31B); (1) striated
 3892 (Fig. 29D). State 1 is a synapomorphy for *Velamysta*.

3893 347. *Ductus bursae* with anterior and posterior sections:
 3894 (0) joined smoothly (Fig. 31I); (1) with anterior section
 3895 projecting posteriorly beyond end of posterior section,
 3896 ductus seminalis arising anterior of junction (Fig. 31H);
 3897 (2) with posterior section joining on to a disc at end of
 3898 much larger anterior section (Fig. 31F); (3) with anterior
 3899 section projecting posteriorly beyond end of posterior
 3900 section, ductus seminalis arising posterior of junction
 3901 (Fig. 31G).

3902 348. *Ductus bursae* near junction with corpus bursae
 3903 with a large, curved sclerotized pad: (0) absent
 3904 (Fig. 29H); (1) present (Fig. 29G).

3905 349. *Corpus bursae anteriorly*: (0) rounded (Fig. 30A);
 3906 (1) attenuated (Fig. 30C). This character is difficult to
 3907 observe unless the corpus bursae is inflated, either
 3908 immediately following dissection, or artificially using a
 3909 syringe and water.

3910 350. *Signae on corpus bursae*: (0) scattered; (1) in lines
 3911 (Fig. 30D). The signae are numerous, tiny sclerotized
 3912 spines on the inner surface of the corpus bursae, and
 3913 they are usually dense and evenly scattered. In state 1
 3914 distinct lines of denser, larger or more strongly sclero-
 3915 tized signae are visible.

3916 351. *Appendix bursae*: (0) absent (Fig. 31A); (1)
 3917 present (Fig. 31C).

3918 *Wing pattern*. 352. *Male VHW with a white marking*
 3919 *in cell Sc + R1-Rs anterior of discocellular veins*: (0)
 3920 absent (Fig. 17AA); (1) present, confined to cell
 3921 Sc + R1-Rs (Fig. 17AB); (2) present and extending
 3922 into cell M1-Rs (Fig. 17AD).

3923 353. *If male with VHW white marking in cell*
 3924 *Sc + R1-Rs anterior of discocellular veins* (Char. 352:
 3925 1), then marking is: (0) single (Fig. 17AB); (1) double
 3926 (Fig. 17AC). The double marking in *Olyras* and *Paititia*
 3927 is regarded as homologous to the single marking in
 3928 *Eutresis* because of similarity of position and because
 3929 the scales forming these white markings are very similar
 3930 in all three taxa, being notably translucent (more
 3931 opaque in other taxa). *Veladyris* also has an additional
 3932 white marking in cell Sc + R1-Rs, but because of much
 3933 more basal position of this marking it is regarded as
 3934 independent of the white discal marking coded in Char.
 3935 352.

Larval hostplant (characters not included in cladistic
analysis coding in Table 3) 3936
 3937

H1 & H2. *Larval hostplant*: (0) Apocynaceae; (1) 3938
 Gesneriaceae; (2) *Brunfelsia* L. (Petunioideae); (3) 3939
Cestrum L. (Cestroideae, Cestreae); (4) *Nicandra* Adans. 3940
 (Solanoideae, Nicandreae); (5) *Datura* L. clade (Solan- 3941
 oideae, Datureae); (6) *Solanum* clade (Solanoideae, 3942
 Solaneae); (7) *Solandra* clade (Solanoideae, Solandreae); 3943
 (8) *Capsicum* L. (Solanoideae, Capsiceae); (9) *Lycianthes* 3944
 Dunal. (Solanoideae, Capsiceae); (A) *Withania* + 3945
Iochroma + *Physalis* clade (Solanoideae, Physaleae). 3946
 See Table 3. 3947

Following Olmstead et al. (1999), Solanaceae clades 3948
 contain the following genera of ithomiine hostplants: (5) 3949
Datura L., *Brugmansia* Pers.; (6) *Solanum* L. (incl. 3950
Cyphomandra Mart., *Lycopersicon* Mill.); (7) *Dyssochro-* 3951
ma Miers, *Juanulloa* Ruiz & Pav., *Markea* A. Rich., 3952
Merinthopodium Donn. Sm., *Schultesianthus* Hunz., 3953
Solandra Sw., *Trianaea* Planch. & Lindeno (A) *Athenaea* 3954
 Sendt., *Aureliana* Sendt., *Cuatresia* Hunz., *Withania* 3955
 Pauq., *Acnistus* Schott, *Dunalia* Kunth, *Iochroma* 3956
 Benth., *Saracha* Ruiz & Pav., *Vassobia* Rusby, *Brachis-* 3957
tus Miers, *Physalis* L., *Witheringia* L'Her. 3958

Appendix 2 3959

Character matrix: "?" = indicates missing data, 3960
 "--" = indicates a non-applicable state. 3961

22 Attached. 3962

Appendix 3

Information sources for included species

Higher taxon	Species	Dissections examined ¹	Immature stage sources ²
Tellervini (Tellervinae)	<i>Tellervo zoilus</i>	M: BMNH 7117; F: BMNH 7118, BMNH 7126	6
Tithoreini	<i>Elzunia pavonii</i>	M: BMNH 6624; F: BMNH 6625	1
Tithoreini	<i>Tithorea harmonia</i>	M: BMNH 6819, BMNH 6622, KWJH, BMNH 6820; F: BMNH 6623, KWJH, BMNH 6818	1
Tithoreini	<i>Tithorea tarricina</i>	M: BMNH 6812, BMNH 6814, BMNH 6816; F: BMNH 6813, BMNH 6815, BMNH 6817	1
Tithoreini	<i>Aeria eurimedia</i>	M: BMNH 6626, BMNH 7106; F: BMNH 7172, BMNH 7119	1
Tithoreini	<i>Aeria olena</i>	M: BMNH 7139; F: BMNH 7173, BMNH 7140	1
Methonini	<i>Methona megisto</i>	M: BMNH 7161; F: BMNH 7160	1
Methonini	<i>Methona themisto</i>	M: BMNH 6629; F: BMNH 6642	1
Melinaeini	<i>Athyrtis mechanitisi</i>	M: BMNH 6634, BMNH 6638; F: BMNH 6647	1
Melinaeini	<i>Eutresis hypereia</i>	M: BMNH 6632, MGCL; F: BMNH 6645, MGCL, BMNH 7159	1
Melinaeini	<i>Melinaea ethra</i>	M: BMNH 7141; F: BMNH 7142	1
Melinaeini	<i>Melinaea ludovica</i>	M: BMNH 6631; F: BMNH 6644	1
Melinaeini	<i>Melinaea menophilus</i>	M: MGCL, BMNH 7143, BMNH 7149, KWJH; F: BMNH 7144	1,2
Melinaeini	<i>Olyras crathis</i>	M: BMNH 6633; F: BMNH 6646	1
Melinaeini	<i>Paititia neglecta</i>	M: BMNH 7133; F: BMNH 7132	1
Mechanitini	<i>Forbestra equicola</i>	M: BMNH 6637; F: BMNH 6650	3
Mechanitini	<i>Forbestra olivencia</i>	M: BMNH 7145; F: BMNH 7146	7
Mechanitini	<i>Mechanitis lysimnia</i>	M: BMNH 7150, KWJH; F: BMNH 7147, BMNH 7176, KWJH	1
Mechanitini	<i>Mechanitis polymnia</i>	M: BMNH 6639; F: BMNH 6651	1
Mechanitini	<i>Sais rosalia</i>	M: BMNH 6636; F: BMNH 6649	8
Mechanitini	<i>Scada karschina</i>	M: BMNH 7151; F: BMNH 7175, BMNH 7152	1
Mechanitini	<i>Scada reckia</i>	M: KWJH, KWJH, KWJH, KWJH, BMNH 6640; F: BMNH 7174, KWJH, BMNH 6652	1
Mechanitini	<i>Thyridia psidii</i>	M: BMNH 6635; F: BMNH 6648	1
New tribe	<i>Athesis clearista</i>	M: MGCL, BMNH 6627; F: BMNH 7112, MGCL	1
New tribe	<i>Patricia deryllidas</i>	M: BMNH 7084, BMNH 7134, BMNH 7137, BMNH 7138, BMNH 6628; F: BMNH 6641	2, 18
Napeogenini	<i>Aremfoxia ferra</i>	M: BMNH 6653; F: BMNH 7131	–
Napeogenini	<i>Epityches eupompe</i>	M: BMNH 6654; F: BMNH 6664, MGCL	1
Napeogenini	<i>Hypothyris xanthostola</i>	M: BMNH 6655; F: BMNH 6665	1
Napeogenini	<i>Hypothyris cantobrica</i>	M: BMNH 6656; F: BMNH 6666	1
Napeogenini	<i>Hypothyris euclea</i>	M: KWJH, KWJH, KWJH, KWJH, BMNH 6662; F: BMNH 6673	1
Napeogenini	<i>Hypothyris moebiusi</i>	M: BMNH 6661; F: BMNH 6671	–
Napeogenini	<i>Hypothyris ninonia</i>	M: BMNH 6660; F: BMNH 6670	1
Napeogenini	<i>Hyaliris coeno</i>	M: BMNH 6657, KWJH; F: BMNH 6667, BMNH 6672	–
Napeogenini	<i>Hyaliris excelsa</i>	M: BMNH 6659; F: BMNH 6669	1
Napeogenini	<i>Hyaliris oca</i>	M: BMNH 6658, KWJH; F: BMNH 6668	2
Napeogenini	<i>Napeogenes apulia</i>	M: BMNH 6349; F: KWJH 6676	2
Napeogenini	<i>Napeogenes inachia</i>	M: BMNH 6333; F: BMNH 6675, BMNH 6678	1, 14
Napeogenini	<i>Napeogenes rhezia</i>	M: BMNH 6332; F: BMNH 6674, BMNH 6677	–
Ithomiini	<i>Ithomia arduinna</i>	M: BMNH 7098; F: BMNH 7097	1
Ithomiini	<i>Ithomia drymo</i>	M: BMNH 6688, BMNH 7169; F: BMNH 6682, BMNH 6686	1
Ithomiini	<i>Ithomia terra</i>	M: BMNH 6687; F: BMNH 6681, BMNH 6685	2
Ithomiini	<i>Pagyris cymothoe</i>	M: BMNH 6690; F: BMNH 6680	1
Ithomiini	<i>Pagyris ulla</i>	M: BMNH 6689; F: BMNH 6679	–
Ithomiini	<i>Placidina euryanassa</i>	M: BMNH 6630; F: BMNH 6643	1, 15
Oleriini	<i>Hyposcada anchiala</i>	M: BMNH 6806, MGCL, KWJH, BMNH 7231; F: BMNH 7122, MGCL	4
Oleriini	<i>Hyposcada taliata</i>	M: BMNH 7107, KWJH OLERIA-39, BMNH 6810; F: KWJH OLERIA-50	–
Oleriini	<i>Hyposcada virginiana</i>	M: KWJH, BMNH 6805; F: MGCL	9
Oleriini	<i>Megoleria susiana</i>	M: BMNH 7227, BMNH 6683; F: BMNH 7228, BMNH 6684	5
Oleriini	<i>Oleria aegineta</i>	M: KWJH; F: KWJH OLERIA-46	–
Oleriini	<i>Oleria aegle</i>	M: BMNH 5941, BMNH 6807, MGCL; F: MGCL, MGCL	1
Oleriini	<i>Oleria aquata</i>	M: BMNH 6780, BMNH 7148; F: BMNH 6781	1
Oleriini	<i>Oleria astrea</i>	M: AME, BMNH 6246, BMNH 6760, BMNH 6761, BMNH 6763, ZMHU, BMNH 6263; F: MGCL, BMNH 6264	–
Oleriini	<i>Oleria canilla</i>	M: BMNH 6270, MGCL; F: BMNH 6271, BMNH 7121	1

Appendix 3 Continued.

Higher taxon	Species	Dissections examined ¹	Immature stage sources ²
Oleriini	<i>Oleria olerioides</i>	M: KWJH OLERIA-15, BMNH 6808; F: KWJH OLERIA-47	–
Oleriini	<i>Oleria santineza</i>	M: BMNH 6402, AMNH, AMNH, BMNH 6399, BMNH 6429, BMNH 6430, ZMHU, MGCL, BMNH 6809, KWJH OLERIA-20, KWJH OLERIA-25; F: BMNH 6403, AMNH, BMNH 6434, BMNH 6435, KWJH, KWJH OLERIA-43	2
Oleriini	<i>Oleria zelica</i>	M: MGCL, BMNH 6691; F: MGCL	10
Dircennini	<i>Callithomia alexirrhoe</i>	M: BMNH 6328, BMNH 7085; F: BMNH 6692	–
Dircennini	<i>Callithomia lenea</i>	M: BMNH 6327; F: BMNH 6693	1
Dircennini	<i>Ceratinia neso</i>	M: BMNH 6776; F: BMNH 6700	1
Dircennini	<i>Ceratinia tutia</i>	M: BMNH 6777, KWJH; F: BMNH 6698, BMNH 7177	1
Dircennini	<i>Dircenna dero</i>	M: BMNH 6772, KWJH; F: BMNH 6695	1
Dircennini	<i>Dircenna jemina</i>	M: BMNH 6771; F: BMNH 6694	–
Dircennini	<i>Dircenna paradoxa</i>	M: BMNH 6326, BMNH 7182, BMNH 7185; F: BMNH 7191, BMNH 6696, BMNH 7183, BMNH 7184	2
Dircennini	<i>Episcada apuleia</i>	M: BMNH 6287; F: 6705	2
Dircennini	<i>Episcada clausina</i>	M: BMNH 6283, KWJH, BMNH 7156, BMNH 6284; F: BMNH 7153	1
Dircennini	<i>Episcada doto</i>	M: BMNH 6275; F: BMNH 6701	–
Dircennini	<i>Episcada hemixanthe</i>	M: BMNH 6292; F: BMNH 7178, BMNH 6706	–
Dircennini	<i>Episcada hymenaea</i>	M: BMNH 6278, BMNH 6778, SMF; F: BMNH 6703	1
Dircennini	<i>Episcada philoclea</i>	M: BMNH 6289, BMNH 7088; F: BMNH 6707	1
Dircennini	<i>Episcada salvinia</i>	M: BMNH 6280, BMNH 6279; F: BMNH 6704	1
Dircennini	<i>Episcada canaria</i>	M: BMNH 6276; F: BMNH 6702	1, 15
Dircennini	<i>Haenschia sidonia</i>	M: ZSBS; F: BMNH 7108	–
Dircennini	<i>Hyalenna pascua</i>	M: BMNH 7055; F: MUSM	1
Dircennini	<i>Hyalenna perasippa</i>	M: BMNH 6775, BMNH 7086; F: BMNH 7186, MUSM	–
Dircennini	<i>Pteronymia aletta</i>	M: BMNH 6305; F: BMNH 6708	1
Dircennini	<i>Pteronymia alida</i>	M: BMNH 6321, KWJH, KWJH, ZMHU, BMNH 6785, BMNH 6784; F: BMNH 6712	2
Dircennini	<i>Pteronymia artena</i>	M: KWJH, BMNH 6782; F: BMNH 6716, BMNH 7179	2
Dircennini	<i>Pteronymia carlia</i>	M: BMNH 6298; F: BMNH 7155	1
Dircennini	<i>Pteronymia euritea</i>	M: BMNH 6299; F: BMNH 7162	1
Dircennini	<i>Pteronymia hara</i>	M: BMNH 6320, USNM, BMNH 7087, KWJH, BMNH 6389, SMNS, KWJH; F: USNM, BMNH 6715	–
Dircennini	<i>Pteronymia inania</i>	M: KWJH; F: BMNH 6713	2
Dircennini	<i>Pteronymia latilla</i>	M: BMNH 6302; F: BMNH 6709	1
Dircennini	<i>Pteronymia lonera</i>	M: USNM; F: USNM 6714	1, 17
Dircennini	<i>Pteronymia zurlina</i>	M: KWJH, KWJH, BMNH 6316; F: BMNH 6711	2
Godyridini	<i>Brevioleria arzalia</i>	M: BMNH 6787, BMNH 6792; F: BMNH 7180, BMNH 6723	1
Godyridini	<i>Brevioleria plisthenes</i>	M: BMNH 7163, UFP; F: UFP	1
Godyridini	<i>Godyris dircenna</i>	M: BMNH 6746; F: BMNH 6735	1
Godyridini	<i>Godyris duillia</i>	M: BMNH 7090, BMNH 6377; F: BMNH 6717	2
Godyridini	<i>Godyris nero</i>	M: BMNH 6369, BMNH 6384; F: BMNH 6734	–
Godyridini	<i>Godyris zavaleta</i>	M: KWJH, BMNH 6786; F: KWJH, BMNH 6719	1
Godyridini	<i>Godyris mantura</i>	M: BMNH 6379, BMNH 7223; F: BMNH 6718, BMNH 7224	–
Godyridini	<i>Greta diaphanus</i>	M: BMNH 6375; F: BMNH 6725	11
Godyridini	<i>Greta morgane</i>	M: BMNH 6371; F: BMNH 6726	12, 19
Godyridini	<i>Heterosais edessa</i>	M: BMNH 7157; F: BMNH 7181, BMNH 7158	1
Godyridini	<i>Heterosais nephele</i>	M: BMNH 6804; F: BMNH 6732	–
Godyridini	<i>Hypoleria lavinia</i>	M: BMNH 6394; F: BMNH 6721	1, 13
Godyridini	<i>Mechungia cymo</i>	M: BMNH 7091, BMNH 7165, BMNH 7166, BMNH 6788, BMNH 7164, BMNH 7167, BMNH 7168; F: BMNH 6724	1
Godyridini	<i>Hypoleria adasa</i>	M: BMNH 6790, BMNH 7171; F: BMNH 6722	1
Godyridini	<i>Pseudoscada erruca</i>	M: BMNH 6386, BMNH 6802; F: BMNH 6729, BMNH 6733	1
Godyridini	<i>Pseudoscada florula</i>	M: BMNH 6803, BMNH 6395; F: BMNH 6731	1
Godyridini	<i>Pseudoscada timna</i>	M: BMNH 6798, BMNH 6791, BMNH 6799, BMNH 6800, BMNH 6795, BMNH 6796, BMNH 6801, BMNH 6797; F: BMNH 6730	1
Godyridini	<i>Greta andromica</i>	M: BMNH 6352, BMNH 6368; F: BMNH 6728	2
Godyridini	<i>Greta ortygia</i>	M: BMNH 6374, BMNH 6354; F: BMNH 7050, BMNH 7051	2